Interactions of Mammalian Retroviruses with Cellular MicroRNA Biogenesis and Effector Pathways

by

Adam Wesley Whisnant

Department of Department of Molecular Genetics and Microbiology
Duke University

Date:_____

Approved:

_____
Bryan R. Cullen, Supervisor

_____
Guido Ferrari

_____
Dennis C. Ko

_____
Micah A. Luftig

_____
David J. Pickup

Dissertation submitted in partial fulfillment of
the requirements for the degree of Doctor
of Philosophy in the Department of
Molecular Genetics and Microbiology in the Graduate School
of Duke University

2014

ABSTRACT

Interactions of Mammalian Retroviruses with Cellular MicroRNA Biogenesis and Effector Pathways

by

Adam Wesley Whisnant

Department of Molecular Genetics and Microbiology
Duke University

Date:_____

Approved:

_____
Bryan R. Cullen, Supervisor

_____
Guido Ferrari

_____
Dennis C. Ko

_____
Micah A. Luftig

_____
David J. Pickup

An abstract of a dissertation submitted in partial
fulfillment of the requirements for the degree
of Doctor of Philosophy in the Department of
Molecular Genetics and Microbiology in the Graduate School of
Duke University

2014

Abstract

The cellular microRNA (miRNA) pathway has emerged as an important regulator of host-virus interactions. While miRNAs of viral and cellular origin have been demonstrated to modulate viral gene expression and host immune responses, reports detailing these activities in the context of mammalian retroviruses have been controversial. Using modern, high-throughput small RNA sequencing we provide evidence that the spumaretrovirus bovine foamy virus expresses high levels of viral miRNAs via noncanonical biogenesis mechanisms. In contrast, the lentivirus human immunodeficiency virus type 1 (HIV-1) does not express any viral miRNAs in a number of cellular contexts. Comprehensive analysis of miRNA binding sites in HIV-1 infected cells yielded several viral sequences that can be targeted by cellular miRNAs. However, this analysis indicated that HIV-1 transcripts are largely refractory to binding and inhibition by cellular miRNAs. In addition, we demonstrate that HIV-1 exerts minimal perturbations on cellular miRNA profiles and that viral replication is not affected by the ablation of mature cellular miRNAs. Together, these data demonstrate that the ability of retroviruses to encode miRNAs is not broadly conserved and that lentiviruses, particularly HIV-1, have evolved to avoid targeting by cellular miRNAs.

Contents

List of Tables

List of Figures

Acknowledgements

I would like to acknowledge the excellent support and guidance offered by Bryan R. Cullen at Duke University and the many members of the laboratory throughout the years. In particular, I would like to acknowledge Jason G. Powers, Omar Flores, Edward M. Kennedy, and Hal P. Bogerd for their advice and direct collaboration on much of the work presented.

I would also like to acknowledge the laboratory of Martin Löchelt at the German Cancer Research Center, especially Timo Kehl and Qiuying Bao, for performing the culture infections with bovine foamy virus and providing their samples. In addition, I thank Magdalena Materniak and Jacek Kuzmak of the National Veterinary Research Institute in Pulawy, Poland for providing leukocytes from bovine foamy virus-infected calves.

The infections with human immunodeficiency virus were done in generous collaboration with Chin-Ho Chen and Phong Ho at Duke University as well as Mario Stevenson and Natalia Sharova at the University of Miami.

1. Introduction

1.1 *MicroRNA Biogenesis and Function*

MicroRNAs are a regulatory class of ~22nt non-coding RNAs that post-transcriptionally regulate gene expression by binding complementary mRNAs. MiRNA-mediated RNA interference is known to play essential roles in many cellular processes including cellular proliferation and differentiation, signaling, immunity, and apoptosis [1-5]. A single miRNA can target hundreds of partially-complementary mRNAs as the major determinant of binding is complementarity between the mRNA and a short stretch of the miRNA, nucleotides 2-8 of the 5′ end, also known as the seed region [1, 6-8]. Additionally, non-canonical miRNA binding to mRNAs that show incomplete seed complementarity can contribute up to 40% of miRNA target sites [9]. Because of the abundance of potential mRNA targets, miRNAs representing <0.1% of the total miRNA are not expressed at levels required to inhibit the expression of any one particular gene target [10]. Thus, miRNAs at or above 0.1% of the population are considered to be significantly expressed in regards to function.

Most miRNAs originate from longer transcripts transcribed by RNA Polymerase (Pol) II called primary-miRNAs or pri-miRNAs [11-13] (Fig. 1-1). A pri-miRNA is typically capped, polyadenylated, and contains one or more ~80nt hairpins consisting of a ~33bp imperfect stem with a >10nt terminal loop flanked by single-stranded sequences

[14]. This structure is recognized by the Microprocessor complex which consists of the RNase III enzyme Drosha and the DiGeorge syndrome critical region 8 (DGCR8) protein. DGCR8 recognizes the stem-loop and positions Drosha to liberate a ~60nt hairpin called a pre-miRNA bearing a 2nt 3′ overhang [15-17]. A pre-miRNA may also be directly transcribed with RNA Pol III, effectively bypassing Drosha cleavage [18, 19]. Yet another Drosha-independent biogenesis mechanism exists with the case of mirtrons and occurs when splicing liberates an intron that folds into a pre-miRNA hairpin [20], however the bulk of mature miRNAs are canonically processed by Drosha.

The pre-miRNA is then recognized by Exportin 5 and shuttled into the cytoplasm for processing by another RNase III enzyme, Dicer [21]. Complexed with the cofactor HIV-1 TAR RNA binding protein (TRBP), Dicer removes the loop of the pre-miRNA yielding duplexed ~22nt RNAs with 3′ 2nt overhangs on both strands [15, 22, 23]. One of these strands is then preferentially bound by the RNA-Induced Silencing Complex (RISC), minimally consisting of one of the four Argonaute (Ago) proteins and one of three members of the GW182 protein family [1, 24]. Dicer is required for the maturation of all known mammalian miRNAs except miR-451, whose pre-miRNA is loaded into Ago2 and processed into the mature miRNA through the action of an RNase H-like domain [25].

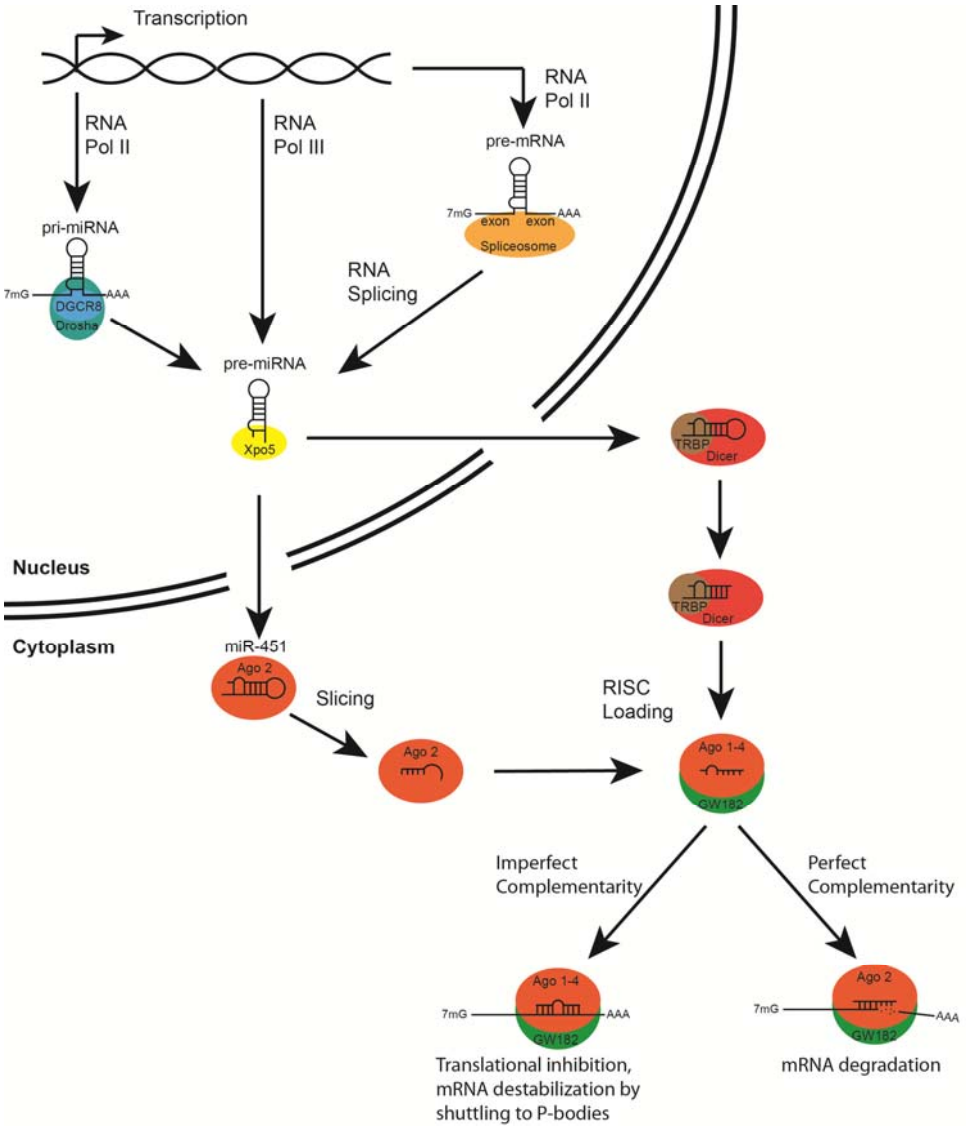

Figure 1-1: Overview of microRNA biogenesis in mammalian cells. Primary-miRNA transcripts are cleaved by the Microprocessor complex consisting of Drosha and DGCR8 to release a pre-miRNA hairpin. A pre-miRNA may also be liberated by the spliceosome or directly transcribed by RNA Pol III. The pre-miRNA is shuttled to the cytoplasm by Exportin 5 (Xpo5) where Dicer-TRBP cleaves the terminal loop. One strand of the resulting duplex is preferentially loaded into RISC where it guides the complex to complementary regions of mRNA. Perfect complementarity can result in cleavage and degradation of the target sequence while imperfect complementarity results in translational inhibition and mRNA destabilization.

In the event of perfect complementarity between a miRNA and an mRNA, the major Ago protein in human cells, Ago2, can nucleolytically degrade the mRNA [26]. However, most miRNA targets are not perfectly complementary and silencing is achieved by other means. GW182 proteins interact with poly(A)-binding protein (PABP) and cause PABP to dissociate from mRNAs targeted by RISC, resulting in translational inhibition through disruption of mRNA circularization as well as dissociation of eIF4G [27]. Most RISC-bound mRNAs are shuttled to cytoplasmic processing bodies (P-bodies) that contain enzymes for decapping and deadenylating mRNAs, as well as exonucleases [24, 27-30]. GW182 recruits the P-body-associated CCR4-NOT deadenylation/exonuclease complex to RISC-bound mRNAs which removes the poly(A) tail and promotes 3′ → 5′mRNA degradation [27, 28]. Alternatively, the 5′ mRNA cap can be removed in P-bodies by the Dcp1/2 enzyme complex, which co-immunoprecipitates with Argonaute proteins [29], and allows for 5′ → 3′ mRNA degradation by the exonuclease Xrn1 [28, 30]. In addition to these enzymes, numerous enhancers of decapping are localized to P-bodies including LSm1-7, EDC3, EDC4, and DDX6 (also known as RCK/p54) [27, 28, 30]. Altogether, these P-body components provide multiple mechanisms to destabilize and degrade RISC-associated mRNAs.

1.2 *Virus-Encoded MicroRNAs*

As miRNAs are non-immunogenic, require only ~80nt of coding capacity, and advantageous point mutants can be rapidly selected for, they are an ideal strategy for viruses to simultaneously regulate the expression of multiple genes. So far over 200 pre-miRNAs have been identified in differing families of DNA viruses including adenoviruses, ascoviruses, herpesviruses, and polyomaviruses [31-33]. Virally-encoded pre-miRNAs are crucial regulators of the cell cycle, apoptosis, innate immunity, viral latency [34], and in the case of adenovirus VA RNAs, used to inhibit cellular miRNA biogenesis by direct competition for Exportin 5 and Dicer [35, 36].

When the work described in this dissertation began, no RNA viruses were known to encode miRNAs. While successful in discovering miRNAs from many DNA viruses, small-RNA cloning techniques were unable to identify any miRNAs encoded by the human T cell lymphophtropic virus 1 (HTLV-1), influenza A, Yellow Fever, Dengue, West Nile, Polio, vesicular stomatitis virus (VSV) and hepatitis C virus (HCV) in human cells [37-40].

Several pieces of evidence suggest that HIV-1 may encode miRNAs. The trans-activation response (TAR) element of the HIV genome has been found to associate with the miRNA-processing enzyme Dicer *in vitro* [41, 42], though the TAR RNA used in these studies was artificially transcribed and, unlike TAR RNA *in vivo*, lacked a 5′ cap.

A known cofactor of Dicer, TRBP, is known to bind to the TAR element in HIV transcripts [43] and could potentially mediate Dicer recruitment to TAR. However, it has not been demonstrated that interactions between Dicer and HIV-1 transcripts give rise to functional miRNAs in the context of an infected cell. Computational prediction of secondary structure along the HIV-1 genome revealed several short-hairpins that could potentially give rise to mature miRNAs [44-46] while Northern blotting revealed the presence of several HIV-1 RNAs, including sequences derived from the TAR element and *nef* gene, that are 20-25 nucleotides in length, the functional size of miRNAs [45, 47, 48]. Overexpression of these sequences from Pol III promoters resulted in an inhibition of viral and cellular gene products, leading to the conclusion that HIV-1 expresses miRNAs [41, 49-51]. However, the inhibitory effects of these shRNAs must be interpreted cautiously as plasmid-based overexpression gives no insight into the regulatory potential of small RNAs at physiological levels and the small stretches of viral sequences that were cloned may have a different structure in the full-length viral genome.

Whether HIV-1 encodes miRNAs remains controversial. The aforementioned small RNA cloning strategies used to identify miRNAs from several viruses failed to identify any of the reported or novel miRNAs encoded by HIV-1 or HTLV-1 [37, 38]. Early high-throughput sequencing studies have generated differing interpretations

about the existence of HIV-1 miRNAs. Aside from lacking significant levels of expression, the miRNA-encoding regions of HIV identified in these studies gave rise to completely heterogeneous 5′ ends [52-54] indicating that these sequences are likely degradation products.

As miRNA biogenesis most often begins with nucleolytic processing, nuclease-sensitive stem-loops existing in a genomic template would likely prove detrimental to viral replication. However, introducing miRNA stem-loops into tick-borne encephalitis virus, influenza A, Sindbis, and VSV has shown that these viruses can efficiently encode miRNAs while remaining replication-competent [55-58]. As the replication cycle of most RNA viruses is relatively short (<24 hours) [59], most stages of the viral lifecycle would be complete before a virally-encoded miRNA is expressed at levels required to downregulate expression of a particular gene. Even with complete translational inhibition, existing proteins may need to be degraded before a phenotype could be observed. Thus, an RNA virus is unlikely to receive a selective advantage by encoding miRNAs in rapid, acute infections. The first known example of a virus with an RNA genome that naturally encodes miRNAs is the retrovirus bovine leukemia virus (BLV) which directly transcribes 5 pre-miRNAs from Pol III promoters in latently-infected cells, bypassing the conundrum of cleaving genomic transcripts to promote replication [19, 60].

1.3 *MicroRNA Regulation of Retroviral Replication*

Retroviruses are small viruses with single-stranded, positive-sense RNA genomes. Each virion contains two copies of the genome that are both capped and polyadenylated and serve as the template for reverse transcription. Upon transcription of the integrated proviral genome, both the viral mRNA and genomic RNA can potentially serve as targets for miRNAs [59]. The RNA interference pathway is indeed able to suppress the mobilization of endogenous retroviruses in plants, yeast, worms, and flies [61].

In mammalian cells, miR-32 has been reported to limit the replication of the retrovirus primate foamy virus (PFV) type 1 by binding to a sequence in the *bet* gene [62] while several studies have shown correlations between host miRNA profiles and susceptibility to HIV-1 infection [63-68]. Numerous microRNAs are computationally predicted to target the HIV-1 genome [66, 67, 69-74]; however, such predictions must be interpreted cautiously as they frequently overestimate the number of binding sites searching for only a small degree of complementarity. Indeed, a recent report predicted >2000 potential miRNA binding sites in the genome of the laboratory HIV-1 strain NL4-3 [72]. Moreover, many potential target sites, that do show full seed complementarity, are not functional and this is often due to the fact that these sites are occluded by mRNA secondary structure [75]. HIV-1 has also been reported to perturb the expression of

several cellular miRNAs upon infection [66, 69, 72, 76-79], including downregulation of the miR-17/92 cluster which targets the p300/CBP-associated factor (PCAF) histone acetyltransferase, a proposed cofactor for the HIV-1 Tat protein [77]. Expression of specific miRNAs has even been correlated with an elite suppressor status, or a status indicating that an individual is chronically infected with HIV but is able to suppress viral loads below transmissible levels without anti-retroviral therapy [65]. A recent study suggests that Vpr targets Dicer for proteasomal degradation [80] to enhance replication in macrophages. It has also been reported that retroviral transcriptional activators such as HIV-1 Tat and PFV Tas have suppressor of RNA silencing (SRS) activity to facilitate replication [45], but these results could not be reproduced in later studies [38, 81]. SRS activity has also been attributed to the HIV-1 Nef protein but this activity was not demonstrated in the context of infection [82].

MicroRNA mimics with perfect complementarity to the HIV-1 genome can indeed inhibit the short term replication of the virus in culture [83-101]. However, the ability of HIV-1 to mutate and adapt resistance to small molecule inhibitors of replication is well known and similar adaption has been continually observed with efforts to target the virus with RNA interference [102-108]. The most direct approach for a retrovirus to escape targeting by a miRNA is to mutate or delete the sequences in the genome that are complementary to the miRNA [102]. Only a small number of mutations are required to disrupt miRNA targeting as the primary determinate for binding is

complementarity between 6-7 nucleotides of the miRNA. Previous studies targeting viral RNAs by overexpressing shRNAs demonstrate that the virus can also adapt secondary structures that make targeted sequences inaccessible [104, 105], providing an alternate escape mechanism if direct mutagenesis of the targeted region is deleterious to replication. Because of the relative ease and demonstrated ability of retroviruses to avoid miRNA recognition, retroviruses are likely to have evolved resistance to targeting by miRNAs expressed in their natural tissue tropisms. Though miR-32 can limit the replication of PFV-1 in kidney cell culture lines [62], it is unknown if this restriction exists in relevant tissues *in vivo*. Reduction in the levels of Ago1 and Ago2 proteins in a fibrosarcoma cell line showed no effect on PFV replication [109], indicating that miRNAs capable of inhibiting the replication of a particular virus may not exist in all cell types.

Understanding how HIV-1 and other retroviruses interact with the cellular miRNA machinery has the potential to illuminate novel aspects of viral lifecycles, provide insight into mechanisms controlling viral gene expression, and discover new therapeutic avenues. Indeed, antisense locked nucleic acids that sequester miR-122, whose binding to the 5′ UTR of the HCV genomic RNA is critical for viral replication, provides long-term suppression of viremia in animals [110].

2. Identification of novel, highly expressed retroviral microRNAs in cells infected by bovine foamy virus

2.1 *Summary*

While numerous viral microRNAs (miRNAs) expressed by DNA viruses, especially herpesvirus family members, have been reported, there have been very few reports of miRNAs derived from RNA viruses. Here, we describe three miRNAs expressed by bovine foamy virus (BFV), a member of the spumavirus family of retroviruses, in both BFV-infected cultured cells and BFV-infected cattle. All three viral miRNAs are initially expressed in the form of an ~122-nt long pri-miRNA, encoded within the BFV long terminal repeat "U3" region, that is subsequently cleaved to generate two pre-miRNA that are then processed to yield three distinct, biologically active miRNAs. The BFV pri-miRNA is transcribed by RNA polymerase III and the three resultant mature miRNAs were found to contribute a remarkable ~70% of all miRNAs expressed in BFV-infected cells. These data document the second example of a retrovirus that is able to express viral miRNAs using embedded proviral polymerase III promoters.

2.2 *Introduction*

While cells express numerous miRNA species, several DNA viruses also express miRNAs that have been shown to play a role in immune evasion and can also regulate viral gene expression [32, 111]. In particular, herpesviruses generally express multiple viral miRNAs, especially in chronically infected cells, and polyoma- and adenoviruses

have also been shown to encode functional miRNAs. In contrast, analysis of numerous RNA viruses has so far failed to identify any viral miRNAs [40] with the exception of two retroviruses, i.e., bovine leukemia virus (BLV), which encodes five viral miRNAs [19, 60] and an avian leucosis virus, termed ALV-J, which was recently shown to express a single viral miRNA in infected cells [112]. One reason why RNA viruses might have only rarely evolved the ability to express miRNAs as a way of downregulating the expression of host genes with antiviral potential is that the excision of a pre-miRNA from a pri-miRNA precursor, in the case of RNA viruses likely the viral genomic RNA, would result in the cleavage of that pri-miRNA by Drosha. This has the potential to result in a reduction in viral replication that would potentially exceed any enhancement caused by the viral miRNA, and this problem would become more extreme if several viral pre-miRNAs were excised from a single viral genome. Indeed, the ability of inserted pri-miRNA stem-loops to reduce viral titers in *cis* has been well documented in the case of retroviral vectors, although this reduction can be largely alleviated by knockdown of Drosha in the producer cells [113, 114].

As noted above, the retrovirus BLV does encode several viral miRNAs. However, in this case each viral miRNA is initially transcribed by RNA polymerase III (Pol III) as a pre-miRNA that is directly exported to the cytoplasm for Dicer cleavage [19, 60]. Importantly, while pre-miRNAs generally contain stems of ~22bp, pri-miRNA stems are ~33bp in length and Drosha cleavage is dependent on this longer stem length [16,

17]. Therefore, BLV is able to express viral miRNAs yet the BLV genomic RNA is not subject to cleavage by Drosha. In contrast, the single miRNA expressed by ALV-J has been reported to be excised by the canonical miRNA processing machinery [112], resulting in Drosha cleavage of some portion of the ALV-J genomic RNA and/or subgenomic envelope mRNA. Whether this results in a drop in the production of the ALV-J viral structural proteins is, however, currently unknown.

2.3 *Materials and methods*

2.3.1 Molecular clones

The complete BFV pri-miRNA sequence was amplified from DNA generated by random hexamer-primed reverse transcription of chronically BFV-infected total cellular RNA using the forward primer 5′-GCCTAAGCTTGGGGTTCGGAGGATGGCTCA-3′ and reverse primer 5′-ATCTGAATTCTCTAGTTATACATCTAAAAA-3′ and cloned into the HindIII and EcoRI sites of pGEM3Z. An EBV-BART-5 miRNA expression vector has been previously described [115]. Luciferase-based reporter vectors were constructed by annealing target site oligonucleotides and ligating them into the XhoI and NotI sites in the 3′UTR of the Renilla luciferase (Rluc) gene of psiCHECK2. The target sequences are complementary to miR-BF1-5p (5′ TTCGGAGGATGGCTCATCAAGC 3′), miR-BF1-3p (5′-TCCCTGAAGCCATATCCGAGGC-3′), miR-BF2-5p (5′-TCAGTAGAAAGACAGTACCTCGCC-3′), or miR-BF2-3p (5′-CAGGCGGTATGCTTTCTACTTTTT-3′).

2.3.2 Cell culture and virus propagation

The BFV Riems isolate was initially propagated by co-cultivation of infected and uninfected calf trachea cells [116]. Subsequently, BFV was adapted to grow by co-cultivation with Madin-Darby bovine kidney (MDBK) cells maintained in Dulbecco's modified Eagle's medium (DMEM; Sigma) supplemented with 10% fetal horse serum (Sigma). MDBK-derived BFV was subsequently serially passaged by co-cultivation of BFV-infected and non-infected MDBK cells, corresponding samples are designated chronically BFV-infected. In parallel, BFV, which is normally highly cell associated, was adapted to cell-free transmission using MDBK cells by serial passage using the culture supernatant, rather than cell co-cultivation. After ten cell-free serial passages, BFV titers were ~10^3 infectious particles/mL and this stock was used in this study to infect 10^6 MDBK cells (acute infection) at a multiplicity of infection of ~0.01. BFV titers were determined using an MDBK-based indicator cell line, containing the BFV long terminal repeat (LTR) promoter linked to an indicator gene, as previously described for primate foamy virus [117]. The BFV LTR is activated by the BFV Tas transactivator upon infection, thus allowing BFV titer to be readily determined. 293 and baby hamster kidney (BHK) cells were cultured in DMEM supplemented with 10% fetal bovine serum.

2.3.3 Peripheral blood leukocyte (PBL)-derived RNA from experimentally BFV-infected calves

Five male calves of the Holstein-Friesian breed (6 weeks old) that tested sero-negative for BFV, BLV and bovine viral diarrhea virus were used in this study. Animals

were adapted to the housing and feeding conditions in the animal facilities of the National Veterinary Research Institute in Pulawy (Poland) before the start of the study. The study was approved by the local ethical commission and was performed in accordance with national regulations for animal experimentation.

Three animals were experimentally infected with the Polish BFV100 isolate [118], which is highly related to, but distinct from, the German BFV Riems isolate [116], by intravenous inoculation of $5x10^6$ Cf2Th cells infected with BFV100. Two calves were inoculated with the same amount of uninfected Cf2Th cells and served as negative controls, as described previously [119]. Throughout the experiment, the control calves were kept isolated from the BFV-infected animals. Successful BFV infection was confirmed in the three infected calves by detection of BFV integrase gene DNA using nested PCR [120] and of BFV Gag specific antibodies by ELISA [119]. Both control calves were negative in both assays, as expected. Six months after BFV infection, blood was collected from the jugular vein into tubes containing anticoagulant (EDTA-Na), hemolyzed with ice cold H_2O and 4% NaCl and centrifuged. The PBLs were washed twice with PBS, divided into aliquots of $5x10^6$ cells, suspended in 0.75 mL of TRIzol (Invitrogen) and frozen at -70°C until RNA extraction. Extracted total RNA (10ng) was then used for RT-PCR analysis, as described below.

2.3.4 Deep sequencing of total small RNA

Total RNA was isolated from BFV-infected MDBK cells using TRIzol. The RNA fraction containing ~15-40nt RNAs was isolated by polyacrylamide gel electrophoresis on 15% Tris-borate-EDTA (TBE)-urea gels (Bio-Rad), electroeluted from the excised gel slice with the Gel Eluter (Hoefer), and processed using the TruSeq Small RNA Sample Preparation Kit (Illumina). Adapter-ligated small RNAs were reverse transcribed using SuperScript III (Life Technologies), amplified using GoTaq green PCR master mix (Promega) with the TruSeq 3′ indices, and sequenced on an Illumina HiSeq 2000. Initial reads were quality filtered with cassava 1.8.2.

RNA species <200nt in length were isolated from chronically BFV-infected MDBK cells using the mirVana miRNA Isolation Kit (Ambion). To prepare the RNA for deep sequencing, the size-fractionated total RNA sample was first treated with calf intestinal phosphatase (CIP; New England Biolabs) in NEB Buffer #3 at 37°C for one hour and precipitated using ethanol and sodium acetate [39]. This treatment was designed to remove any 5′ triphosphates from the RNA. The RNA was then re-phosphorylated with T4 polynucleotide kinase (T4 PNK; New England Biolabs) at 37°C for one hour. RNA >25nt was collected using CENTRI-SPIN 40 columns (Princeton Separations) and sequenced with the TruSeq Small RNA Sample Preparation Kit as described above.

For the 50bp single-end reads, adapter sequences were clipped and reads >15nt in length were quality filtered using the FASTX-toolkit v0.0.13 (http://hannonlab.cshl.edu/fastx_toolkit/index.html). Read mates of >15nt from the 50bp paired-end sequencing were clipped and quality filtered using Trimmomatic v0.30 [121]. Bowtie v.0.12.7 [122] was used to sequentially filter and assign reads to adapter sequences, the viral genome (Accession No. JX307862.1), miRbase v.20 bovine miRNA hairpins [123], and Ensembl annotations of the UMD3.1 bovine non-coding RNAs and genome [124]. While one mismatch was allowed for alignments to the viral and bovine RNA libraries, two mismatches were allowed when aligning to bovine genomic DNA.

2.3.5 Northern blotting

Northern blotting was performed as previously described [18]. Briefly, 25μg of total RNA was fractionated on a 15% TBE-urea gel (Bio-Rad) and transferred to GeneScreen Plus Hybridization Transfer Membrane (PerkinElmer) and UV-crosslinked (Stratalinker, Stratagene). Membranes were pre-hybridized in ExpressHyb (Clontech) and then incubated at 37°C with ^{32}P-end labeled oligonucleotide probes complementary to miR-BF1-5p (5'-GCTTGATGAGCCATCCTCCGAA-3'), miR-BF1-3p (5'-GCCTCGGATATGGCTTCAGGGA-3), miR-BF2-5p (5'-GGCGAGGTACTGTCTTTCTACTGA-3'), and miR-BF2-3p (5'-AGAAAGCATACCGCCTGACC-3'). Membranes were washed with a buffer containing 2x SSC and 0.1% SDS at 37°C then visualized by autoradiography.

2.3.6 Quantitative reverse transcription PCR

Custom TaqMan small RNA reverse transcription primers and PCR probes were ordered through Invitrogen. The target sequences were 5'-UUCGGAGGAUGGCUCAUCAAGC-3'for miR-BF1-5p and 5'-UCAGUAGAAAGACAGUACCUCGCC-3' for miR-BF2-5p. 10ng of total RNA were reverse transcribed on a Programmable Thermal Controller (MJ Research) and amplified according to manufacturer's protocol using a StepOnePlus Real-Time PCR System (Applied Biosystems). Relative miRNA abundance in bovine cells was determined using the ΔΔCt method [125] with cellular U6 snRNA (assay ID 001973) as the reference.

To determine if BFV miRNA expression is Pol III dependent, 10^5 293 cells were plated in 24-well plates and treated with 50μg/mL of α-amanitin (Sigma) the next day as previously described [18]. Briefly, 250ng of each miRNA expression vector was transfected via calcium phosphate, with addition of α-amanitin or carrier 2 h post-transfection. At 24 h post-transfection, cells were harvested with TRIzol (Ambion) and total RNA treated with RQ1 DNase (Promega) then assayed as above for miR-BF2-5p and EBV-BART-5-5p (assay ID 197237_mat) with RNU48 (assay ID 001006) as the reference. The mock sample was transfected with the parental expression vectors, lacking any miRNA sequence, and treated with carrier (water).

2.3.7 Luciferase indicator assays

A total of 50ng of each reporter plasmid was co-transfected with 500ng of a pGEM3Z-based BFV-miRNA expression vector using polyethylenimine (PEI), into 24-well plates containing 10^5 BHK cells per well, plated the previous day. At 24 h post-transfection, lysates were harvested and luciferase activity measured using the Dual-Luciferase Reporter Assay System (Promega) on a TD-20/20 Luminometer (Turner Designs). The ratio between the RLuc and internal control firefly luciferase (FLuc) proteins was determined for each sample and normalized to the ratio of the parental psiCHECK2 vector.

2.4 *Results*

2.4.1 Identification of three novel BFV microRNAs

To identify potential BFV-encoded miRNAs, we performed deep sequencing of small RNAs present in newly BFV-infected MDBK cells as well as MDBK cells chronically infected with BFV. The chronically BFV-infected MDBK cells were derived by long-term co-cultivation of BFV-infected and uninfected MDBK cells and are predicted to be essentially uniformly infected. In contrast, the acutely infected MDBK cells were generated by infection of MDBK cells at ~0.01 infectious units of BFV per cell followed by cultivation for 72 h prior to RNA harvest. Therefore, only a small percentage, perhaps 1-5% of the MDBK cells, was likely to be infected at this time point. As shown in Fig. 2-1A, we detected three different small RNAs of BFV origin in acutely

BFV-infected MDBK cells, one of which was recovered in two different isoforms differing by 1nt at their 5′ end. These same BFV-derived small RNAs were also recovered from chronically BFV-infected cells but, as expected, at far higher levels. The most highly expressed BFV small RNA, miR-BF2-5p, was found to contribute ~52% of all small RNA reads in these chronically BFV-infected cells, while a second BFV-derived small RNA, miR-BF1-5p, contributed a further 19% of all small RNA reads (Fig. 2-1B). In contrast, the most highly expressed cellular miRNA, miR-21, only comprised ~4% of all recovered small RNA reads. A third BFV-derived small RNA, miR-BF1-3p, contributed ~1% of all recovered small RNA reads in the chronically infected cells (Fig. 2-1B) and no other small RNAs of BFV origin contributed significant numbers of sequence reads in either chronically or acutely infected cells (Fig. 2-1A).

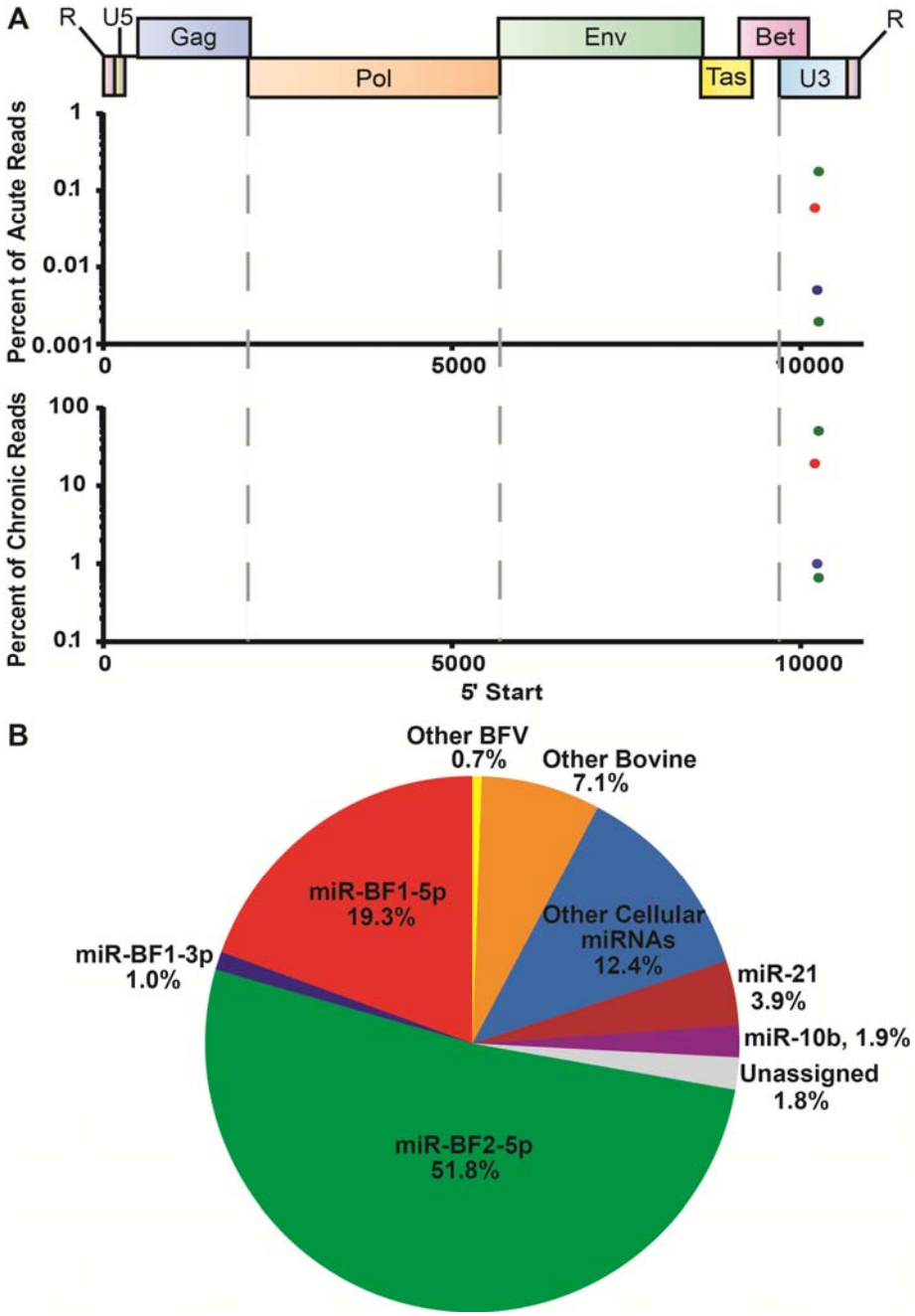

Figure 2-1: Alignment of small RNA reads to the BFV genome. (A) RNA reads that mapped to the viral genome are shown relative to their genomic origin (x axis). The number of reads is plotted as a percentage of the total number of small RNA deep-sequencing reads (y axis) from MDBK cells at 72 h post-infection (top) or from chronically infected MDBK cells (bottom). (B) Assignment of deep-sequencing reads in chronically BFV-infected MDBK cells.

Key characteristics of authentic viral miRNAs include 1) that they derive from a small number of discrete locations in the viral genome, 2) that they are close to the canonical miRNA size, which ranges from ~20nt to ~25nt and 3) that they have a discrete 5′ end that results in a specific miRNA seed sequence [31]. As shown in Fig. 2-1A, the BFV reads we obtained are indeed derived from one specific location in the BFV genome, located in the long terminal repeat (LTR) "U3" region slightly 3′ to the end of the BFV *bet* gene. In the integrated BFV provirus, they would therefore be predicted to be present in two copies. Moreover, as shown in Fig. 2-2, the BFV reads we obtained all cluster at or near the predicted miRNA size of ~22nt.

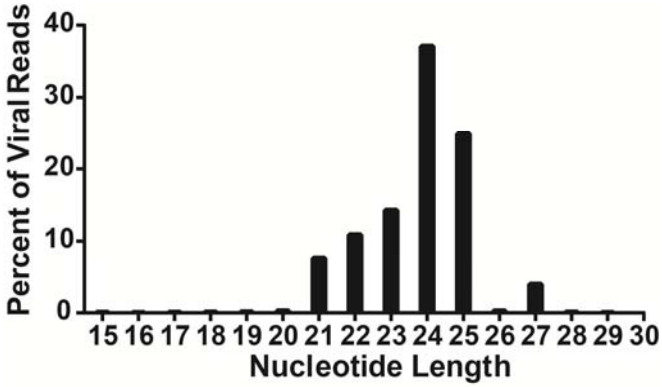

Figure 2-2: Small RNAs expressed by BFV cluster at the size expected for miRNAs. Reads from chronically BFV-infected MDBK cells mapping to the BFV genome for a given nucleotide length (x axis) are graphed as percentages of total reads aligning to the BFV genome (y axis).

Finally, in Table 2-1, we provide a breakdown of the sequence reads derived from miR-BF1-5p, miR-BF1-3p and miR-BF2-5p that contribute >2% of the reads obtained for that miRNA. As may be observed, essentially all the BFV reads obtained for each of these three viral miRNA species start with the same 5′ nucleotide. (A small

percentage, <1%, of the miR-BF2-5p reads had a 5′ end displaced by one nucleotide from the more common 5′ start site. This sub-population explains the additional miR-BF2-5p species shown in Fig. 2-1A). Therefore, these BFV-derived small RNA reads conform to the characteristics expected for authentic viral miRNAs. The miRNA sequence variation that was observed was almost entirely at the 3′ end, which plays a less important role than the seed sequence found near the miRNA 5′ end in promoting mRNA target recognition [1]. In addition, we also saw some evidence for the addition of non-templated bases at the viral miRNA 3′ ends, as has also been reported previously for some cellular miRNAs [126].

Mapping of the obtained reads onto the BFV genome shows that these small RNAs are closely adjacent to each other (Fig. 2-1A). In fact, miR-BF1-5p and miR-BF1-3p are separated by only 12nt and show extensive complementarity, so that they are predicted to fold into an RNA stem-loop structure (Fig. 2-3A). Moreover, miR-BF2-5p begins immediately after miR-BF1-3p ends and also has the potential to form a stem-loop structure (Fig. 2-3A). Further analysis of our deep sequencing data indeed revealed a small number of reads that could represent the passenger strand for miR-BF2-5p, though this putative miR-BF2-3p RNA was present at a level ~10^5 times lower than the highly expressed miR-BF2-5p (Table 2-1). Curiously, many of the reads obtained for miR-BF2-3p contained a non-templated “C” residue at the 5′ end. This “C” is not present

in any of the reported BFV sequences [116] and was not observed by sequencing of PCR products obtained from this region in infected MDBK cells, so its origin is unclear.

The ability of the small RNA reads of BFV origin to fold into two adjacent RNA stem-loop structures suggested that these might be initially transcribed as a single structured RNA, containing two stem-loops (Fig. 2-3A). To address this possibility, we performed 50bp pair-end deep sequencing of RNAs <200nt but >30nt in length from chronically BFV-infected MDBK cells. As shown in Fig. 2-3B, we observed two major 5′ start sites, one coincident with the 5′ end of miR-BF1-5p and one located 4nt 5′ to miR-BF1-5p. We also detected a third 5′ end coincident with the 5′ end of miR-BF2-5p. At the 3′ end, we detected a major termination site after the third "U" of a run of 5 U residues and a minor termination site in a second "U" rich sequence (5′-UUUCU-3′) located immediately 5′ to these 5 U residues (Fig. 2-3C). Runs of U residues, generally five or more, serve as a terminator for Pol III and a run of three Us at the end of a small RNA is characteristic of Pol III transcripts [127].

Table 2-1: Summary of BFV small RNAs recovered from chronically BFV-infected MDBK cells. RNA species that contribute >2% of the total reads for a given BFV miRNA are shown, with their position relative to the reference BFV strain (JX307862.1) indicated by genome coordinates. Non-templated nucleotides are indicated in bold.

miRNA	Sequence	Length (nt)	Start	End	Reads	%
miR-BF1-5p	TTCGGAGGATGGCTCATCAAGC	22	11,190	11,211	878,086	32
	TTCGGAGGATGGCTCATCAAGCT	23	11,190	11,212	836,116	30
	TTCGGAGGATGGCTCATCAAG	21	11,190	11,210	659,169	24
	TTCGGAGGATGGCTCATCAAGC**C**	23	11,190	11,212	127,154	5
miR-BF1-3p	TCCCTGAAGCCATATCCGAGGC	22	11,224	11,245	86,127	58
	TCCCTGAAGCCATATCCGAGG	21	11,224	11,244	28,224	19
	TCCCTGAAGCCATATCCGAGG**T**	22	11,224	11,245	6,142	4
	TCCCTGAAGCCATATCCGAGGCT	23	11,224	11,246	3,400	2
	TCCCTGAAGCCATATCCGAGGC**A**	23	11,224	11,246	3,185	2
miR-BF2-5p	TCAGTAGAAAGACAGTACCTCGCC	24	11,246	11,269	3,514,215	47
	TCAGTAGAAAGACAGTACCTCGCCT	25	11,246	11,270	2,052,969	28
	TCAGTAGAAAGACAGTACCTCGCC**C**	25	11,246	11,270	384,581	5
	TCAGTAGAAAGACAGTACCTCGC	23	11,246	11,268	369,154	5
	TCAGTAGAAAGACAGTACCTCGCCTGT	27	11,246	11,272	301,059	4
miR-BF2-3p	**C**CAGGCGGTATGCTTTCTACT	21	11,285	11,305	35	58
	CCAGGCGGTATGCTTTCTACTT	22	11,285	11,306	11	18
	TCAGGCGGTATGCTTTCTACT	21	11,285	11,305	3	5
	CCAGGCGGTATGCTTTCTAC	20	11,285	11,304	2	3
	CCAGGCGGTATGCTTTCTACTTTT	24	11,285	11,308	2	3

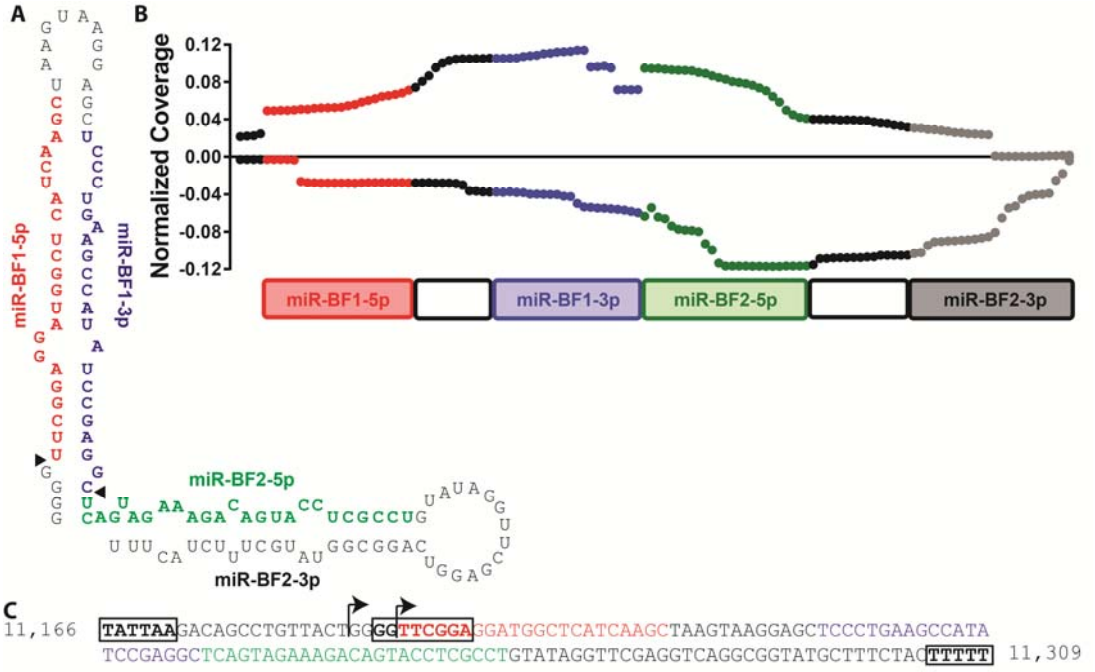

Figure 2-3: Origin of BFV miRNAs. (A) Predicted sequence and RNA secondary structure of the BFV pri-miRNA. Black triangles indicate the sites of cleavage during BFV pri-miRNA processing to yield the two viral pre-miRNAs. (B) Paired-end deep sequencing of BFV sequences of ≥30nt. The y axis shows the number of reads containing a given nucleotide divided by the total number of viral reads in the library. Values obtained with the forward sequencing primer are plotted on the positive y axis, with values obtained with the reverse primer plotted on the negative y axis. (C) Proviral DNA sequence with potential Pol III transcription factor binding sites and termination sequences boxed. Numbers represent the nucleotide locations within the reference BFV strain.

Interestingly, we observed that reads starting with the run of 4 "G" residues located 5′ to miR-BF1-5p invariably terminated at one of these two U stretches, while reads initiating at the first nucleotide of miR-BF1-5p generally terminated at the end of miR-BF1-3p. Runs initiating at the first nucleotide of miR-BF2-5p also ended at the distal U stretch. Based on this analysis, it appears that all three BFV small RNAs are initially transcribed as a single RNA, that normally ends at the stretch of U residues at ~11,309 in

the BFV genome and that folds into a structured pri-miRNA with two simple stem-loops, as shown in Fig. 2-3A. Because many full-length reads contain a 4nt 5′ extension of 5 GGGG-3′ (Fig. 2-3), while reads beginning at the first nucleotide of miR-BF1-5p generally end at the last nucleotide of miR-BF1-3p, we favor the hypothesis that the BFV pri-miRNA is initially transcribed by Pol III starting at the first "G" residue, at position 11,186, and is then processed by simultaneous cleavage after the 4nt G run, at position 11,190, and between miR-BF1-3p and miR-BF2-5p, at position 11,245, to yield two canonical pre-miRNAs that are then exported to the cytoplasm and cleaved by Dicer to liberate the observed BFV miRNA species.

If this hypothesis is correct, then Northern analysis of RNA derived from chronically BFV-infected MDBK cells should yield a single pri-miRNA of ~122nt, recognized by probes specific for all four mature BFV miRNAs, and two pre-miRNAs of 56nt and 62nt in length, recognized by both miR-BF1 and both miR-BF2-derived miRNA probes, respectively. Indeed, as shown in Fig. 2-4, that is exactly what is observed. In particular, all four probes, including one specific for the miR-BF2-3p miRNA that is not recovered at significant levels as a mature miRNA (Table 2-1), recognize a single ~120nt pri-RNA. Moreover, the two miR-BF1 and two miR-BF2 miRNA pairs each recognize one of two distinct pre-miRNAs with the latter, as expected, migrating slightly more slowly than the former. Finally, only three distinct mature miRNAs are recognized, although both miR-BF1-5p and, especially, miR-BF2-5p appear to migrate as dimers, as

expected based on the sequencing data (Table 2-1). Moreover, miR-BF2-5p appears slightly larger than miR-BF1-5p or miR-BF1-3p, again as predicted by our sequencing data (Table 2-1).

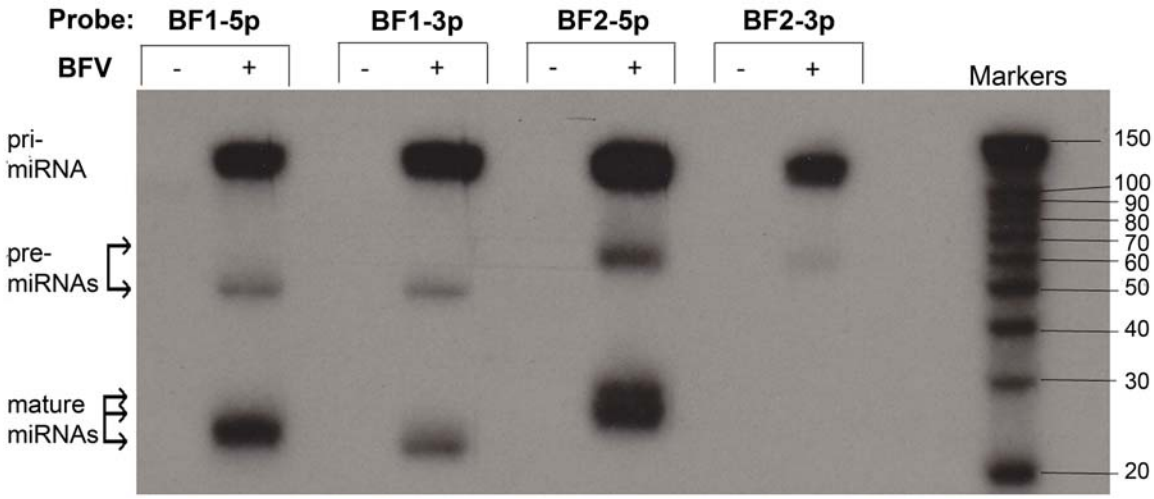

Figure 2-4: Northern blot analysis of RNAs from uninfected (–) and chronically BFV-infected (+) MDBK cells. The antisense oligonucleotide probes used for the indicated lanes are shown at the top. The predicted migration locations of the BFV pri-miRNA, the two pre-miRNAs, and the mature miRNAs are indicated.

2.4.2 BFV-derived microRNAs are transcribed by RNA polymerase III

As noted above, the major putative BFV pri-miRNA species ends within a run of U residues, and is only ~122nt in length (Fig. 2-3A), and is therefore predicted to be transcribed by cellular Pol III. Indeed, analysis of the BFV DNA sequence reveals the existence of a possible "TATA" box located upstream of the pri-miRNA transcription start site, and a possible "box B" sequence (consensus 5′-GGTTCGANNCC-3′) that is closely adjacent to the pri-miRNA transcription start site (Fig. 2-3C). Canonical Pol III promoters often contain "TATA" boxes and/or box B sequences [128]. However, we

have not been able to identify a version of the "box A" sequence that is also found in many Pol III promoters.

To test whether the BFV miRNAs are indeed transcribed by RNA Pol III, we transfected 293 cells with a construct containing the entire BFV pri-miRNA sequence shown in Fig. 2-3C cloned into pGEM3Z, which does not contain any known eukaryotic Pol II or Pol III promoters. As a control, we also transfected 293 cells with an expression vector encoding the Epstein-Barr virus (EBV) miRNA miR-BART5, which is known to require transcription by Pol II [129]. We then treated the transfected cells with α-amanitin, which is a specific inhibitor of Pol II-dependent transcription [18, 19]. At 24 h post-transcription, the cells were lysed, total RNA isolated, and expression of miR-BF2-5p and miR-BART5 measured by quantitative RT-PCR. Both viral miRNAs were readily detected in the untreated 293 cells (Fig. 2-5). However, in the α-amanitin treated cells, miR-BART5 expression was almost entirely lost. In contrast, expression of miR-BF2-5p was still detected at levels comparable to those seen in the control cells. Therefore, these data confirm that the BFV miRNAs are indeed transcribed by cellular Pol III.

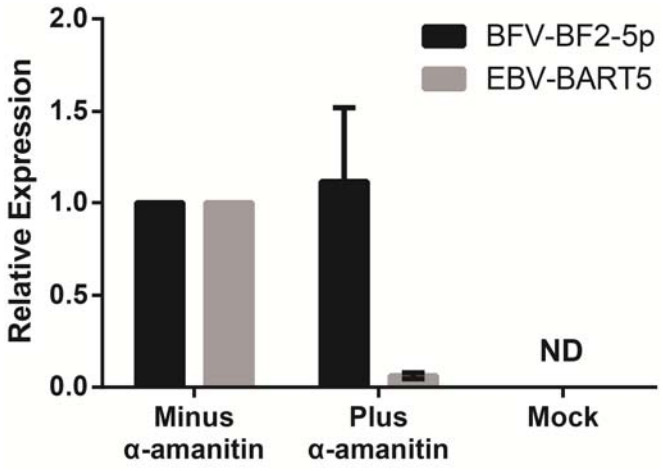

Figure 2-5: BFV miRNAs are transcribed by Pol III. Relative expression is shown for BFV miR-BF2-5p and EBV miR-BART5-5p in 293 cells transfected with the cognate miRNA expression vectors in the presence and absence of the Pol II inhibitor *α*-amanitin. Expression levels were determined by the ΔΔCT method (26), using RNU48 as the internal reference, with the carrier-treated cell value set at 1.0. "Mock" refers to 293 cells transfected with the parental vector lacking any miRNA sequence and treated with carrier. Averages for three independent experiments, with standard errors of the means, are shown. ND, no detectable amplification.

2.4.3 The BFV microRNAs are functional

While the BFV-derived small RNAs described above show all the characteristics of authentic miRNAs, we have not yet demonstrated that they are in fact able to repress the expression of an mRNA bearing complementary mRNA targets. To demonstrate that this is indeed the case, we utilized an indicator vector, psiCHECK2, which contains two independent luciferase genes, firefly luciferase (Fluc) and Renilla luciferase (Rluc), under the control of two different promoters. We inserted a single artificial target sequence that is fully complementary to miR-BF1-5p, miR-BF1-3p, miR-BF2-5p or miR-BF2-3p into the 3'UTR of RLuc. We then co-transfected BHK cells with the pGEM3Z-based BFV pri-miRNA expression vector described above, along with one of the four BFV-miRNA

indicator vectors, or with the parental psiCHECK2 vector. At 24 h post-infection, the cells were lysed and the levels of RLuc and the FLuc internal control determined. As shown in Fig. 2-6, we saw strong and specific downregulation of the RLuc gene present in the indicator plasmids specific for miR-BF1-5p, miR-BF1-3p and miR-BF2-5p when compared either to the psiCHECK2 negative control or the indicator specific for miR-BF2-3p, consistent with the very low expression of miR-BF2-3p as determined by deep sequencing (Table 2-1) or Northern blot (Fig. 2-4).

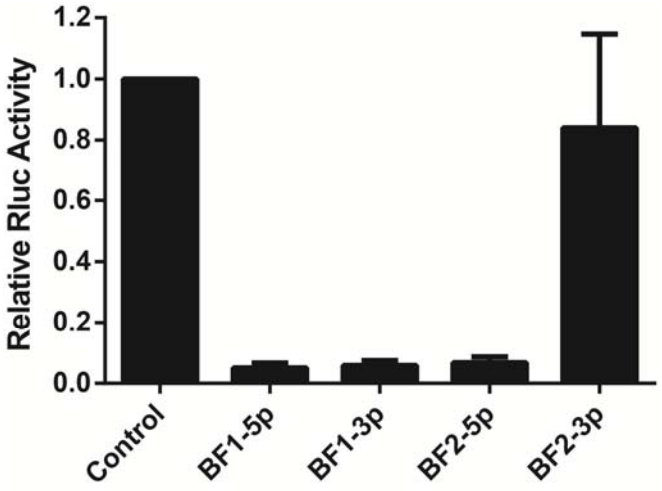

Figure 2-6: Functional analysis of BFV miRNAs. A single perfectly complementary target sequence for each BFV miRNA was inserted into the 3′ UTR of the RLuc indicator gene and co-transfected with a BFV pri-miRNA expression vector lacking any known exogenous Pol II or Pol III promoter. RLuc values are shown normalized to the FLuc internal control and to the level seen with the parental vector lacking an inserted miRNA binding site, which was set at 1.0. Averages for three independent experiments, with standard deviations, are indicated.

2.4.4 BFV microRNAs are expressed *in vivo*

Our data demonstrate that BFV expresses three functional miRNAs in newly or chronically infected MDBK cell cultures. To test whether these same BFV miRNAs are expressed in vivo, we used RT-PCR to test for the expression of miR-BF1-5p and miR-BF2-5p in peripheral blood leukocytes (PBLs) drawn from three BFV-infected calves 6 months after experimental infection with BFV, as previously described [119]. As controls, we used PBLs from two similar mock infected calves. Productive infection of the three BFV-infected calves, and lack of BFV-infection of the two negative control calves, was confirmed by nested PCR using primers specific for the BFV integrase gene [120], at one month and six months after experimental infection, and by detection of antibodies specific for the BFV Gag protein by ELISA exclusively in the three infected animals [119]. As shown in Table 2-2, we did not detect any BFV miRNA expression using RNA from uninfected animals but we did detect miR-BF1-5p and miR-BF2-5p expression in the BFV-infected calves at levels comparable to what was seen in newly BFV-infected MDBK cells, although we estimate that only ~1% of the cells in this latter culture were actually infected by BFV at the time of RNA harvest. Therefore, we conclude that these BFV miRNAs are indeed expressed in infected cells *in vivo*.

Table 2-2: BFV miRNAs are expressed *in vivo*. Relative expression of miR-BF1-5p and miR-BF2-5p in PBLs from three BFV-infected calves (A, B and C) and two uninfected calves (D and E) as well as uninfected, freshly infected and chronically infected MDBK cells. Expression was calculated by the $\Delta\Delta C_T$ qPCR method [125] using the endogenous U6 snRNA as the reference, with PBLs from calf A arbitrarily set to 1.0. ND refers to no detectable amplification.

		$\Delta\Delta C_T$ value	
Sample	**BFV**	**BF1-5p**	**BF2-5p**
Calf A PBLs	+	1.00	1.00
Calf B PBLs	+	1.21	1.05
Calf C PBLs	+	2.02	1.97
Calf D PBLs	-	0.014	ND
Calf E PBLs	-	0.003	ND
MDBK cells	-	0.001	ND
	Acute	2.68	10.7
	Chronic	3,880.00	10,390.00

2.5 *Discussion*

Spumaviruses, more commonly referred to as foamy viruses, are an ancient group of generally non-pathogenic retroviruses that infect many mammalian species, with the notable exception of humans [130, 131]. However, while no human foamy virus has been identified, there have been several reports documenting the zoonotic infection of individuals who came into contact with primates by a range of primate foamy virus (PFV) species [132, 133]. Moreover, several PFV species replicate efficiently in human cells in culture and retroviral vectors based on PFVs and other foamy viruses are under development for use in gene therapy or antigen delivery in humans and animals [134-136].

Among species that are susceptible to foamy viruses, infection is often common and BFV has been detected in a considerable fraction of domesticated cattle in several different countries [119, 120]. However, as is also the case for PFVs in either their natural hosts or in zoonotically infected humans, there is little evidence that BFV exerts a significant deleterious effect in infected cows [119, 130].

Previous work has demonstrated that BLV, a deltaretrovirus that can induce B-cell lymphomas in cattle, expresses high levels of five viral miRNAs in BLV-transformed cells and it has been proposed that these miRNAs can facilitate B-cell transformation [19, 60]. Interestingly, these viral miRNAs were shown to be transcribed by Pol III and it was predicted, based on computational analysis, that "a number of spumaviruses" might also encode Pol III-driven viral miRNAs [19]. To test this hypothesis, we have performed deep sequencing of small RNAs expressed in acutely or chronically BFV-infected cells and our results indeed demonstrate that BFV expresses high levels of three distinct, fully functional viral miRNAs both in culture and in vivo. However, in contrast to BLV, which expresses each of its five viral miRNAs in the form of separate ~60nt long pre-miRNA stem-loop structures [19, 60], BFV encodes a pri-miRNA of ~122nt that must be processed to remove a 4nt 5' extension, and also cleaved between the two viral pre-miRNA species, to generate two distinct BFV pre-miRNAs (Figs. 2-3A, 2-4). At present, we do not know which nuclease(s) is mediating this initial processing event. The finding, based on paired-end deep sequencing, that the BFV pri-miRNA precursor is

apparently cleaved simultaneously on both sides of the miR-BF1 stem-loop, to generate a pre-miRNA bearing a 2nt 3′ overhang, may implicate the Drosha/DGCR8 microprocessor complex in this processing event. We note, however, that cleavage of cellular pri-miRNA stem-loops requires both an ~33bp stem and flanking single-stranded RNA sequences [16, 17], neither of which is present in the BFV pri-miRNA (Fig. 2-3A), so it is also possible that a different nuclease(s) is involved.

A comparison of the sequence of the BFV miRNAs defined in Table 2-1 shows that they are all fully conserved across the four reported BFV sequences, including sequences obtained for Chinese, American and European BFV isolates [116]. Indeed, the entire 122nt BFV pri-miRNA sequence is fully conserved, with the exception of two nucleotides in the terminal loop of the miR-BF2 stem-loop that, based on previous work [129], are not predicted to affect miRNA processing or expression.

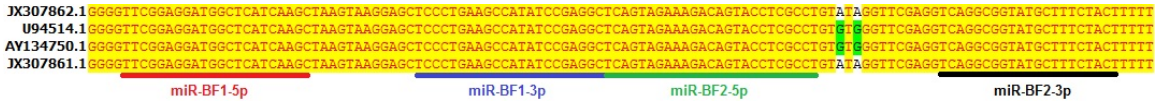

Figure 2-7: Conservation of the BFV pri-miRNA. Sequences of the BFV pri-miRNA shown in Fig. 2-3A from all annotated BFV strains are aligned with conserved nucleotides highlighted in yellow. The strain used in this study is listed first, with common variant nucleotides highlighted in green. The locations of mature miRNAs are indicated below the alignment.

Interestingly, comparison of the three highly expressed BFV miRNAs with known viral and cellular miRNAs revealed that the entire miR-BF1-5p seed sequence (nt 2-8) is conserved in miR-B5, which is expressed by bovine herpesvirus-1 (BHV-1) in

infected cells [137]. However, as the mRNA targets for miR-B5 are not currently known, this conservation is not currently informative as to miR-BF1-5p function.

An interesting aspect of the BFV miRNAs described in this report is that they all derive from a single locus in the U3 region of the BFV LTR, at a site located ~50nt 3′ to the end of the BFV *bet* gene (Fig. 2-1A). As such, they would be duplicated during reverse transcription so that the integrated BFV provirus would actually express these viral miRNAs from two independent locations. Perhaps more importantly, the Pol III transcription unit in the 5′ LTR would be located 5′ to both BFV Pol II transcription units, driven respectively by the LTR promoter and the internal promoter located immediately 5′ to the viral *tas* gene (Fig. 2-1A). Therefore, this Pol III transcription unit would not be subject to transcriptional interference caused by these two viral Pol II dependent promoters [138] and it is possible that the majority of BFV pri-miRNA transcription is actually derived from the Pol III transcription unit located in the 5′ LTR of BFV.

The observation that BLV, ALV-J and BFV encode one or more viral miRNAs [19, 60, 112], while HIV-1 and HTLV-I do not [37, 38], suggests either that miRNA expression has evolved independently in these three retroviral species or that HIV-1 and HTLV-I (the latter, like BLV, a deltaretrovirus) have lost the ability to express miRNAs. The former seems more likely, as BLV, ALV-J and BFV express viral miRNAs that are initially transcribed by different RNA polymerases (Pol III for BLV and BFV, Pol II for

ALV-J) and are subjected to different miRNA processing steps (Drosha-independent for BLV, Drosha-dependent for ALV-J). Regardless, it is now clearly of interest to examine whether other retroviral species, including other foamy viruses, encode miRNAs and whether, if they do, these exert any phenotypic effects in culture or *in vivo*. In this context, it is interesting to note that vectors based on PFV have been proposed as potential gene therapy vectors in humans [139, 140] and it would appear important to determine whether this PFV isolate encodes any viral miRNAs and, if so, whether these are retained in these viral vectors. If this is the case, then it would be important to delete these miRNAs or at least demonstrate that they do not exert any deleterious effects in transduced human cells. Similarly, while HIV-1 does not encode any miRNAs [37, 38], so that vectors based on this lentivirus do not face this concern, it would be important to examine any retrovirus, or indeed any virus, that has the potential for use as a gene therapy vector to confirm that these vectors do not encode any viral miRNAs.

3. In-depth analysis of the interaction of HIV-1 with cellular microRNA biogenesis and effector mechanisms

3.1 *Summary*

The question of how HIV-1interfaces with cellular microRNA (miRNA) biogenesis and effector mechanisms has been highly controversial. Here, we first used deep sequencing of small RNAs present in two different infected cell lines (TZM-bl and C8166) and two types of primary human cells (CD4+ PBMCs and macrophages) to unequivocally demonstrate that HIV-1 does not encode any viral miRNAs. Perhaps surprisingly, we also observed that infection of T cells by HIV-1 has only a modest effect on the expression of cellular miRNAs at early times after infection. Comprehensive analysis of miRNA binding to the HIV-1 genome using the photoactivatable ribonucleoside-induced crosslinking and immunoprecipitation (PAR-CLIP) technique revealed several binding sites for cellular miRNAs, a subset of which were shown to be capable of mediating miRNA-mediated repression of gene expression. However, the main finding from this analysis is that HIV-1 transcripts are largely refractory to miRNA binding, most probably due to extensive viral RNA secondary structure. Together, these data demonstrate that HIV-1 neither encodes viral miRNAs not strongly influences cellular miRNA expression, at least early after infection, and suggest that HIV-1 transcripts may have evolved to avoid inhibition by pre-existing cellular miRNAs by adopting extensive RNA secondary structures that occlude most potential miRNA binding sites.

3.2 *Introduction*

Analysis of the miRNA coding potential of HIV-1 has led to considerable controversy. HIV-1 was initially reported to lack any viral miRNAs by conventional sequencing of small RNAs in HIV-1-infected HeLa cells [37], and this report was supported by a subsequent report that failed to detect any HIV-1 miRNAs in chronically HIV-1-infected ACH-2 T cells, again using conventional sequencing [38]. In contrast, the first HIV-1 miRNA was reported in 2004, based on Northern analysis of RNA derived from HIV-1 infected cells using probes specific for the viral *nef* gene [47]. This viral miRNA was subsequently proposed to inhibit HIV-1 LTR function at the transcriptional level by targeting the LTR U3 region [49]. The second HIV-1 miRNA to be proposed derives from the HIV-1 TAR element, a 59nt long RNA stem-loop located at the 5′ end of all HIV-1 miRNAs [41, 42, 48]. This miRNA was proposed to affect chromatin remodeling and to downregulate pro-apoptotic cellular genes. More recently, two groups have used moderately deep sequencing approaches to analyze HIV-1-derived small RNAs in infected cells. Yeung *et al*. [52] obtained 47,773 total reads, of which 125 (0.26%) were of HIV-1 origin, representing a diverse group of small viral RNA sequences that the authors nevertheless proposed likely represented functional viral miRNAs. Similarly, Schopman *et al*. [53] performed deep sequencing of small RNAs present in HIV-1 infected SupT1 cells and found that HIV-1 contributed ~1% of the total small RNA pool, and several viral small RNA species were recovered at ≤175 total reads

each. As cellular miRNAs contributed ~71% of the total of 2,522,374 small RNA reads recovered in this study, this means that even the most prevalent candidate viral miRNAs only represented ~0.01% of the total miRNA pool in these HIV-1-infected T cells, which equates to <5 copies per cell in total [141].

In considering whether small RNA reads of viral origin indeed represent authentic viral miRNAs, the following parameters need to have been satisfied: 1) miRNAs are almost always 22±2nt in length [1]. Therefore, an authentic viral miRNA will be recovered at a discrete size that is close to 22nt. If viral small RNA reads extend over a wider size range, then this is more consistent with RNA breakdown products. 2) Because the seed region of the miRNA, nucleotides 2 through 8 from the 5′ end, is the key determinant of mRNA target recognition, authentic viral miRNAs will have a discrete, not a diffuse, 5′ end. 3) miRNAs tend to regulate >100 mRNA species, due to the small size of the seed recognition sequence, so functional miRNAs are generally highly expressed. Importantly, recent data demonstrate that miRNAs that represent <0.1% of the total viral miRNA pool are unlikely to be functionally relevant [10]. 4) Viral miRNAs should derive from one or a small number of discrete sites in the viral genome that coincide with predicted pri-miRNA stem-loops. If viral small RNA reads are scattered across the genome, they are less likely to represent real miRNA reads [32, 34]. 5) Relative to the total small RNA pool, authentic viral miRNAs will be enriched in RNA

preparations derived from immunoprecipitated RISCs while RNA breakdown products will be depleted.

In addition to the question of whether HIV-1 actually encodes miRNAs, it has also been proposed that HIV-1 can modulate cellular miRNA expression to promote its replication [77]. Finally, HIV-1 transcripts are, of course, potential targets for binding by RISCs programmed by cellular miRNAs, which could repress virus replication and possibly favor entry into latency [69]. Here, we have used deep sequencing as well as techniques that directly recover RISC binding sites to address how HIV-1 interfaces with the miRNA machinery in infected T cells and macrophages. We clearly demonstrate that HIV-1 does not encode any viral miRNAs and also reveal that HIV-1 only minimally affects cellular miRNA expression patterns within 72 h of infection. We also identify a number of cellular miRNA binding sites on the HIV-1 RNA genome and show that some of these can potentially mediate inhibition of viral gene expression. However, we also demonstrate that HIV-1 genomic-length mRNAs represent very poor targets for RISC binding, most probably because large stretches of the HIV-1 genome are occluded by RNA secondary structure.

3.3 *Materials and methods*

3.3.1 Viral isolates

The viruses used in this study include the uncloned, CCR5-tropic BaL isolate [142]; a CCR5-tropic virus derived from the pWT/BaL proviral clone [143], which contains a SalI/XhoI fragment of BaL, encompassing the HIV-1 *tat*, *rev*, *vpu* and *env* genes, cloned into an HXB-3-derived proviral backbone; a CXCR4-tropic virus derived from the widely used pNL4-3 proviral clone [144]; and lastly, a CCR5-tropic virus derived from pNLHXADA [145], which contains the *env* gene of the ADA isolate cloned into a proviral backbone derived primarily from NL4-3 but also partly from HXB-2.

3.3.2 Molecular clones

The pWT/BaL [143], pNL4-3 [144] and pNLHXADA [145] HIV-1 proviral expression vectors have been previously described [146]. The pMSCV/amiRNA-N2 and -N4 expression plasmids were designed to encode the N2 and N4 amiRNAs previously shown to inhibit HIV-1 replication [100]. These retroviral vectors were generated by annealing the amiRNA-encoding oligonucleotides and ligating them into the polylinker present in pMSCV-Puro (Clontech).

300bp fragments of the HIV-1 genome, centered on miRNA target sites detected by PAR-CLIP, were cloned into the 3′ UTR of codon-optimized Rluc via the XhoI and NotI sites of psiCheck2 (Promega), which also contains the Fluc gene in *cis* as an internal control. pri-miRNA stem-loops were cloned into the XhoI and XbaI sites of pLCE as

~200bp DNA fragments generated by PCR of human genomic DNA, as previously described [147].

3.3.3 Cell culture

293T and TZM-bl cells [148] were cultured in Dulbecco's Modified Eagle Medium (DMEM) (Sigma) supplemented with 10% Fetal Bovine Serum (FBS). The human CD4+ T cell line C8166 [149] was cultured in RPMI 1640 media (Sigma) supplemented with 10% FBS. Peripheral blood mononuclear cells (PBMCs) were isolated from total blood by density gradient centrifugation (Lymphocyte Separation Medium, Cellgro #25-072-CV) and CD4+ T cells then isolated using the DynaBead CD4 Positive Isolation Kit from Invitrogen (#1131D). Cells were activated by incubation in phytohemagglutinin (PHA) and mouse monoclonal antibodies specific for human CD28 and CD49d (BD Biosciences #347690) for three days. Activation of the CD4+ T cells was confirmed by FACS using an anti-CD69 antibody and the cells then cultured in RPMI supplemented with 10% FBS and interleukin 2 prior to infection. Peripheral blood monocytes were obtained by elutriation and cultured for 4 days in DMEM containing 10% human serum, 1% L-glutamine, and 6ng/mL monocyte colony stimulating factor (MCSF) to activate macrophages.

TZM-bl amiRNA cell lines were generated by transfecting 293T cells with 15μg of a pMSCV amiRNA expression vector, 5μg of pMLV-gag/pol, and 1μg pHIT. 48 h post-transfection, virus-containing supernatants were collected, filtered and used to

transduce TZM-bl cells. Transduced cells were selected for puromycin resistance and then maintained in complete DMEM supplemented with puromycin dihydrochloride (Sigma) at a final concentration of 1μg/mL. Expression of amiRNAs was confirmed by deep sequencing of small RNAs.

3.3.4 Viral stocks and infection

NL4-3 virus was prepared in 293T cells via Fugene6 transfection with the pNL4-3 plasmid. Virus-containing supernatants were used to infect MT4 cells maintained in RPMI 1640 supplemented with 10% heat-inactivated FBS. Virus stocks were harvested 4, 5 and 6 days after infection and filtered through a 0.45μm filter Acrodisc syringe filter. The virus stock with the highest level of infectious virus, as determined by ELISA for the p24 Gag protein and by viral titer, was used for subsequent experiments. NL4-3 titers were measured by staining TZM-bl cells with the β-Gal Staining Kit (Mirus Bio) 24 h post-infection and counting blue foci. The HIV-1 BaL isolate stock was maintained in primary CD4+ human T cells and titered on TZM-bl as described above. Viral stocks were used to infect C8166 T cells and/or activated CD4+ T cells via spinoculation at 2000 rpm for 3 h. T cells were infected with HIV-1 using ~0.7 TZM-bl infectious units per cell.

The WT-BaL (as opposed to BaL isolate) virus stock was prepared by transfection of $5x10^6$ 293T cells with 15μg of pWT-BaL using FuGENE6 (Roche). Virus-containing supernatants were collected 48 h post-transfection, filtered through a 0.45μm filter

Acrodisc filter and then used to infect the parental TZM-bl cells or TZM-bl cells engineered to stably express HIV-1-specific amiRNAs.

The NLHXADA virus stock was prepared by transfection of 293T cells with the pNLHXADA proviral clone [145], essentially as described above for pWT-BaL. After four days of culture in medium lacking MCSF, $7x10^5$ macrophages were seeded in 24-well plates and directly infected with NLHXADA virus (500ng p24 total per well) overnight. Supernatants were replaced with fresh media and the cells cultured at 37°C until 10 days after the initial detection of reverse transcriptase activity in the supernatant, a total of 27 days.

3.3.5 Flow cytometry

0.3 mL of each infected T cell culture was resuspended in 1% FBS in phosphate-buffered saline (PBS) and stained with pooled human anti-HIV-IgG (1:100) (AIDS Reagent #3957) as the primary antiserum and FITC-conjugated goat α-human IgG (Invitrogen) as the secondary antibody (1:100), and analyzed on a FACSCalibur flow cytometer (BD Biosciences).

3.3.6 HIV-1 strand determinations

Sections of the NL4-3 and BaL LTR U3 region were cloned into pGEM3 (Promega) using primers 5′-GGGCGAATTCAAGACAAGATATCCTTGATCT -3′ with 5′-GCACTCTAGAAGCTTTATTGAGGCTTAAGC-3′ for NL4-3 and 5′-GGGCGAATTCATCTACCACACACAAGGCTA-3′ with 5′-

CTCTCTAGAAGTCCCCAGCGGAAAGTCCCT-3′ for BaL. Vectors were cleaved with XbaI and linear fragments purified by agarose gel electrophoresis. 1μg of each linear vector was subjected to in vitro transcription followed by DNase treatment with the MEGAscript T7 kit (Invitrogen), and purified with the MEGAclear kit (Invitrogen), both according to manufacturer's instructions. Five-fold dilution series beginning at $2x10^{11}$ RNA strands were diluted into 250ng of uninfected C8166 RNA and subjected to DNase treatment.

250ng of cellular RNA were subjected to RQ1 DNase treatment (Promega) according to the manufacturer's instructions. One-half of each sample was subjected to reverse transcription using 100ng of random hexamers (Bioline) and the SuperScript III Reverse Transcription kit (Invitrogen). Samples were diluted 1:4 and 5μl of each diluted cDNA were amplified using SYBER-Green master-mix on a StepOnePlus Real-Time PCR system (Applied Biosystems) in triplicate using 5pmol of each of the following primers: 5′-TACAAGCTAGTACCAGTTGA-3′ and 5′-GCTGTCAAACCTCCACTCTAAC-3′. Ten five-fold standard dilutions amplified in parallel were used to quantify total HIV-1 U3 RNA strands in each sample. Primary cells and C8166 cells were estimated to contain ~20pg of total RNA per cell and TZM-bl cells were estimated to have 40pg RNA per cell, based upon multiple total RNA extractions by TRIzol.

3.3.7 Deep sequencing of total small RNA

Total RNA was isolated using TRIzol. The RNA fraction containing ~15-30nt length RNAs was isolated by polyacrylamide gel electrophoresis (PAGE) purification on 15% TBE-Urea gels (BioRad), electroeluted from the excised gel slice (Gel Eluter/Hoefer), and cloned as previously described [146]. Adapter-ligated small RNAs were reverse transcribed using SuperScript III, amplified using GoTaq Green PCR Master Mix (Promega) with the Tru-Seq 3′ indices (Illumina), and sequenced on an Illumina HiSeq 2000.

3.3.8 TZM-bl deep sequencing and RIP-Seq

RISC-bound miRNAs from uninfected and WT-BaL infected TZM-bl cells at 72 h post-infection were isolated by immunoprecipitation using a monoclonal antibody specific for Ago1, Ago2 and Ago3 (Abcam: AB 57113) and proteins removed by digestion with proteinase K. Recovered small RNAs were then isolated using a mirVana kit (Ambion). The immunoprecipitated RNA (RIP-Seq) cDNA library was constructed essentially as described (56) using an Illumina TruSeq small RNA kit, prior to sequencing using an Illumina HiSeq 2000.

3.3.9 Photoactivatable-ribonucleoside-enhanced crosslinking and immunoprecipitation (PAR-CLIP)

48 h post-infection, cells were labeled with 100μM 4-thiouridine (Sigma) for 16 h. Cells were washed with PBS and crosslinked using a Stratagene UV Stratalinker 2400 at 365nm. The samples were then processed as previously described [150, 151]. RISC cross-

linked RNAs were isolated using anti-Ago2 (Abcam AB57113). This antibody also recognizes Ago1 and Ago3, (data not shown). Cloning of isolated small RNAs was performed using the TruSeq small RNA cloning kit (Illumina). TZM-bl cells expressing individual HIV-1-specific amiRNAs were infected independently but the cell lines were pooled into one sample for PAR-CLIP processing. A sample from each culture untreated with 4-thiouridine was harvested in parallel and deep sequenced in order to determine both the miRNA population present in each PAR-CLIP sample and the number of HIV-1 strands per cell.

3.3.10 Data analysis

Reads >15nt were collapsed into FASTA format with the FASTX-Toolkit (http://hannonlab.cshl.edu/fastx_toolkit/index.html) using the following pipeline: fastq_quality_filter –Q 33| fastq_to_fasta –Q 33 | fastx_clipper -a TruSeq-Index# -l 15 –c | fastx_collapser. All reads were then subject to alignment using Bowtie v.0.12.7 [122] with the following options: –a --best --strata –m 25.

3.3.10.1 Deep sequencing analysis

Sequences were sequentially filtered and assigned using the following pipeline (displayed as Database: additional bowtie alignment parameters)-

1. Markers (18- and 24mer radiolabeled oligos, 3′ and 5′ adapters): -v 0 --noRC
2. HIV genome: -v 1

3. miRbase v19 Homo sapiens: -v 1 –noRC [152]

4. Ensembl ncRNAv70 Homo sapiens: -v 1 –noRC [153]

5. fRNAdb v3.4 Homo sapiens: -v 1 --noRC [154]

6. Human Genome 19: -v 2

MiRNA sequences were given a -5p or -3p designation if they aligned to the 5′ or 3′ stem region of the miRNA precursor, as annotated in miRbase v19, respectively. MiRNAs that represented >0.1% of the total cellular miRNA population were considered significant [10]. Reads for sequences aligning to two or more entries in a database were distributed equally between each entry except that reads aligning to both piwi-interacting RNAs (piRNAs) and rRNAs, tRNAs, snRNAs, Y RNAs or snoRNAs were assigned to the latter RNA species.

3.3.10.2 PAR-CLIP analysis

Alignments to a combined human and HIV-1 genome were performed as previously described [150, 151] allowing 3 mismatches. Alignments containing (+)sense T>C and (-)sense A>G conversions were used to generate clusters with PARalyzer v1.1 [155] using the following parameters: a minimum of 5 reads for a sequence to be included in a cluster, a minimum cluster read-depth of 5, at least 1 conversion event in a read for cluster inclusion, and no non-conversion mismatches allowed for each read determining the cluster. Clusters with a read depth >50 and a conversion event to read-depth ratio of >0.75 were considered significant. Significant miRNAs (≥0.1% of the total

miRNA pool) expressed in each library were determined as above, from samples untreated with 4-thiouridine, and were then used by PARalyzer to predict which miRNAs were likely to target a given cluster.

3.3.11 Luciferase indicator assays

50ng of each reporter plasmid was co-transfected with 500ng of a pLCE-based miRNA expression vector [147], via calcium phosphate co-precipitation, into 24-well plates containing 10^5 293T cells per well, plated the previous day. 24 h post-transfection, lysates were harvested and luciferase levels determined using a Dual Luciferase Kit (Promega) according to manufacturer's instructions. The ratio between the Rluc and internal control Fluc proteins was determined for each sample and compared to the same reporter plasmid co-transfected with pLCE lacking a miRNA precursor.

3.3.12 Analysis of HIV-1 infection and production by NoDice cells

To analyze HIV-1 production in NoDice cells, we transfected 2×10^6 293T, NoDice(2-20), or NoDice(4-25) cells in a 10cm dish using Fugene6 (Promega) according to the manufacturer's protocol, with 10μg pNL-GFP-HXB and 500ng pKH3-GST as an internal control for transfection efficiency [156, 157]. At 48 h post-transfection, the virus-containing supernatant media were filtered through a 0.45μm-pore-size filter (Acrodisc filter; Pall) and then used to infect TZM-bl cells (55). Twenty-four hours post-infection, the TZM-bl cells were lysed in Passive Lysis Buffer (Promega) and analyzed for firefly luciferase (FLuc) activity, using a luciferase assay system (Promega). In parallel, the

virus producer cells were lysed, the whole-cell lysate was subjected to gel electrophoresis and transferred to a nitrocellulose membrane, and the level of expression of the co-transfected glutathione S-transferase (GST) internal control was analyzed by Western blotting using a rabbit polyclonal anti-GST antibody (sc-459; Santa Cruz) and anti-rabbit IgG peroxidase (A6514; Sigma). GST levels were visualized by chemiluminescence (WesternBright Sirius kit; Advansta), and the image was captured using G:Box (SynGene) and then quantified with GeneTools (SynGene) software.

To analyze HIV-1 infection efficiency in NoDice cells, we transfected 2×10^6 293T cells using Fugene6 with 10μg of pNL-Luc-HXB and 500ng pCMV-VSV-G [158]. Forty-eight hours post-infection, virus-containing supernatants were filtered and used to infect 293T, NoDice(2-20), and NoDice(4-25) cells. Twenty-four hours post-infection, cells were lysed and analyzed for FLuc expression.

For pseudotyped HIV-1 virus production experiments, 2×10^7 293T cells were transfected in a 15cm dish using polyethylenimine with 25μg of pD3-HIV-GFP [159] and 10μg of pCMV-VSV-G. At 48 and 72 h post-transfection, the supernatant media were filtered and pooled and equal amounts were used to infect 293T, NoDice(2-20), and NoDice(4-25) cells. At 48 h post-infection, cells were analyzed by flow cytometry for green fluorescent protein (GFP) expression to determine the percentage of 293T and NoDice cells infected by HIV-1.

3.4 *Results*

3.4.1 HIV-1 fails to express any viral miRNAs in infected cells

To determine the miRNA expression profile in HIV-1 infected cells, we performed deep sequencing of small ~15-30nt long RNAs in a range of infected cell types. These included TZM-bl cells, a variant of HeLa cells that expresses the CD4 receptor and both the CXCR4 and CCR5 co-receptor [148], infected with the CCR5-tropic HIV-1 variant WT/BaL [143]; the human CD4+ T cell line C8166 [149] infected with the CXCR4-tropic HIV-1 laboratory isolate NL4-3 [144]; CD4+ peripheral blood mononuclear cells (PBMCs) infected with either the CCR5-tropic BaL isolate [142] or the CXCR4-tropic NL4-3 isolate; and finally, primary human monocyte-derived macrophages (MDMs) infected with an NL4-3-derived HIV-1 variant, NLHXADA, bearing the CCR5-tropic ADA *env* gene [145].

TZM-bl cells were directly infected with WT/BaL virus derived from 293T cells transfected with the pWT/BaL proviral clone [143]. Uniform infection of the TZM-bl cells was confirmed by staining of a control TZM-bl culture at 72 h post-infection for viral activation of the integrated β-galactosidase (β-gal) indicator gene [148], which confirmed a >90% infection rate (Fig. A-1). Quantitation of the level of viral RNA transcripts, by qRT-PCR of a region derived from the HIV-1 LTR U3 region that is present in all viral transcripts, indicated that the infected TZM-bl cells contained an average of ~130,367 viral RNA strands per cell (Table 3-1).

Table 3-1: Overview of the HIV-1 deep sequencing libraries analyzed. This table indicates the cell type used (column 1), the virus used to infect (column 2), and the source of the env gene in that virus (column 3), as well as the total number of HIV-1 transcripts per cell at the time of harvest (column 4) and how many days post-infection RNA was harvested (column 5).

Cell Type	HIV-1 Virus Isolate Used	Envelope Gene Source	No. of HIV-1 RNA Strands/Cell	No. of Days of Post-infection
TZM-bl	WT/BaL	BaL	130,367	3
C8166	NL4-3	NL4-3	20,546	3
CD4+ PBMC	BaL	BaL	8,303	3
CD4+ PBMC	NL4-3	NL4-3	1,949	3
MDM	NLHXADA	ADA	12,110	27

C8166 cells and CD4+ PBMCs were infected with NL4-3 virus cultured in MT4 cells or with BaL virus cultured in CD4+ PBMCs. Cells were initially infected with ~0.7 TZM-bl infectious units per cell and then cultured for 72 h. At this time, infectivity levels were determined by FACS analysis using pooled human anti-HIV-1 IgG followed by FITC-conjugated goat anti-human IgG. This analysis indicated that ~97% of the C8166 cells, ~78% of the BaL infected CD4+ PBMCs and ~94% of the NL4-3 infected CD4+ PBMCs were HIV-1 positive (Fig. A-2). qRT-PCR analysis of viral transcript levels (Table 3-1) indicated that these infected cultures contained an average of ~20,546, ~8,303 and ~1,949 viral RNA strands per cell, respectively (Table 3-1).

Finally, primary MDMs were infected with an HIV-1 virus, NLHXADA, derived from an NL4-3-based proviral clone bearing the CCR5-tropic ADA *env* gene [145]. MDMs were initially infected with a virus stock obtained from pNLHXADA-transfected 293T cells and supernatant RT levels then monitored. Once significant RT levels were detected, at 17 days post-infection, the MDMs were cultured for an additional 10 days, for a total of 27 days, prior to lysis and RNA isolation. Previous work has shown that this protocol leads to essentially uniform infection of the MDM culture [160]. Analysis indicated an average of ~12,110 HIV-1 RNA strands per cell (Table 3-1).

Deep sequencing analysis of the small RNA profile in all five HIV-1 infected cell cultures and in matched uninfected cultures revealed that cellular miRNAs were, as expected, the major RNA variant detected in all 9 deep sequencing libraries (Fig. 3-1). In addition, we also detected significant levels of reads that could be aligned to human rRNAs, tRNAs, snRNAs, snoRNAs or mRNAs and likely represent RNA breakdown products (Fig. 3-1). Very few reads were found to align to the genomes of any of the HIV-1 virus variants in any of the infected cell cultures. This contrasts with previous reports showing that viruses known to encode viral miRNAs, such as Epstein-Barr virus (EBV), Kaposi's sarcoma-associated herpesvirus (KSHV) and the retrovirus BLV contribute a substantial share of the small RNAs seen in infected cells [19, 37, 151].

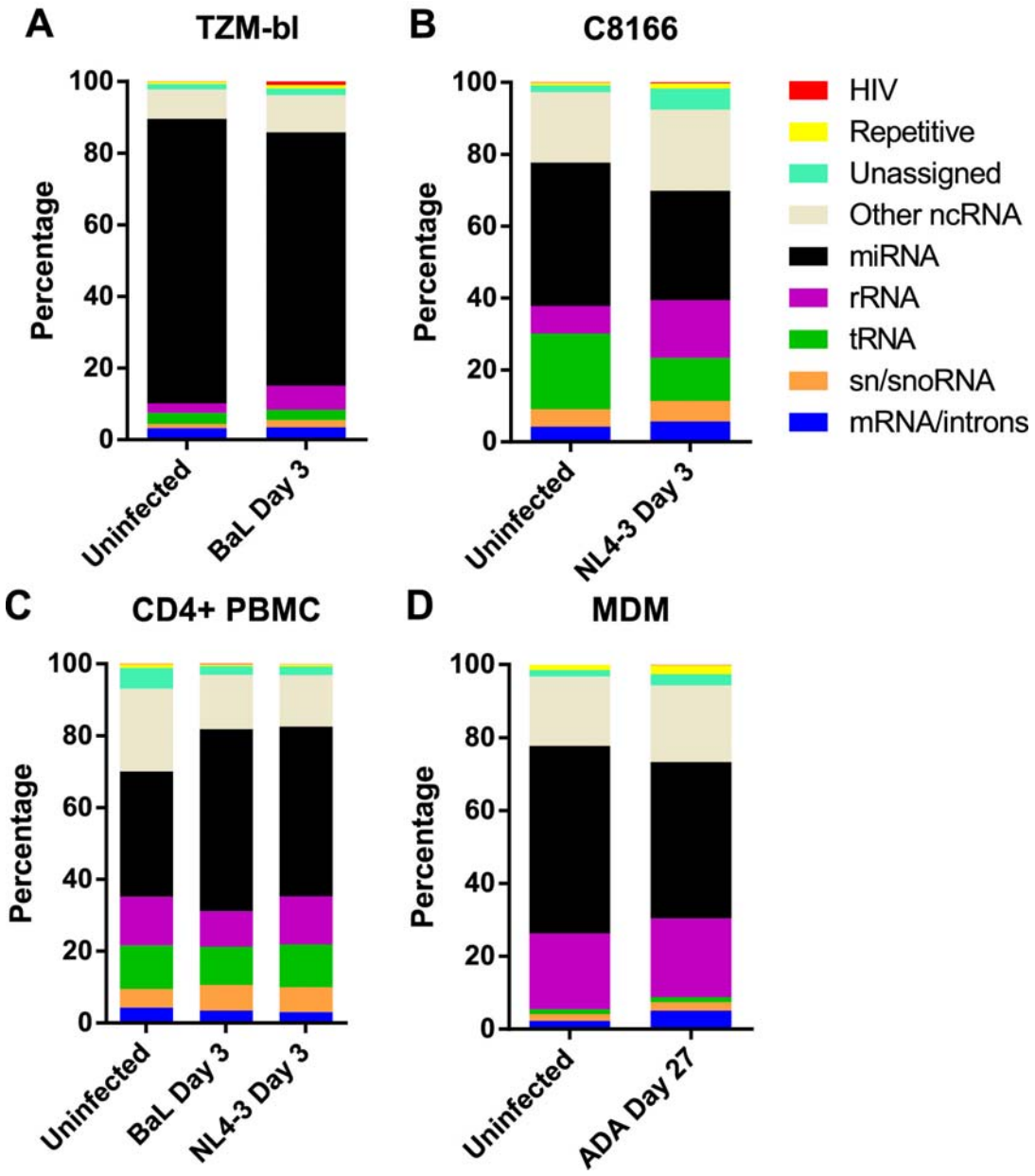

Figure 3-1: Assignment of deep sequencing reads to cellular and viral RNA classes. Small RNA deep sequencing reads were aligned to the human or HIV-1 genome and are shown by their assignment to different subclasses of RNA. Samples were derived from uninfected cells or from cells infected with HIV-1, as indicated. Repetitive sequences are defined as those that map to ≥25 locations in the human genome.

One key characteristic of miRNAs is their size, which ranges from ~20nt to ~24nt in length [1]. Analysis of the length profile of the total cellular small RNAs recovered in HIV-1 infected TZM-bl, C8166, CD4+ PBMC and MDMs shows that these indeed peak at ~22nt in size, as expected (Fig. 3-2, panels A, C, E and G). In contrast, the RNA reads that align to the HIV-1 genome are not only rare but also showed a fairly random size distribution, with a tendency for more reads at smaller sizes. Certainly, there was no evidence for high levels of HIV-1-derived small RNAs in the 22±2nt size range characteristic of miRNAs (Fig. 3-2, panels B, D, F and H).

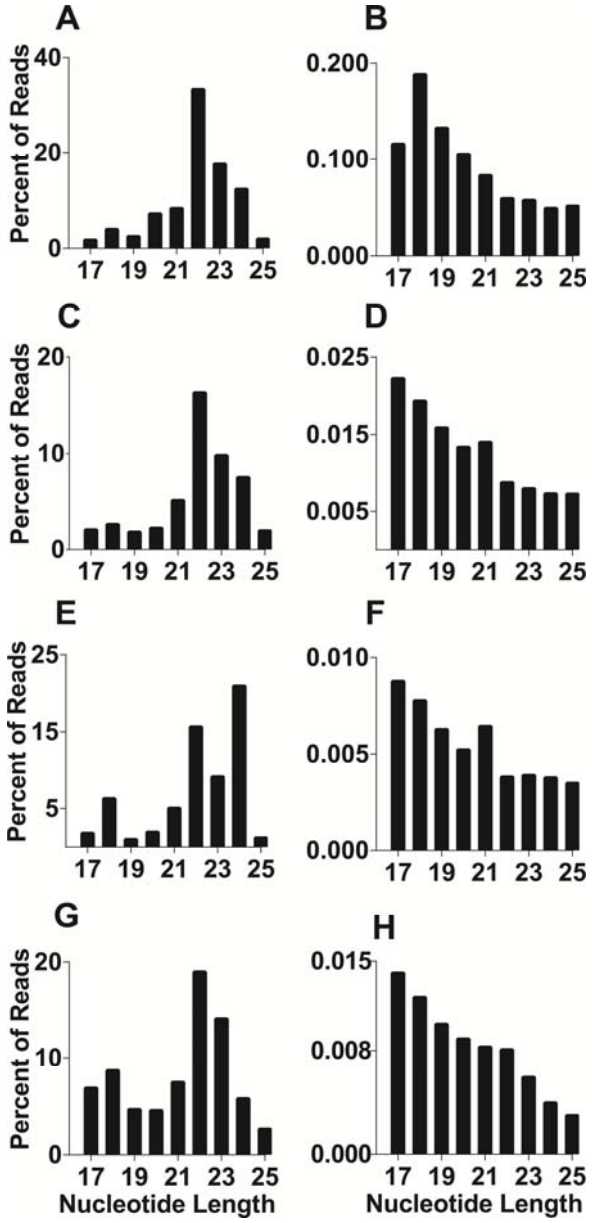

Figure 3-2: HIV-1-specific small RNAs do not cluster at the ~22nt size predicted for miRNAs. Small RNA reads from 17 to 25nt in length, derived from HIV-1-infected cells that align either to the human genome (A, C, E, and G) or the HIV-1 genome (B, D, F, and H) are shown assigned by their size. (A and B) TZM-bl cells infected with the WT/BaL virus. (C and D) C8166 T cells infected with NL4-3. (E and F) CD4+ PBMCs infected with the BaL HIV-1 isolate. (G and H) MDMs infected with the NLHXADA virus.

Analysis of viral small RNAs in cells infected by EBV or KSHV, which are known to encode viral miRNAs, has revealed that virus-derived small RNAs are almost all derived from a small number of locations in the viral genome that coincide with the pri-miRNA RNA stem-loops that are processed to yield viral miRNAs [34]. Moreover, these viral miRNAs are characterized by high level expression [151]. Indeed, recent data have shown that miRNAs that contribute <0.1% of the total cellular miRNA pool make no significant functional contribution [10]. Cellular and authentic viral miRNAs are also characterized by a discrete 5′ end, consistent with the finding that it is nucleotides 2 through 8 from the 5′ end, the so-called seed region, that primarily determines the mRNA target specificity of the miRNA [1, 37, 151]

Alignment of the HIV-1-derived small RNAs to the relevant proviral genome, in contrast, shows that these are scattered over the entire proviral sequence (Fig. 3-3). Some "hot-spots" of small RNA reads were noted, but even these are found to contribute <0.02% of the total miRNA pool in the infected cells (Fig. 3-3). Moreover, these "hot-spots" were generally not conserved between virus variants and/or cell types. An exception to this generalization arises in the case of small RNA reads that map to the overlap between the HIV-1 Gag and Pol open reading frames, which represent the major reads in the C8166/NL4-3 and CD4+ PBMC/BaL libraries (albeit still contributing only ~0.015% and ~0.0035% of total miRNA reads respectively) and were also readily detected in TZM-bl/BaL cells (Fig. 3-3).

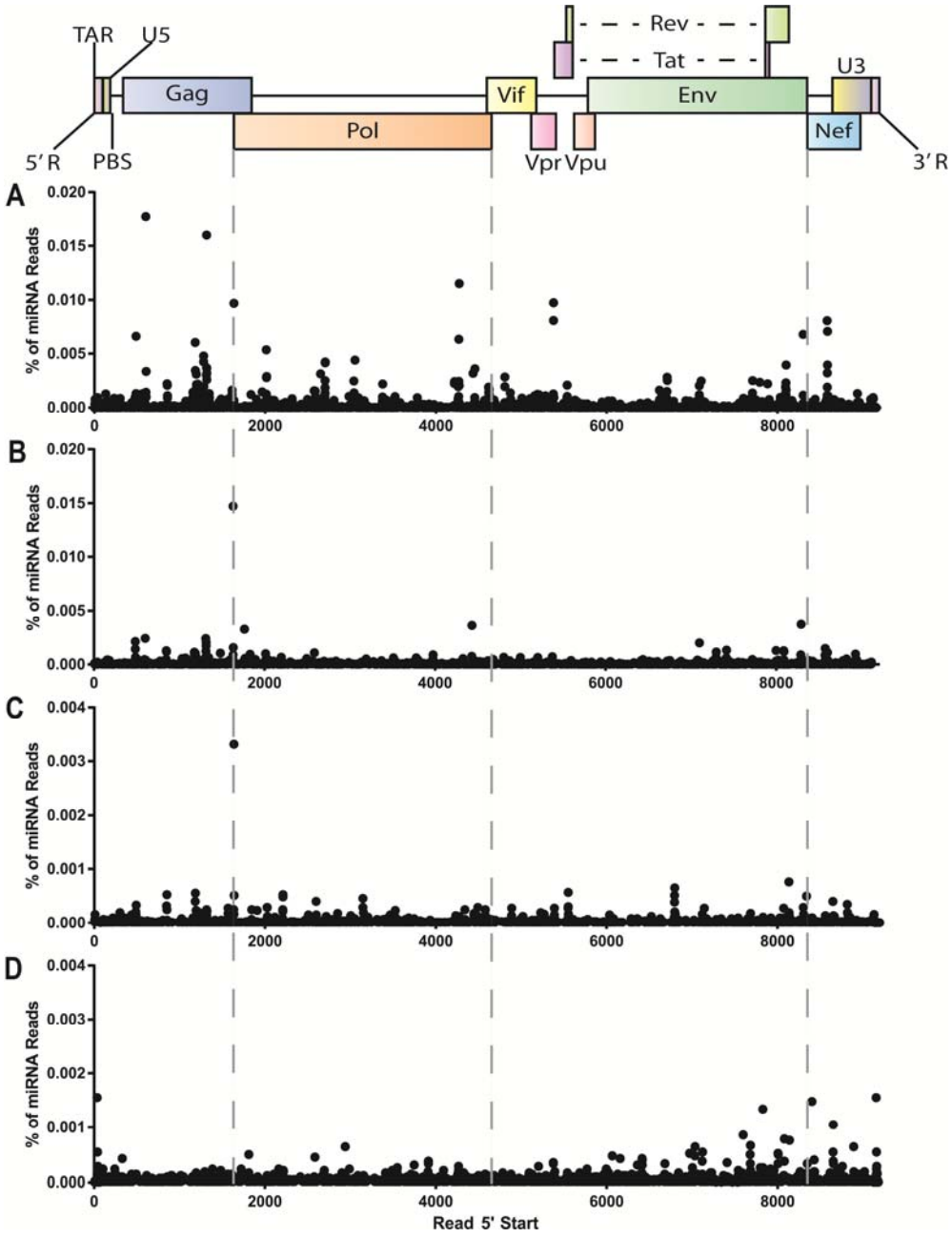

Figure 3-3: Alignment of small RNA reads to the HIV-1 genome. RNA reads of 19 to 25nt in length that mapped to the HIV-1 genome were aligned based on their 5′ ends and are shown relative to their genomic position of origin (x axis). The y axis shows the number of reads as a percentage of the total number of cellular miRNA reads in the same RNA sample. (A) TZM-bl infected with WT/BaL; (B) C8166 infected with NL4-3; (C) CD4+ PBMCs infected with BaL; (D) MDMs infected with NLHXADA.

Analysis of the reads at this hot-spot shows that their 5′ ends map to a stretch of 6 "U" residues found immediately 5′ to an RNA hairpin that facilitates the Gag/Pol frameshift during translation of genome length HIV-1 mRNAs by promoting ribosome stalling at the six "U" residue "slippery site" (Fig. 3-4) [161]. However, this short hairpin does not share any of the characteristics that are typical of a pri-miRNA hairpin structure; in particular, this predicted viral RNA hairpin is only 11bp long rather than the ~33bp typical of pri-miRNA hairpins [16, 17]. It seems possible that these reads, which almost all begin in the "U" stretch and then extend into the adjacent hairpin, are actually Gag/Pol mRNA fragments that are protected by the stalled ribosomes that are known to accumulate at this site on the viral mRNA [161].

Reads	TAATTTTTTAGGGAAGATCTGGCCTTCCCACAAGGGAAGGCCAGGGAAT	% Total HIV Reads
1620	....TTTTTAGGGAAGATCTGGCCT.....	0.796%
177	......TTTAGGGAAGATCTGGCCT.....	0.087%
93	...TTTTTTAGGGAAGATCTGGCCT.....	0.046%
73	....TTTTTAGGGAAGATCTGGCC.....	0.036%
67	..ATTTTTTAGGGAAGATCTGGCCT.....	0.033%
54	..ATTTTTTAGGGAAGATCTGGCCT.....	0.027%
33	TAATTTTTTAGGGAAGATCTGGCCT.....	0.016%
23	.....TTTTAGGGAAGATCTGGCCT.....	0.011%
18	....TTTTTAGGGAAGATCTGGC.....	0.009%
12	...TTTTTTAGGGAAGATCTGGCC.....	0.006%

Figure 3-4: Alignment of HIV-1 deep sequencing reads with the viral Gag/Pol frameshift signal. The region of the HIV-1 RNA genome that coincides with the Gag/Pol frameshift signal [161] represents the major source of HIV-1-specific small RNA reads in most infected cell types (Fig. 3-3). This figure collates all the reads, from all four infected cell types shown in Fig. 3-3, and aligns them to this region of the HIV-1 genome. At the top is shown the HIV-1 sequence, with the loop of the predicted frameshift stem-loop indicated in red. The predicted structure of this stem-loop is shown at the right. Note that most reads initiate 5′ to the actual stem-loop in a U-rich region that also plays a key role in HIV-1 frameshifting and is known to be a site of ribosome pausing.

Two groups have reported that HIV-1 encodes miRNAs derived from the TAR RNA stem-loop that is located at the 5′ end of all viral transcripts [41, 42, 48]. The TAR stem, at ~24bp, is again much shorter than the optimal, ~33bp stem characteristic of pri-miRNA stem-loops [16, 17] and TAR also differs from authentic pri-miRNAs in that the terminal loop is only 6nt, not the ≥10nt characteristic of pri-miRNAs (Fig. 3-5) [16]. Most importantly, Drosha cleavage of pri-miRNAs requires unstructured RNA sequences both 5′ and 3′ to the pri-miRNA stem [17, 162]; while TAR is located at the very 5′ end of all HIV-1 RNAs and, moreover, likely has a cap and cap-binding proteins associated with its 5′ end. In fact, we recovered almost no reads that mapped to TAR in all cases except ADA-infected MDM, where these reads contributed ~0.002% of the viral short RNA reads (Fig. 3-3). Analysis of these rare TAR-derived RNAs revealed a heterogeneous population of small RNAs that mapped to both sides of the TAR RNA stem-loop and that, in particular, did not have a discrete 5′ end (Fig. 3-5).

Reads	GGGTCTCTCTGGTTAGACCAGATCTGAGCCTGGGAGCTCTCTGGCTAACTAGGGAACCC	% Total HIV Reads
113	.........TGGTTAGACCAGATCTGAGCC..............................	0.055%
94	....................................TCTGGCTAACTAGGGAACCC...	0.046%
74	........CTGGTTAGACCAGATCTGAGCCT.............................	0.036%
56	....................................TCTCTGGCTAACTAGGGAACC....	0.028%
56	....................................TGGCTAACTAGGGAACCCACT	0.028%
54	....................................TCTCTGGCTAACTAGGGAACCC...	0.027%
54	.......TCTGGTTAGACCAGATCTGAGCCT.............................	0.027%
49	......CTCTGGTTAGACCAGATCTGAGCCT.............................	0.024%
48	....................................TCTCTGGCTAACTAGGGAAC.....	0.024%
43	........CTGGTTAGACCAGATCTGAGCC..............................	0.021%

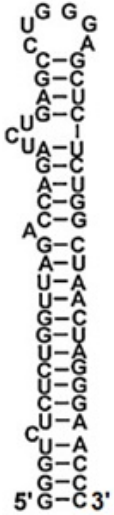

Figure 3-5: Alignment of HIV-1 small RNA reads to the HIV-1 TAR RNA element. This figure aligns HIV-1-derived small RNA reads, compiled from all four small RNA libraries described in Fig. 3-3, and aligns them to the HIV-1 TAR RNA stem-loop that forms the 5′ end of all HIV-1 transcripts. The sequence of the TAR region is shown at the top, with the loop indicated in red, and the predicted RNA structure adopted by TAR is shown at the right.

It could be argued that some of the HIV-1 small RNA reads, despite their low level of expression, are nevertheless functional miRNAs that are efficiently loaded into RISC. To address whether this is the case, we immunoprecipitated RISC using an antibody able to specifically bind Ago1, Ago2 and Ago3, each of which can interchangeably function as a key component of RISC [1] and then compared the profile of small RNAs recovered from the RISC immunoprecipitate with that seen when the total small RNA profile was determined in parallel in WT/BaL-infected TZM-bl cells. As expected, the RNA library derived from the RISC immunoprecipitate indeed showed a strong enrichment in miRNAs, with known cellular miRNAs increasing from ~71% to ~93% of the total RNA library. In contrast, the HIV-1 derived small RNA reads were selectively lost when RISC-associated small RNAs were sequenced (Fig. 3-6). In this library, no viral RNA was found to contribute >0.005% of the total human miRNA pool, a level that is far lower than the >0.1% contribution previously reported to be characteristic of functionally relevant miRNAs [10].

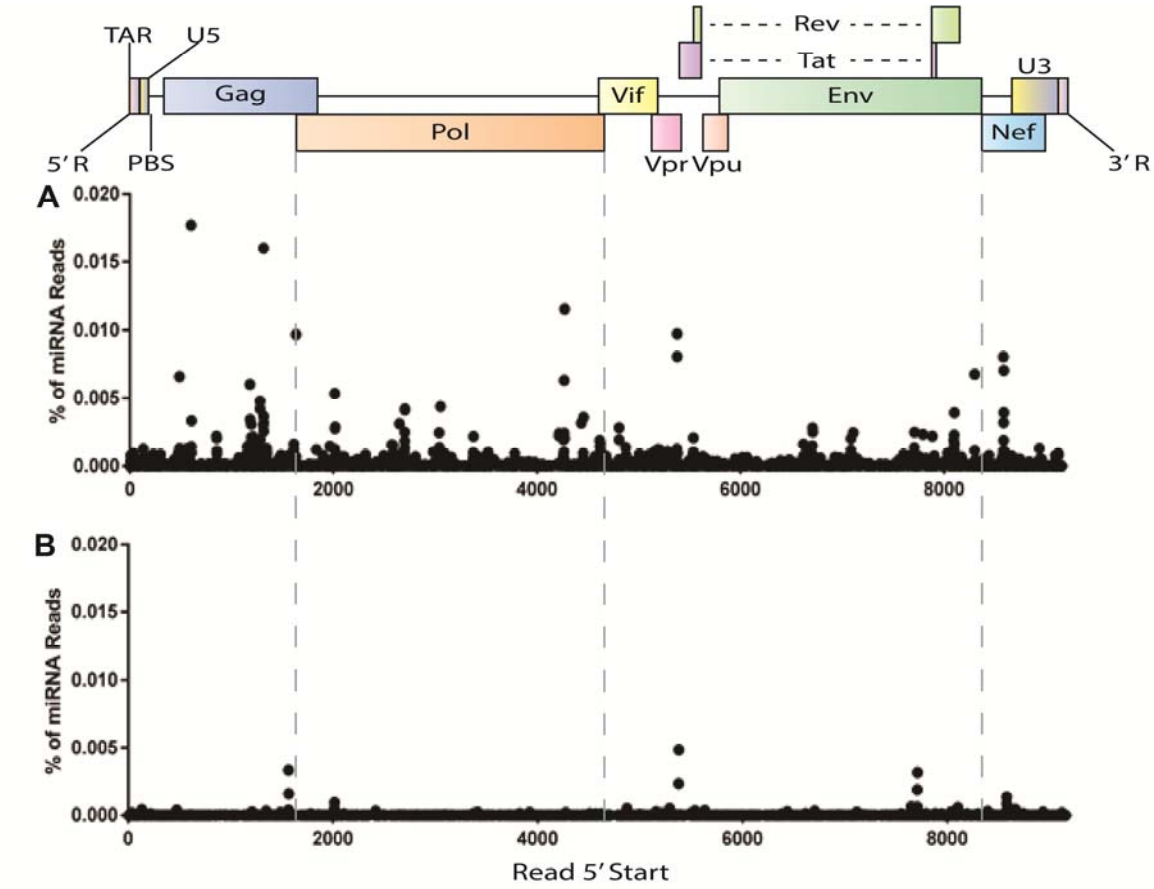

Figure 3-6: Comparison of HIV-1 small RNA reads obtained from a total small RNA and RISC-associated small RNA sample. This figure compares the pattern of total HIV-1 small RNA reads detected in TZM-bl cells infected with the WT/BaL viral clone to the pattern of small RNAs seen in the RISC-associated small RNA fraction, prepared from the same culture in parallel by immunoprecipitation with an Ago-specific monoclonal antibody. Data are presented as in Figure 3-3.

Previously, it has been suggested that HIV-1 might generate miRNAs, or even small interfering RNAs (siRNAs), from transcripts derived from the negative-sense RNA strand [53]. Even though retroviruses do not generate minus strand RNAs during their replication cycle, minus-sense strands could in principle arise by transcription from cellular promoters located 3' to, and in the opposite orientation from, integrated

proviruses. However, we failed to detect a significant level of small RNA reads derived from the HIV-1 antisense strand in either infected TZM-bl cells (Fig. 3-7) or in any other infected cell types (data not shown). While most regions of the HIV-1 minus strand gave read numbers equivalent to ≤0.0002% of the total miRNA population, one region, complementary to the HIV-1 primer binding site, did give rise to a substantial number of reads (Fig. 3-7A). These have been previously noted by others [52, 53] and proposed to derive from breakdown products of the lysine tRNA that serves as the primer for HIV-1 reverse transcription. Indeed, reads complementary to the HIV-1 primer binding site were recovered at comparable levels in non-infected cells (data not shown) and analysis of small RNAs bound to RISC in infected TZM-bl cells failed to detect any reads derived from the region complementary to the viral primer binding site, thus strongly suggesting that these are indeed tRNA breakdown products (Fig. 3-7B).

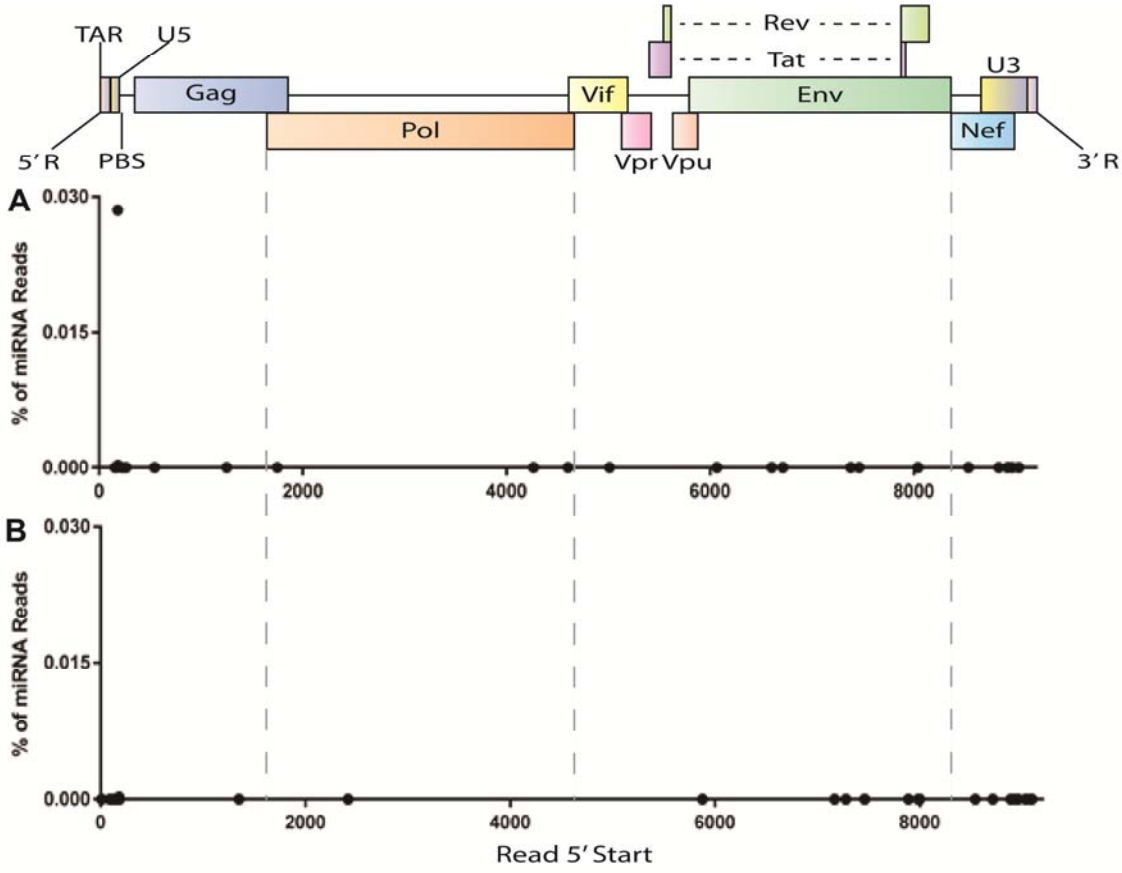

Figure 3-7: Alignment of small RNA reads from the HIV-1-infected TZM-bl cells with the minus strand of the HIV-1 genome. This analysis was performed as described in Figure 3, except that small RNA reads are aligned to the hypothetical antisense strand complementary to the HIV-1 genome. (A) uses total small RNA reads, obtained from WT/BaL infected TZM-bl cells. (B) uses reads obtained by analysis of RISC-associated small RNAs. The major peak shown in (A) is located antisense to the HIV-1 primer binding site and likely represents lysine tRNA breakdown products that are not loaded into RISC.

3.4.2 HIV-1 fails to significantly affect cellular miRNA expression early after infection

There are a number of reports documenting cases where cellular miRNAs facilitate aspects of a viral replication cycle and/or where viruses manipulate the cellular miRNA expression profile to enhance some aspect of their replication or pathogenic potential [4, 163-168]. This has also been suggested for HIV-1, which has been reported to downregulate the miR-17/92 miRNA cluster, consisting of the six cellular miRNAs miR-17, miR-18a, miR-19a, miR-20a, miR-19b and miR-92a, to upregulate expression of the PCAF histone acetyltransferase which has been proposed to function as a co-factor for the HIV-1 Tat transcription factor [77]. To examine whether HIV-1 indeed exerts a significant effect on the cellular miRNA profile, we therefore compared the level of expression of cellular miRNAs in uninfected and matched HIV-1 infected cells, measured either by total small RNA sequencing or, in the case of TZM-bl cells infected with BaL, by deep sequencing RISC-associated small RNAs (Fig. 3-6). This analysis was performed 72 h after initial infection in all cases. We believe this short time frame is appropriate, given that HIV-1 infected T cells have been reported to have a half-life of only ~24 h in vivo [169].

As shown in Fig. 3-8, and presented in detail in Table A-1, analysis of the expression level of cellular miRNAs in HIV-1 infected TZM-bl cells, C8166 T cells and, most importantly, primary CD4+ PBMCs revealed few differences between the infected and uninfected cells despite clear evidence of efficient infection and high levels of viral

transcripts (Table 3-1). In particular, only one cellular miRNA, miR-30b-5p, increased >2 fold in BaL infected PBMCs and no cellular miRNAs increased or decreased >2 fold in NL4-3 infected PBMCs. In both TZM-bl and C8166 cells, several cellular miRNAs changed their expression, in either a positive or negative direction, by slightly over the 2-fold limit indicated in Fig. 3-8. The functional significance of these changes, if any, is unclear. Perhaps surprisingly, we failed to see any significant (≥2-fold) effect of HIV-1 infection on the expression of members of the miR-17/92 cluster, as previously proposed [77].

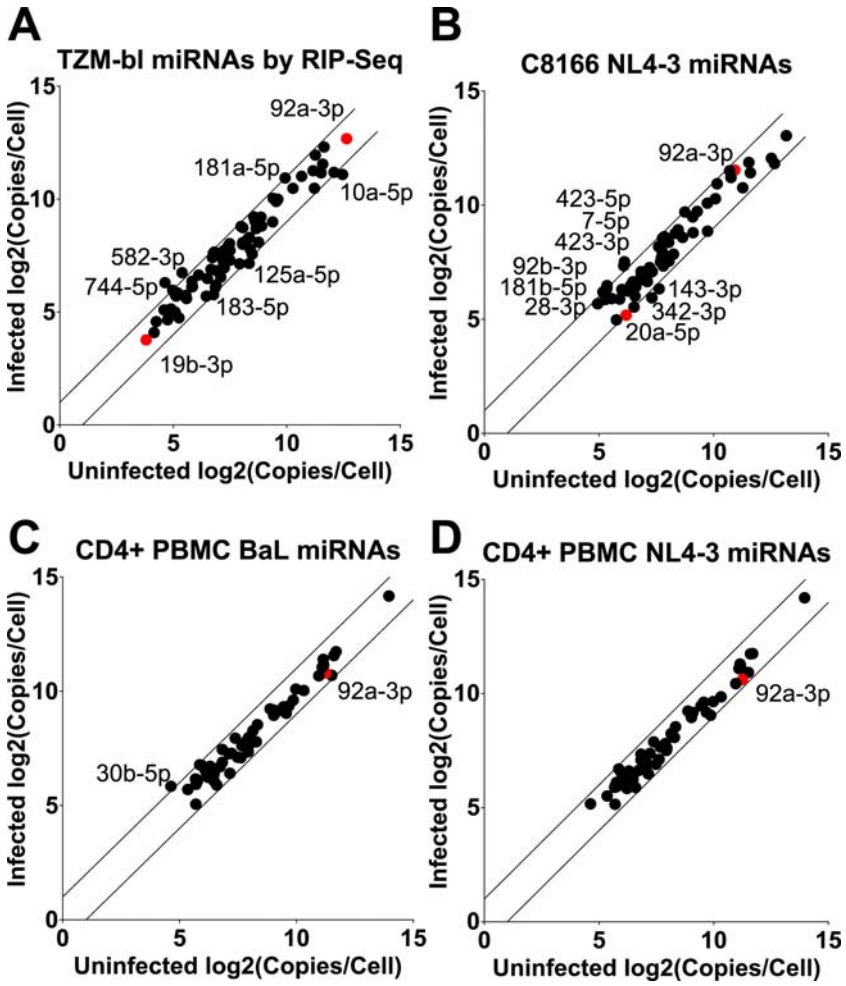

Figure 3-8: Effect of HIV-1 infection on cellular miRNA expression levels. This figure presents a comparison of the level of each cellular miRNA detected in uninfected and HIV-1-infected cells. Only miRNAs that represent ≥0.1% of the total miRNA pool were included. Panel A shows data obtained by comparison of RISC-associated small RNAs, while panels B, C, and D compare total miRNA levels. The lines delineate changes of 2-fold between samples. miRNAs that fall outside this 2-fold limit are indicated by name. Red dots represent miRNAs derived from the miR-17/92 cluster. For illustrative purposes, this figure assumes that cells each express 5×10^4 miRNAs.

3.4.3 Cellular miRNAs bind HIV-1 transcripts inefficiently

Viruses that infect cells encounter a range of different cellular miRNAs that have the potential to inhibit viral mRNA function and it is largely unclear how viruses avoid this problem. One virus family, the poxviruses, has been shown to globally degrade cellular miRNAs [170]. However, most viruses, including HIV-1, do not block miRNA function in infected cells [81]. It is also possible that a virus that is highly tissue tropic, e.g., HIV-1 which only infects CD4+ T cells and macrophages, has simply evolved to avoid mRNA binding sites for the miRNAs specific to these cell types. In that case, however, one would expect HIV-1 to be susceptible to inhibition by the diverse miRNAs found in other, normally non-target cell types.

To address this question, we used the recently described photoactivatable ribonucleoside-enhanced crosslinking and immunoprecipitation (PAR-CLIP) technique [150, 151] to globally identify all the binding sites for miRNA-programmed RISCs on the HIV-1 genome in infected C8166 T cells or TZM-bl epithelial cells. At 48 h post infection with the NL4-3 (C8166) or WT-BaL (TZM-bl) virus isolate, the infected cells were incubated with 100 μM 4-thiouridine (4SU) for 16 h prior to crosslinking by irradiation using UV light at 365nm. mRNAs bound to RISC were then isolated by immunoprecipitation using a monoclonal antibody specific for the human Ago proteins. After RNase treatment, mRNA fragments bound to RISC were gel purified, cDNA cloned and subjected to Illumina deep sequencing. The resultant reads were then

aligned to the human or HIV-1 genome and analyzed using the PARalyzer program, which partitions reads into individual clusters, each of which defines a single RISC binding site (Fig. 3-9) [155]. The PARalyzer program also seeks to use sequencing data defining the cellular miRNAs present in the infected cells, obtained in parallel, to identify the cellular miRNA that is most likely responsible for guiding RISC to that particular viral binding site. This assignment, which assumes perfect complementarity to nucleotides 2-7 in the miRNA seed region, is, however, unable to identify "non-canonical" miRNA binding sites, which can contribute a significant percentage of the RISC interaction sites [9].

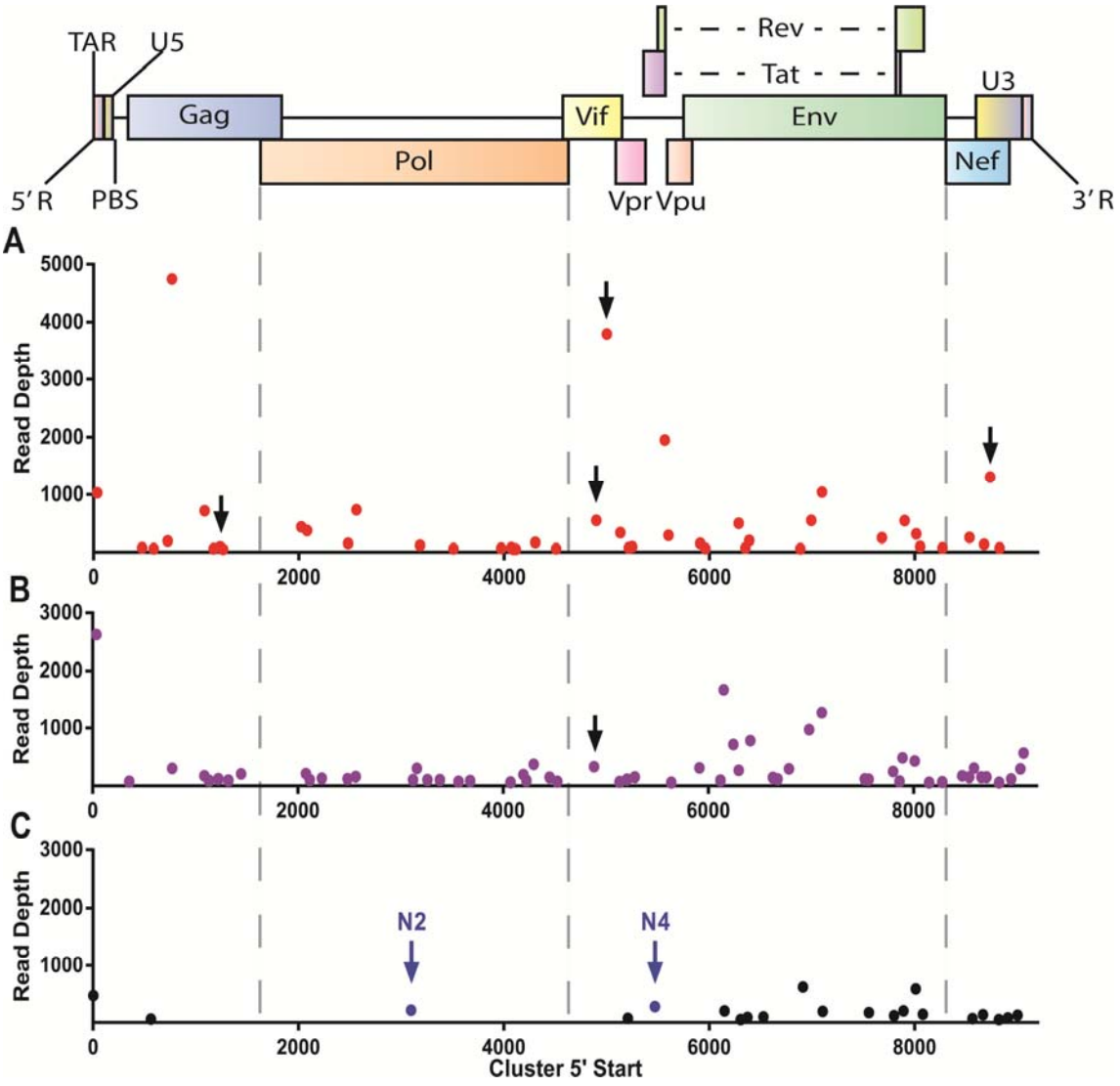

Figure 3-9: Alignment of PAR-CLIP clusters with the HIV-1 genome. The PAR-CLIP technique was performed on HIV-1-infected cells using a monoclonal antibody specific for RISC. Each HIV-1-specific PAR-CLIP cluster, identified by bioinformatic analysis using the PARalyzer program [155], is aligned to the HIV-1 genome based on the 5′-most nucleotide of the read cluster. Clusters indicated by black arrows were successfully assigned to specific cellular miRNAs and are analyzed in Fig. 3-10. Clusters indicated by blue arrows derive from the amiRNAs N2 and N4 [100] that were expressed in the TZM-bl ami cells. (A) C8166 cells infected with NL4-3; (B) TZM-bl cells infected with WT/BaL; (C) TZM-bl ami cells infected with WT/BaL.

As shown in Fig. 3-9, we identified a number of RISC binding clusters on the HIV-1 RNA genome in both C8166 and TZM-bl cells. However, we were surprised by the low level of RISC binding to the viral RNA genome observed. As shown in Table 3-2, we recovered ~$1.7x10^7$ assignable PAR-CLIP reads from the HIV-1 infected C8166 cells, of which only 0.21% aligned to the HIV-1 RNA genome. Similarly, we recovered $6.8x10^6$ assignable PAR-CLIP reads from the HIV-1 infected TZM-bl cells, of which only 0.3% aligned to the HIV-1 genome. Analysis of the number of HIV-1 RNA strands present in the C8166 cells at the time of crosslinking revealed ~20,707 HIV-1 transcripts, while analysis of the crosslinked TZM-bl cells revealed ~407,661 HIV-1 strands per cell. Previous work has suggested that cells contain between ~10^5 and ~$5x10^5$ mRNA molecules per cell, depending on the size of the cell and particularly of the cell cytoplasm [171]. As T cells have a small cytoplasm, we can estimate that they likely contain ~200,000 total mRNA molecules per cell, which would mean that HIV-1 contributes ~10% of the total mRNA pool in the infected C8166 cells. In the larger TZM-bl cells, HIV-1 would appear to be responsible for at least 50% of the total mRNA pool, even assuming that the 407,661 HIV-1 strands are largely added to a pre-existing mRNA pool of ~$5x10^5$ molecules. Therefore, HIV-1 contributes 10% of the total mRNA in C8166 cells but is only bound to ~0.21% of the available RISC, an underrepresentation of ~48 fold. This effect is even more extreme in TZM-bl cells, where HIV-1 contributes ~50% of the total mRNA pool but only ~0.31% of the total RISC binding events, an

underrepresentation of ~160 fold. It therefore appears that RISC recruitment to HIV-1 mRNAs is inefficient.

Table 3-2: Overview of the HIV-1 PAR-CLIP libraries analyzed. This table summarizes the characteristics of the HIV-1-infected cell PAR-CLIP libraries, including the total number of assignable (≤1 mismatch) PAR-CLIP reads (column 2), the percentage of PAR-CLIP reads that can be assigned to HIV-1 RNAs (column 3), and the total number of HIV-1 transcripts per cell at the time of cross-linking and RNA harvest (column 4), as determined by qRT-PCR with RNA standards.

Library	**Total no. of assignable PAR-CLIP reads**	**HIV-1 PAR-CLIP reads (%)**	**No. of HIV-1 RNA strands per cell**
C8166/NL4-3	17,347,389	0.21%	20,707
TZM-bl/WT-BaL	6,817,180	0.30%	407,661
TZM-bl ami/WT-BaL	11,077,171	0.05%	15,756

While low, RISC binding to HIV-1 is certainly detectable and we therefore wished to ask if the observed binding sites were functional. In fact, for unclear reasons, relatively few RISC binding sites could be assigned to any of the miRNAs present in the infected cells. However, our analysis did predict that four RISC binding clusters detected in HIV-1 infected C8166 cells, indicated by black arrows in Fig. 3-9, were likely caused by miR-423 (cluster at position 1233), miR-301a (cluster 4898), miR-155 (cluster 5001) and miR-29a (cluster 8735), respectively. We note that miR-423 represented ~0.63% of total cellular miRNA reads in the C8166 cells used in this experiment, miR-301a ~0.10%, miR-155 ~5.43% and miR-29a ~3.24% of total miRNA reads, as determined by deep sequencing performed in parallel. We note that the putative miRNA-29a-specific cluster has previously been reported by two other groups, who argued that miR-29a is,

in fact, able to inhibit HIV-1 replication [70, 71]. In contrast, another group has reported that this proposed miR-29a target site is largely blocked by HIV-1 RNA secondary structure [72]. Of these four clusters, only one cluster was also detected in TZM-bl cells, which express miR-301a and miR-423 but not miR-29a or miR-155. The PAR-CLIP reads that contribute to each of these clusters are listed in Fig. A-3, where they are aligned to the relevant cellular miRNA.

To test whether these miRNAs are indeed able to bind to these regions of the HIV-1 NL4-3 genome, we used PCR to clone ~300bp segments of the HIV-1 genome centered on each of the PAR-CLIP clusters we had detected. These segments were inserted 3' to the Renilla luciferase (Rluc) indicator gene present in the psiCHECK2 indicator plasmid, which also contains an internal control firefly luciferase (Fluc) expression cassette in *cis*. We also constructed derivatives of each of these indicator plasmids in which the predicted seed sequence present in the HIV-1 DNA fragment was mutated, to prevent miRNA binding, as shown in Fig. A-3. Co-transfection of the indicator plasmids bearing the 1233, 4898 and 5001 clusters into 293T cells, together with either the cognate miRNA expression vector or a control plasmid, revealed specific downregulation in the presence of the relevant cellular miRNA that was lost when the seed target sequence in HIV-1 was mutated (Fig. 3-10. In contrast, the 8735 cluster did not confer downregulation on the Rluc gene in the presence of a miR-29a expression plasmid, even though we observed strong downregulation of a control Rluc vector

bearing two perfect miR-29a target sites (Fig. 3-10). We therefore conclude that HIV-1 transcripts can indeed bind miR-423, miR-301a and miR-155 in infected C8166 T cells and that this interaction has the potential to reduce HIV-1 gene expression. In contrast, even though we did detect a RISC binding cluster at a *nef* miRNA target site previously reported to bind miR-29a, we failed to see downregulation by miR-29a when this cluster was inserted into an Rluc indicator plasmid, a result which agrees with data previously reported by Sun et al. [72]. Therefore, it appears that miR-29a binding to this region of the HIV-1 nef gene, while detectable by PAR-CLIP (Fig. 3-9A), is too inefficient to mediate significant gene repression (Fig. 3-10). It remains possible that this interaction is functionally significant in other contexts, for example, in cells expressing very high levels of miR-29a and/or very low levels of HIV-1 transcripts.

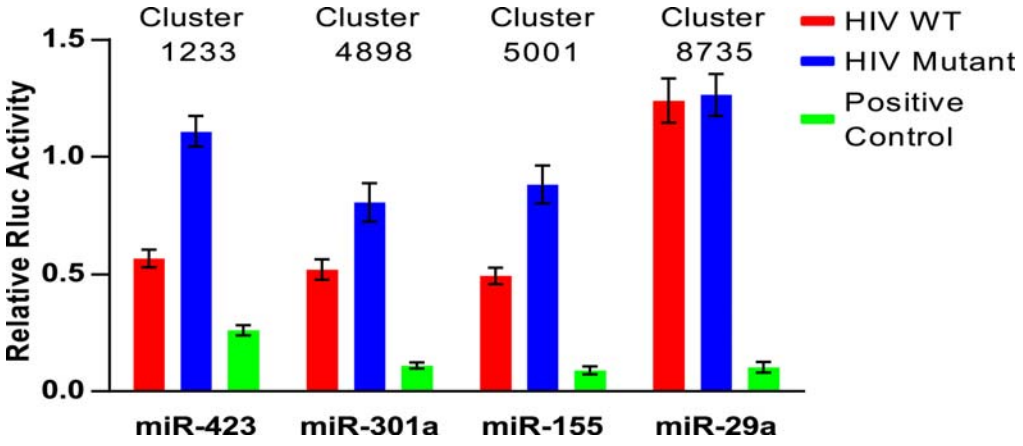

Figure 3-10: Identification of specific cellular miRNA binding sites in the HIV-1 genome. We constructed indicator plasmids containing ~300bp segments of the HIV-1 genome, encompassing the clusters indicated by black arrows in Fig. 3-9A, inserted 3′ to the Rluc indicator gene. Derivatives in which the predicted seed target for a cellular miRNA were mutated were also generated (see Fig. 3A), as was a positive-control indicator plasmid containing two perfect target sites for each of the four miRNAs being tested. These were then co-transfected into 293T cells along with the cognate cellular miRNA expression plasmid or a control plasmid. Rluc values are shown normalized to the Fluc internal control and to the level seen in cells lacking the cognate miRNA expression vector, which was set at 1.0. Note that the inhibition in Rluc expression seen with the wild-type (WT) indicator in the presence of the cognate miRNA is lost when the seed target in the HIV-1 sequence is mutated. This figure shows the average of four independent experiments, with the standard error of the mean indicated.

As a further demonstration that miRNAs can indeed guide RISC to the HIV-1 genome, we took advantage of a recent study that identified artificial miRNAs (amiRNAs) that are able to effectively inhibit HIV-1 gene expression and replication by testing over 9,000 different amiRNAs, tiled at 1nt increments across the HIV-1 RNA genome, for their ability to block HIV-1 replication in culture [100]. Interestingly, few of these amiRNAs proved to be effective, thus suggesting that access to the HIV-1 RNA genome was largely occluded for most of the RISCs programmed with these amiRNAs [100]. We expressed two amiRNAs that were shown to be effective, termed N2 and N4,

by engineering these amiRNAs into retroviral expression vectors and then selecting TZM-bl cells that stably expressed the N2 or N4 amiRNA, as determined by small RNA deep sequencing. The N2- and N4-expressing TZM-bl cells were then infected with HIV-1 strain WT/BaL and PAR-CLIP performed as described above. As expected based on previous work [100], we observed that these TZM-bl cells were largely non-permissive for HIV-1 replication, as the level of HIV-1 transcripts detected in TZM-bl cells expressing N2 and N4, which are fully complementary to the HIV-1 RNA genome, was reduced ~25 fold relative to infected wild-type TZM-bl cells (Table 3-2). Nevertheless, despite the much lower level of HIV-1 RNAs present in these cells, we were able to readily detect PAR-CLIP clusters that precisely aligned with the expected binding sites of RISCs programmed with either the N2 or N4 amiRNA. These interactions were detected despite the potential for Ago2-containing RISCs programmed by these amiRNAs to cleave the viral genome within the binding cluster (Fig. 3-9) [1]. Therefore, these data demonstrate that miRNAs are indeed able to guide RISC to the HIV-1 RNA genome if the target area is accessible.

To address the question of whether endogenous cellular miRNAs limit viral replication, we used 293T cell lines incapable of generating mature miRNAs due to Dicer ablation with transcription activator-like effector nucleases (TALENs) targeted to exon 5 of the *dcr* gene. Two clonal lines of these NoDice cells, NoDice(2-20) and NoDice(4-25), have been previously shown to lack the ability to generate mature miRNAs [172].

To examine how HIV-1 replicates in the absence of miRNAs, we divided our analysis of the HIV-1 replication cycle into two parts, i.e., from infection to proviral integration and gene expression (Fig. 3-11A and B) or from viral gene expression through virion release to target cell infection (Fig. 3-11C). The ability of NoDice cells to support productive HIV-1 infection was analyzed using stocks of HIV-1 indicator viruses bearing either the FLuc gene (Fig. 3-11A) or the green fluorescent protein (GFP) gene (Fig. 3-11B). The levels of infection of the 293T and NoDice cells were analyzed at 24 h post-infection by luciferase assay (Fig. 3-11A) or at 48 h post-infection by quantitation of the number of GFP-positive cells by fluorescence-activated cell sorter (FACS) (Fig. 3-11B). No difference in the level of infection was observed in either case. Next we tested whether NoDice cells would be able to produce infectious HIV-1 virions by transfecting wild-type 293T cells or NoDice(2-20) or NoDice(4-25) cells with a vector encoding a replication-competent HIV-1 provirus. Supernatant media were then harvested and used to infect the indicator cell line TZM-bl, which expresses FLuc only after HIV-1 infection [148]. As may be observed (Fig. 3-11C), we detected at most a modest reduction in the ability of NoDice cells to produce infectious HIV-1 virions and certainly no evidence of enhanced virus production.

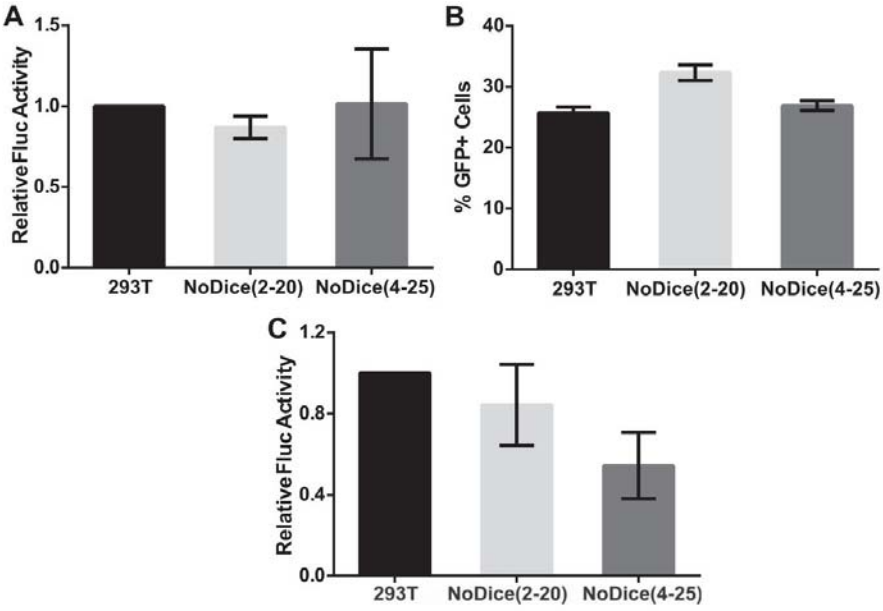

Figure 3-11: Analysis of HIV-1 infection and progeny production in the presence and absence of Dicer function. (A) Wild-type 293T cells or the NoDice(2-20) and NoDice(4-25) cell lines were infected with an equal amount of a previously described HIV-1 derivative engineered to express FLuc [158]. At 24 h post-infection, the cells were lysed and the level of FLuc expression was quantitated. (B) Shown are the results of an experiment similar to that for panel A, except that the cells were infected with an HIV-1 derivative engineered to express GFP. The level of transduced cells was quantitated by FACS at 48 h post-infection. (C) 293T or NoDice cells were transfected with a plasmid encoding a full-length replication-competent HIV-1 provirus together with an internal control plasmid expressing GST. At 48 h post-transfection, the supernatant media and transfected cells were harvested, and the former was filtered and then used to infect the indicator cell line TZM-bl, which expresses FLuc only after HIV-1 infection. Induced FLuc expression levels were determined at 24 h post-infection. In parallel, the level of expression of the GST internal control in the transfected cells was determined by Western blotting and used to correct the level of FLuc expression. Averages of three independent experiments are shown in each panel with SDs indicated.

Analysis of the production of infectious HIV-1 virions by the NoDice cells demonstrated that these cells were comparable to the parental 293T cells, i.e., neither cellular miRNAs nor the Dicer protein are required for the production of infectious HIV-1 (Fig. 3-11).

3.5 *Discussion*

In this work we have attempted to comprehensively address how HIV-1 interacts with cellular miRNA biogenesis and effector mechanisms. Our first goal was to unequivocally answer the previously controversial question of whether HIV-1 itself encodes any miRNAs. While two previous studies, that used conventional sequencing techniques, had failed to detect any HIV-1-encoded miRNAs [37, 38], there are also a substantial number of papers suggesting that HIV-1 does encode miRNAs and/or siRNAs, particularly in the viral *nef* gene, the viral TAR element, within the HIV-1 RRE or derived from some form of viral antisense RNA [41, 42, 45, 47-49, 52, 53]. Here, we have used both CXCR-4-tropic and CCR5-tropic HIV-1 infection of a range of cell types, combined with deep sequencing of total and RISC-associated small RNAs, to address whether any of these proposed miRNAs or siRNAs in fact exist. The cells used were analyzed at 3 days after infection, with the exception of MDMs which were analyzed at 27 days after infection, yet FACS analysis, in the case of CD4+ PBMCs (Fig. A-2), or analysis of β-gal expression in the case of the indicator cell line TZM-bl (Fig. A-1), reveal that these cells were efficiently infected, and we also detected high levels of viral RNA transcripts in all four infected cell types (Table 3-1). Nevertheless, we failed to detect any HIV-1-specific miRNAs or siRNAs, including from the *nef* region, TAR and RRE, even though these putative viral miRNA sequences are all present in one or more of the viruses analyzed (Fig. 3-3, Fig. 3-7). The one region that did give rise to a readily

detectable level of viral small RNA reads did not show loading into RISC (Fig. 3-6) and likely represents a region of the HIV-1 Gag/Pol mRNA that is protected by stalled ribosomes, as it precisely coincides with the sequence that induces ribosome frameshifting (Fig. 3-4) [161]. In general, HIV-1-derived small RNAs did not show the predicted 22±2nt length (Fig. 3-2), were not loaded into RISC (Fig. 3-6), did not show the expected discrete 5' ends (Figs. 3-4 and 3-5) and, perhaps most importantly, never exceeded the 0.1% level of the total cellular miRNA pool recently shown to be critical for miRNA function [10].

In addition to encoding viral miRNAs, viruses can also facilitate their replication by enhancing or repressing the expression of specific cellular miRNAs. HIV-1 infection has in fact been proposed to affect, especially repress, the expression of a number of cellular miRNAs, including the cellular miR-17/92 miRNA cluster [72, 77]. This latter effect has been proposed to facilitate HIV-1 replication by de-repressing expression of the PCAF acetyltransferase, a proposed co-factor of the HIV-1 Tat transcription factor.

A shared characteristic of these two earlier studies is that they looked at changes in cellular miRNA expression at a substantial time after initial infection with HIV-1. Thus, Triboulet *et al*. [77] measured cellular miRNA expression at 21 and 42 days post-infection while Sun *et al*. [72] only saw significant changes in cellular miRNA expression at 21 days post-infection. However, data obtained in vivo using inhibitors of HIV-1 replication have revealed that HIV-1-infected T cells only survive an average of ~24

hours after infection [169]. Moreover, long term culture of HIV-1-infected T cells maximizes the level of cytopathic effect that is observed, and this undoubtedly has the potential to influence cellular gene expression. We therefore felt it was most appropriate to examine the effect of HIV-1 infection at early times after infection, specifically at 72 h post-infection, and our data do not suggest that, at this time point, HIV-1 infection has a strong effect, either positively or negatively, on cellular miRNA expression (Fig. 3-8). In particular, we saw no significant effect on the expression of members of the miR-17/92 miRNA cluster, including miR-92a itself, which was one of the more highly expressed miRNAs in both TZM-bl cells and T cells (Fig. 3-8). Nevertheless, we did see some modest but perhaps significant increases or decreases in the expression of some cellular miRNAs (Fig. 3-8), though these are not the miRNAs previously reported by others. The functional significance of these ≤3-fold changes in a small number of cellular miRNAs is unclear and may not be significant, at least during lytic HIV-1 replication.

In a recent study, Chang *et al*. [78] reported an analysis of cellular miRNA expression in the SUP-T1 T cell line at 5, 12 and 24 h post-infection with HIV-1. They reported that 14 known cellular miRNAs showed significant changes in expression, generally reductions, and they also proposed the existence of a novel cellular miRNA (miR-EPB41L2) that was down-regulated by ~10-fold in HIV-1 infected SUP-T1 cells. Analysis of our data in primary CD4+ T cells, C8166 T cells and TZM-bl cells showed that only one of these 14 miRNAs (miR-21-3p) was expressed at significant (>0.1%)

levels in primary T cells and miR-21-3p expression was not affected by HIV-1 infection (Table A-1C). Only two of these 14 miRNAs were expressed in C8166 cells at significant levels (miR-21-3p and miR-143-3p) and miR-143-3p indeed showed an ~60% reduction in expression after HIV-1 infection (Table A-1B). Finally, 7 of the 14 miRNAs reported by Chang *et al*. [78] to be significantly affected by HIV-1 infection were expressed at significant levels in TZM-bl cells, but only one, miR-10a-5p, showed a significant, ~60% reduction in expression level (Table A-1A). Therefore, while we agree with Chang *et al*. [78] that some cellular miRNAs do show modest changes in expression after HIV-1 infection, these miRNAs vary with the cells being examined and observed changes are quite limited in the most relevant experimental system, i.e., primary CD4+ T cells (Fig. 3-8, Table A-1C).

Given that HIV-1 neither encodes viral miRNAs nor substantially alters cellular miRNA expression during lytic replication in culture, we are left with the question of how the cellular miRNAs encountered by HIV-1 in infected cells affect HIV-1 replication. Previously, others have proposed that cellular miRNAs might promote HIV-1 latency in resting primary CD4+ T lymphocytes [69] and inhibit productive HIV-1 replication in primary monocytes [66]. One particular cellular miRNA, miR-29a, has been suggested to efficiently bind to an RNA target site in the HIV-1 viral *nef* gene [70, 71] although others have reported that this miR-29a target sequence is actually blocked by viral secondary structure [72].

To comprehensively identify sites on the HIV-1 RNA genome that are actually occupied by miRNA-programmed RISC in infected T cells or epithelial cells, we used the previously described PAR-CLIP technique [150, 151], which uses deep sequencing of short mRNA sequences cross-linked to RISC to identify miRNA binding sites. As shown in Fig. 3-9, we were able to identify a number of RISC binding sites on the HIV-1 genome. Many of these either did not show seed homology to any of the miRNAs found to be expressed in these cells at the time that PAR-CLIP was performed, as determined by deep sequencing performed in parallel, or did not prove to be inhibited by the cellular miRNAs that were predicted to bind there, when analyzed by indicator assays (data not shown). However, we were able to assign three RISC-binding clusters identified in HIV-1-infected C8166 cells, one of which was conserved in TZM-bl cells, to the cellular miRNAs miR-423, miR-301a and miR-155 and to further show that these targets could indeed confer downregulation in the presence of these miRNAs, when tested in indicator constructs (Fig. 3-10). Interestingly, we also detected a significant cluster of PAR-CLIP reads in C8166 cells coincident with the previously reported miR-29a target located in the *nef*/LTR U3 region overlap (Fig. 3-9A) [70, 71]. However, an indicator construct containing this region of the HIV-1 genome was not inhibited by miR-29a when co-expressed in 293T cells, even though we could show that miR-29a was able to inhibit a control indicator construct (Fig. 3-10). We conclude that miR-29a

binding to this site in *nef* likely occurs but is inefficient, as also previously proposed by others [72].

Two miRNAs in particular, miR-29a and miR-28, have been reported to suppress HIV-1 gene expression [69, 70] and both of which are expressed at substantial levels in 293T cells, comprising ~0.16% and ~1.0% of the total miRNA pool, respectively (Table A-2). To determine if cellular miRNAs are indeed refractory to HIV-1 replication, we used two previously reported 293T-derivative cell lines, NoDice(2-20) and NoDice(4-25) [157, 172], in which the *dcr* gene has been mutated by TALENs resulting in a loss of both Dicer and mature miRNA biogenesis. The expression of virally-encoded firefly luciferase was comparable between infected cultures of NoDice cells and wild type 293T (Fig. 3-11A). The transduction efficiency of target cells by HIV-1 was also not affected by the loss of Dicer (Fig. 3-11B). Similarly, viral production was not enhanced in cells lacking miRNAs, with at most a modest reduction detected in viral titers (Fig. 3-11C). Together these data indicate that early stages of HIV-1 infection and viral production are not affected by the absence of Dicer and mature miRNAs.

A possibly surprising result that arose from this PAR-CLIP analysis is that HIV-1 transcripts, despite constituting from 10% to as much as 50% of the total mRNA population in infected cells only account for ~0.3% of the total assignable PAR-CLIP reads, i.e., HIV-1 transcripts are ~100-fold less likely to bind RISC than the cellular mRNAs present in the same cells. Extensive biochemical analysis has in fact revealed

that the HIV-1 RNA genome is highly structured [173] and it has previously been reported that this RNA structure greatly limits the ability of amiRNAs to effectively block HIV-1 replication in culture [100]. We have confirmed that two amiRNAs that were reported previously to inhibit HIV-1 replication [100] are indeed able to recruit RISC to the HIV-1 RNA genome (Fig. 3-9C) and inhibit HIV-1 replication (Table 3-2), so these data, in total, are most consistent with the hypothesis that miRNA-programmed RISCs can inhibit HIV-1 replication if they can access a target site but that the majority of the HIV-1 genome is occluded, most probably by RNA secondary structure. This may explain why HIV-1 seems able to grow in almost any human cell line that expresses the relevant cell surface receptors, even though these cells can exhibit very different miRNA expression patterns, i.e., HIV-1 is resistant to miRNAs not because it has evolved to selectively exclude binding sites for T cell or macrophage specific miRNAs but because it has evolved a mechanism to render the viral transcripts largely refractory to RISC binding by adopting extensive secondary structure. While this viral RNA secondary structure may indeed have evolved as a means to reduce inhibition of viral mRNA function by cellular miRNAs, we note that extensive viral RNA secondary structure might also have evolved as a way to reduce inhibition by other cellular innate immune factors, e.g., RNase L, or to facilitate viral RNA packaging into virion particles. Nevertheless, it will be interesting to see whether this is a common mechanism by which

viruses, especially RNA viruses, avoid inhibition by the cellular miRNA machinery in infected cells.

4. Conclusions

Retroviruses may principally interact with the host microRNA machinery in two ways: viral transcripts may serve as miRNA precursors that are processed into mature miRNAs and/or viral transcripts may be targeted by cellular miRNAs. Regulation by viral and/or host miRNAs has the potential to facilitate or restrict replication and to promote viral latency. Here, we have demonstrated that certain retroviruses encode their own miRNAs and that endogenous miRNAs are unable to limit replication of particular retroviruses, especially HIV-1.

4.1 *Retrovirally-encoded microRNAs*

A large number of miRNAs encoded by DNA viruses have been reported to facilitate replication through repression of host genes and to regulate stages of the viral lifecycle by targeting viral transcripts [31, 32, 174-176]. Numerous investigations, however, have failed to identify bona fide miRNAs in mammalian cells that are encoded by an RNA virus [37, 39, 40]. While early investigations into retrovirally-encoded miRNAs were controversial, there are now several known examples of distantly-related retroviruses that encode miRNAs.

The first example of a retrovirus known to encode miRNAs is the deltaretrovirus bovine leukemia virus (BLV) [19, 60]. BLV expresses high levels of five pre-miRNAs in latently-infected cells, each directly transcribed from separate RNA Pol III promoters. After transcription, the pre-miRNAs are exported to the cytoplasm and processed into

mature miRNAs by Dicer. It is important to note that the ~22bp stems of the BLV pre-miRNAs are too short for processing by Drosha which requires a longer stem length of ~33bp [16, 17]. Thus, by directly transcribing pre-miRNAs with Pol III, BLV is able to express high levels of mature miRNAs without encoding genomic RNA sequences that can be cleaved by Drosha. One BLV miRNA is homologous to the oncogenic host miRNA miR-29a and likely promotes cell growth and survival to maintain infection *in vivo* [19].

In contrast, avian leukosis virus subgroup J (ALV-J), an alpharetrovirus, encodes a single miRNA from RNA transcribed by RNA Pol II [112]. This miRNA is believed to be processed as a canonical pri-miRNA as knockdown of endogenous Drosha and Dicer with RNA interference resulted in decreased production of the ALV-J miRNA. However, it is unclear what effects Drosha processing has on the levels of genomic transcripts or subgenomic mRNAs during infection. While the genes regulated by this miRNA are currently unknown, it is likely this miRNA as well promotes the growth and survival of infected cells as the non-coding element from which this miRNA originates, E (XSR), is essential for ALV-J oncogenicity in birds [177].

Bovine foamy virus (BFV), a spumaretrovirus, is the third documented example of a retrovirus that encodes miRNAs as discussed in Chapter 2. BFV expresses high levels of three mature miRNAs that, similar to BLV miRNAs, originate from a Pol III transcript. This BFV transcript, however, is transcribed as one ~122nt pri-miRNA that is

subsequently cleaved into two separate ~60nt pre-miRNAs which then give rise to three mature miRNAs that account for over 70% of all small RNAs in persistently-infected cells. Though the transcripts targeted by these miRNAs are currently unknown, the high levels of viral miRNAs in persistently-infected cells provide an ideal setting for their determination by RISC PAR-CLIP. Interestingly, the seed sequence of one BFV miRNA, miR-BF1-5p, is identical to another miRNA encoded by a bovine virus, bovine herpesvirus-1 miR-B5 suggesting that this miRNA may target host genes involved in broad anti-viral responses.

A pri-miRNA structure with two adjacent pre-miRNA stem-loops in mammalian cells was first reported with BFV. Shortly after this observation was published, Kincaid *et al* reported seven Pol III-driven pre-miRNAs encoded by simian foamy viruses (SFV), some of which originate from similar dumbbell-shaped pri-miRNA transcripts [178]. This noncanonical miRNA biogenesis strategy may therefore be conserved across a wide number of foamy viruses and other retroviruses.

The function of these SFV miRNAs is better understood as two mature SFV miRNAs, miR-S4-3p and miR-S6-3p, share seed identity to host miR-155 and miR-132, respectively [178]. Expression of miR-155 is associated with lymphoproliferation [163] and cell survival while miR-132 downregulates transcription of the type I interferon response [179], indicating that the SFV miRNAs function in immunosuppression and to promote the growth of infected cells.

Another retrovirus examined in detail for the ability to express miRNAs is human immunodeficiency virus type 1 (HIV-1). Several studies have suggested that structured regions of the genome are processed into mature miRNAs [45, 47, 50]. However, subsequent studies have failed to detect any highly-expressed HIV-1 miRNAs [37, 38], or miRNAs encoded by human T cell leukemia virus type 1 (HTLV-1). As discussed in Chapter 3, analysis of small RNAs in numerous infected contexts using modern high-throughput sequencing techniques confirms that no HIV-1-derived small RNAs are expressed at levels required for functional activity. The majority of HIV-1 small RNAs are $\leq$18nt and therefore too small to serve as functional miRNAs. Coupled with the fact that the HIV-1 small RNAs have widely diffuse genomic origins, this suggests that HIV-1 small RNAs result from degradation of viral transcripts. Furthermore, unlike cellular miRNAs, the vast majority of HIV-1 small RNAs are not RISC-associated. Together, these data unequivocally demonstrate that HIV-1 does not express mature miRNAs.

It appears then that the ability to encode miRNAs is not universally conserved among retroviruses. Currently, only four retroviruses are known to express mature miRNAs. As these four viruses are quite distantly related, it is likely that a wide variety of other retroviruses are capable of generating miRNAs. The majority of known retroviral miRNAs are transcribed by Pol III, which bypasses the issue of maintaining nuclease-sensitive regions in the viral genome. Pol III transcripts have been identified

[180] or predicted [19] in a number of other retroviruses and these are ideal candidates to examine for the ability to generate mature miRNAs, now a facile task with modern RNA sequencing technologies.

4.2 *MicroRNA Targeting of HIV-1 Transcripts*

Cellular miRNAs have been shown to bind and regulate the expression of numerous viral genes [62, 115, 181]. Given the demonstrated ability of HIV-1 to rapidly evolve resistance to RNA interference [102-108], it is likely that HIV-1 and other retroviruses have adapted to avoid inhibitory targeting by miRNAs expressed in their tissue tropisms. While miR-32 may inhibit primate foamy virus replication in kidney cell lines [62], it is unknown if this inhibition occurs *in vivo*. Though the cellular miRNA profile has been associated with host susceptibility to HIV-1 [63-67], it is not clear if the endogenous miRNA pool directly regulates viral replication through interactions with viral transcripts or indirectly by controlling the expression of host genes. In addition, Argonaute proteins have been reported to directly interact with Gag to facilitate viral production [182] but this phenomenon has not been consistently observed [183].

There are numerous examples of viruses that manipulate the expression of host miRNAs to enhance various stages viral lifecycle [4, 163, 167, 179]. This activity has been attributed to HIV-1 for a large number of cellular miRNAs [66, 69, 72, 76-79]. However, the majority of these conclusions were based on sequencing of long-term infected cultures, which contain different subpopulations of infected cells and exhibit increased

cytopathic effects, conditions likely to induce changes in gene expression. As discussed in Chapter 3, no global disturbances in endogenous miRNA levels were observed in a number of infected backgrounds at three days post-infection. While a $\geq$2-fold change in the relative abundance of a few individual miRNAs was observed, these changes were not observed in other cell types expressing these particular miRNAs suggesting that HIV-1 does not have a reliable mechanism to alter the host miRNA profile.

Several cellular miRNAs are predicted to target HIV-1 transcripts; however, a consistent antiviral activity for these miRNAs has not been observed throughout multiple studies [66-71]. As discussed in Chapter 3, sequencing of RISC-associated transcripts using photoactivatable ribonucleoside-induced crosslinking and immunoprecipitation (PAR-CLIP) revealed that over 99% of miRNA targets in HIV-1-infected cells are cellular transcripts. As HIV-1 transcripts comprise 10-50% of the mRNA pool, this suggests that viral transcripts are refractory to RISC binding, most likely due to the extensive secondary structure reported in the viral genome. Nevertheless, we identified three separate viral sequences that can be targeted by miRs -155, -301a, and -423 in the context of reporter assays. However, no effects on HIV-1 infectivity and production were observed from ablation of mature miRNAs in the 293T cell line, which expresses high levels of several miRNAs predicted to target the viral genome including miR-301a and miR-423 (Table A-2). This suggests that the majority of cellular miRNAs are not capable of binding viral transcripts at a level required to impact

viral replication. The question remains of whether miR-155, which is highly expressed in lymphoid tissues, is capable of inhibiting viral replication in cell types relevant to infection *in vivo*.

Overall, this work demonstrates that different retroviruses interact with the host miRNA machinery in differing ways. While some retroviruses are capable of expressing mature miRNAs, this activity is not observed with others, particularly HIV-1. Though the replication of PFV may be limited in cells expressing miR-32 [62], HIV-1 appears refractory to regulation by endogenous miRNAs, most likely by occluding RISC-targeting with extensive RNA secondary structure. Thus, while the endogenous miRNA profile has been associated with host susceptibility to HIV-1 [63-68], this is most likely due to regulation of host factors rather than direct targeting of viral transcripts. Understanding the nature of retroviral interactions with cellular miRNA effectors will provide insight into viral lifecycles and may identify novel regulators of viral replication. Of interest will be ablating expression of Ago2, Dicer, specific miRNAs, or other RISC-associated proteins to elucidate their roles in regulating the replication of specific retroviruses in cell types relevant to infection *in vivo*. Additionally, therapeutic approaches using RNA interference against HIV-1 are likely to be more efficacious when targeting non-essential cellular factors critical for replication such as CD4 [86], CCR5 [90], and LEDGF/p75 [184] over viral sequences which can be readily mutated.

Appendix

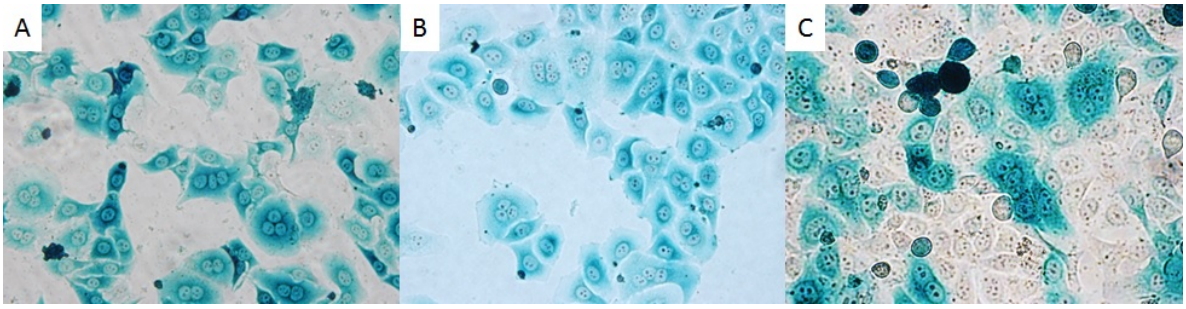

Figure A-1: β-galactosidase staining of TZM-bl cell cultures. This figure shows β-galactosidase staining of the TZM-bl cells analyzed 72 h post-infection with WT/BaL in Fig. 3-1 and 3-9. A) TZM-bl culture used for deep of total sequencing and RISC-associated RNAs. B) TZM-bl culture used for PAR-CLIP. C) TZM-bl ami cells used for PAR-CLIP.

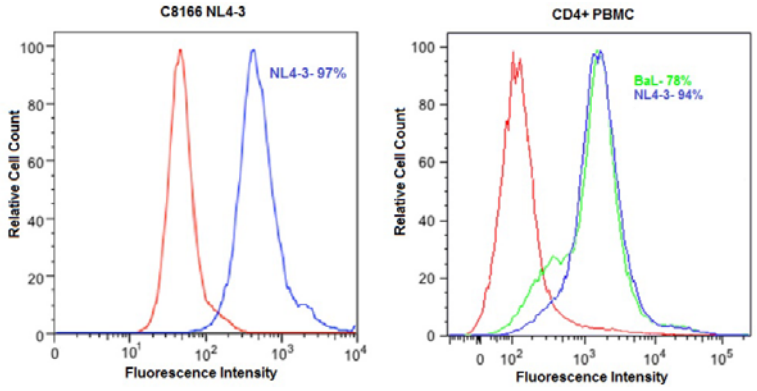

Figure A-2: FACS analysis of uninfected and HIV-1-infected C8166 and CD4+ PBMCs. This figure shows a FACS analysis of the C8166 cells and CD4+ PBMCs analyzed in Fig. 3-1 to 3-5 and 3-8. Coincident with RNA harvest, HIV-1-infected cells and control cells grown in parallel were stained with pooled human anti-HIV-1 IgG followed by FITC-conjugated goat anti-human IgG and analyzed by FACS, which revealed a substantial and specific increase in the detected level of fluorescence. Red indicates uninfected cells, blue or green indicates HIV-1-infected cells. The approximate percentage of cells infected with HIV-1 in each sample was calculated based on this analysis and is indicated.

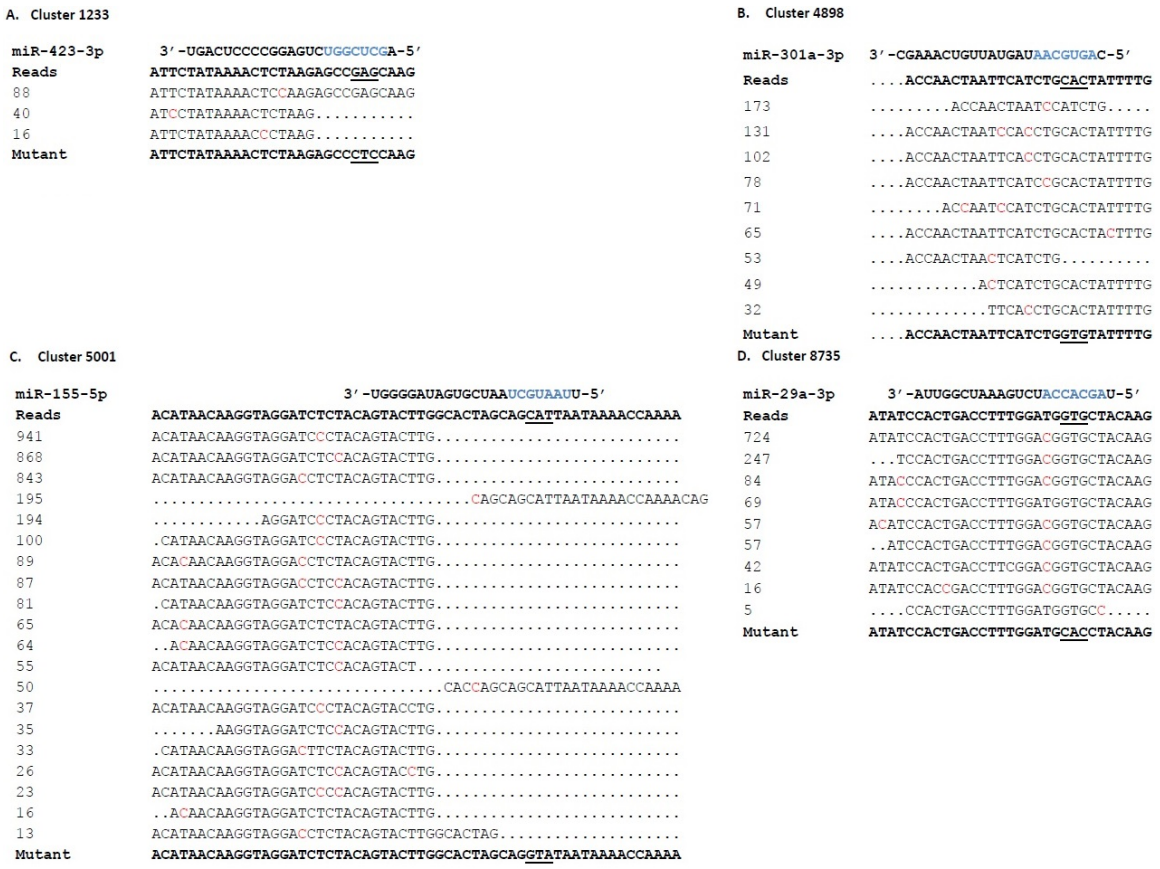

Figure A-3: PAR-CLIP reads that contribute to the 1233, 4898, 5001, and 8735 clusters indicated in Fig. 3-9. The reads that form each of these clusters are listed, including the number of times each read was recovered, and are aligned to the WT HIV-1 sequence (second row) and the likely responsible miRNA, with the seed sequence shown in blue (first row). T to C conversions, resulting from the PAR-CLIP procedure, are indicated in red. The mutant HIV-1 sequences analyzed in Fig. 3-10 are given at the bottom of each panel, with the mutated bases underlined.

Table A-1: Highly-expressed microRNAs in HIV-1-infected cells. The total number of reads shown represents the sum of the reads recovered from uninfected and HIV-1-infected cells. For each miRNA, the percentile representation in the uninfected and infected cell contexts is shown, with miRNAs showing ≥2-fold differences indicated in red. (A) TZM-bl cells; (B) C8166 cells; (C) CD4+ PBMCs. These data are presented graphically in Fig. 3-8.

A) TZMbl RIP-Seq Rank	miRNA	Total Reads	% of Total miRNAs	
			Uninfected	WT-BaL Day 3
1	miR-92a-3p	5,569,650	12.73%	13.07%
2	miR-21-5p	3,554,294	6.39%	10.14%
3	miR-10a-5p	3,399,397	11.23%	4.37%
4	miR-191-5p	2,890,452	8.64%	4.66%
5	let-7i-5p	2,752,334	4.90%	7.90%
6	let-7f-5p	2,621,534	6.14%	5.99%
7	miR-92b-3p	2,260,012	5.85%	4.59%
8	let-7a-5p	2,044,521	4.57%	4.90%
9	miR-10b-5p	1,653,895	4.76%	2.86%
10	miR-182-5p	1,583,216	3.22%	4.13%
11	miR-181a-5p	1,259,240	1.95%	3.93%
12	miR-27b-3p	1,148,133	2.47%	2.86%
13	miR-22-3p	775,211	1.56%	2.04%
14	miR-30a-5p	741,984	1.35%	2.10%
15	miR-30d-5p	729,185	1.48%	1.90%
16	miR-151a-5p	507,840	1.33%	1.02%
17	miR-151a-3p	454,292	0.93%	1.18%
18	miR-423-5p	416,660	0.75%	1.19%
19	miR-28-3p	398,686	0.95%	0.90%
20	miR-143-3p	390,892	0.78%	1.04%
21	let-7b-5p	352,074	0.80%	0.83%
22	miR-26a-5p	305,680	0.86%	0.55%
23	miR-181b-5p	298,799	0.51%	0.88%
24	miR-21-3p	298,407	0.54%	0.85%
25	miR-25-3p	277,638	0.65%	0.63%
26	miR-196a-5p	263,878	0.62%	0.60%
27	miR-186-5p	241,415	0.67%	0.44%
28	miR-99b-5p	237,313	0.71%	0.38%
29	miR-192-5p	231,167	0.53%	0.54%
30	miR-16-5p	224,988	0.53%	0.51%

31	miR-125a-5p	203,397	0.65%	0.28%
32	miR-378a-3p	189,339	0.36%	0.52%
33	miR-486-5p	176,737	0.34%	0.48%
34	let-7g-5p	169,271	0.36%	0.42%
35	miR-100-5p	166,260	0.48%	0.28%
36	let-7c-5p	160,442	0.33%	0.42%
37	miR-222-3p	153,511	0.29%	0.42%
38	miR-320a-3p	148,294	0.29%	0.40%
39	let-7e-5p	146,057	0.36%	0.31%
40	miR-98-5p	138,867	0.29%	0.36%
41	let-7d-5p	137,988	0.30%	0.34%
42	miR-103a-3p	134,824	0.22%	0.40%
43	miR-30a-3p	131,784	0.23%	0.38%
44	miR-423-3p	131,720	0.25%	0.36%
45	miR-181a-3p	130,242	0.22%	0.39%
46	miR-30e-5p	127,998	0.30%	0.30%
47	miR-130a-3p	119,445	0.30%	0.25%
48	miR-148a-3p	118,593	0.21%	0.34%
49	miR-27a-3p	101,002	0.24%	0.23%
50	miR-23a-3p	99,626	0.27%	0.19%
51	miR-125b-3p	94,720	0.20%	0.24%
52	miR-125b-5p	82,917	0.24%	0.15%
53	miR-941-3p	79,789	0.23%	0.14%
54	miR-148b-3p	77,799	0.18%	0.18%
55	miR-204-5p	72,886	0.14%	0.20%
56	miR-183-5p	71,269	0.22%	0.11%
57	miR-582-3p	63,752	0.08%	0.21%
58	miR-941-5p	60,602	0.18%	0.10%
59	miR-30e-3p	59,877	0.11%	0.16%
60	miR-199a-3p	54,780	0.12%	0.14%
61	miR-93-5p	54,150	0.11%	0.14%
62	miR-744-5p	44,258	0.05%	0.16%
63	miR-31-5p	43,284	0.09%	0.11%
64	miR-1304-3p	42,026	0.09%	0.10%
65	miR-421-3p	41,600	0.10%	0.10%
66	miR-1307-3p	40,400	0.07%	0.12%
67	miR-107-3p	40,249	0.06%	0.12%
68	miR-30c-5p	38,022	0.07%	0.11%

69	miR-140-3p	37,504	0.07%	0.10%

B) C8166 Rank	miRNA	Total Reads	% of Total miRNAs	
			Uninfected	NL4-3 Day 3
1	miR-146a-5p	1,409,946	18.43%	16.87%
2	let-7a-5p	824,399	12.92%	7.24%
3	miR-191-5p	816,165	11.73%	8.47%
4	let-7f-5p	526,826	5.93%	7.47%
5	miR-146b-5p	467,264	6.21%	5.46%
6	miR-92a-3p	382,029	3.88%	5.93%
7	miR-155-5p	353,367	3.32%	5.82%
8	miR-98-5p	339,838	4.93%	3.47%
9	miR-182-5p	320,155	3.45%	4.73%
10	miR-142-5p	239,631	2.28%	3.91%
11	miR-21-5p	183,455	2.16%	2.49%
12	miR-26a-5p	151,587	1.69%	2.17%
13	miR-181a-5p	114,797	1.24%	1.69%
14	miR-183-5p	107,718	1.70%	0.93%
15	miR-148a-3p	98,583	1.09%	1.43%
16	let-7i-5p	96,923	0.86%	1.66%
17	let-7g-5p	79,719	1.10%	0.89%
18	miR-30e-5p	65,228	0.70%	0.97%
19	miR-16-5p	62,557	0.80%	0.77%
20	miR-25-3p	59,172	0.64%	0.87%
21	miR-30a-5p	48,310	0.46%	0.79%
22	miR-222-3p	47,476	0.47%	0.75%
23	miR-205-5p	46,656	0.53%	0.66%
24	miR-30d-5p	46,460	0.52%	0.67%
25	miR-186-5p	45,807	0.44%	0.75%
26	let-7d-5p	43,117	0.61%	0.46%
27	miR-26b-5p	37,734	0.39%	0.58%
28	miR-221-3p	36,681	0.43%	0.50%
29	let-7b-5p	36,553	0.53%	0.37%
30	miR-27b-3p	34,742	0.45%	0.42%
31	miR-425-5p	33,335	0.42%	0.42%
32	miR-21-3p	31,087	0.45%	0.32%
33	miR-486-5p	30,997	0.41%	0.36%
34	miR-378a-3p	23,894	0.29%	0.31%

35	miR-27a-3p	23,760	0.32%	0.27%
36	miR-181c-5p	22,995	0.29%	0.28%
37	miR-143-3p	22,993	0.39%	0.16%
38	miR-9-5p	22,261	0.29%	0.26%
39	miR-93-5p	20,753	0.26%	0.27%
40	let-7c-5p	19,741	0.27%	0.22%
41	miR-30c-5p	19,725	0.23%	0.27%
42	miR-24-3p	19,225	0.28%	0.20%
43	miR-7-5p	19,130	0.14%	0.37%
44	miR-423-5p	18,646	0.14%	0.35%
45	miR-29a-3p	18,493	0.23%	0.24%
46	miR-342-3p	18,198	0.32%	0.12%
47	miR-423-3p	17,528	0.14%	0.32%
48	miR-941-3p	15,710	0.20%	0.19%
49	miR-103a-3p	15,574	0.19%	0.20%
50	miR-30e-3p	14,972	0.18%	0.20%
51	miR-148b-3p	14,675	0.19%	0.17%
52	miR-130b-3p	13,821	0.17%	0.18%
53	miR-23a-3p	12,936	0.19%	0.13%
54	miR-941-5p	12,084	0.15%	0.15%
55	miR-192-5p	11,368	0.18%	0.09%
56	miR-769-5p	11,236	0.13%	0.16%
57	miR-92b-3p	9,904	0.08%	0.18%
58	miR-140-3p	9,438	0.12%	0.12%
59	miR-28-3p	9,333	0.08%	0.16%
60	miR-20a-5p	8,949	0.15%	0.07%
61	miR-345-5p	8,394	0.09%	0.12%
62	miR-181b-5p	8,394	0.07%	0.15%
63	miR-449c-5p	8,050	0.08%	0.13%
64	miR-22-3p	7,553	0.08%	0.12%
65	miR-361-5p	6,978	0.11%	0.06%
66	miR-142-3p	6,348	0.06%	0.10%

C) CD4+ PBMC Rank	miRNA	Total Reads	% of Total miRNAs		
			Uninfected	BaL Day 3	NL4-3 Day 3
1	miR-146b-5p	7,086,693	31.85%	36.75%	37.63%
2	miR-21-5p	1,351,759	6.64%	6.81%	6.91%
3	miR-181a-5p	1,269,073	6.22%	6.05%	6.85%
4	miR-146a-5p	996,615	4.53%	5.39%	5.02%
5	miR-26a-5p	921,882	4.59%	4.57%	4.74%
6	miR-142-5p	861,682	4.40%	4.24%	4.37%
7	let-7f-5p	845,760	5.84%	3.31%	3.88%
8	miR-92a-3p	757,467	4.89%	3.58%	3.14%
9	let-7a-5p	656,919	3.98%	3.27%	2.77%
10	miR-191-5p	426,582	2.55%	2.09%	1.86%
11	miR-16-5p	384,142	2.01%	2.19%	1.60%
12	miR-155-5p	292,855	1.86%	1.56%	1.06%
13	let-7i-5p	272,486	1.52%	1.05%	1.57%
14	miR-148a-3p	270,110	1.40%	1.28%	1.41%
15	let-7g-5p	269,671	1.64%	1.31%	1.17%
16	miR-30e-5p	223,593	0.94%	1.20%	1.20%
17	miR-21-3p	218,576	1.09%	1.05%	1.15%
18	miR-30d-5p	217,493	1.04%	1.16%	1.07%
19	miR-150-5p	199,809	1.04%	0.98%	0.99%
20	miR-186-5p	142,342	0.65%	0.74%	0.75%
21	miR-363-3p	119,038	0.56%	0.62%	0.61%
22	miR-25-3p	105,394	0.62%	0.44%	0.54%
23	miR-26b-5p	91,826	0.50%	0.50%	0.39%
24	miR-423-5p	91,695	0.47%	0.46%	0.45%
25	miR-342-3p	87,288	0.33%	0.49%	0.47%
26	miR-98-5p	83,080	0.49%	0.39%	0.38%
27	miR-27b-3p	79,638	0.41%	0.39%	0.40%
28	miR-486-5p	76,954	0.49%	0.33%	0.36%
29	miR-22-3p	62,785	0.30%	0.31%	0.33%
30	miR-28-3p	61,623	0.39%	0.27%	0.28%
31	miR-29a-3p	60,751	0.23%	0.35%	0.33%
32	let-7d-5p	57,110	0.36%	0.28%	0.24%
33	miR-181b-5p	54,768	0.28%	0.31%	0.24%
34	miR-192-5p	49,167	0.23%	0.24%	0.27%
35	miR-423-3p	41,070	0.28%	0.17%	0.18%

36	miR-103a-3p	40,933	0.21%	0.21%	0.20%
37	miR-221-3p	36,870	0.12%	0.22%	0.21%
38	miR-30c-5p	35,675	0.12%	0.22%	0.19%
39	miR-27a-3p	34,679	0.16%	0.17%	0.19%
40	miR-140-3p	34,330	0.16%	0.21%	0.15%
41	miR-181c-5p	33,843	0.16%	0.16%	0.19%
42	let-7b-5p	32,699	0.18%	0.17%	0.15%
43	miR-24-3p	32,081	0.14%	0.18%	0.16%
44	miR-30e-3p	31,696	0.18%	0.13%	0.17%
45	miR-93-5p	31,523	0.14%	0.19%	0.15%
46	miR-92b-3p	27,908	0.19%	0.12%	0.12%
47	miR-425-5p	27,338	0.15%	0.15%	0.11%
48	miR-15b-5p	25,772	0.11%	0.14%	0.14%
49	miR-210-3p	24,372	0.10%	0.14%	0.12%
50	miR-23a-3p	24,324	0.11%	0.13%	0.12%
51	miR-142-3p	23,406	0.10%	0.12%	0.12%
52	miR-130b-3p	18,490	0.08%	0.10%	0.09%
53	miR-30b-5p	16,026	0.05%	0.11%	0.07%
54	miR-125a-5p	15,723	0.10%	0.07%	0.07%

Table A-2: Highly-expressed microRNAs in 293T cells. The total number of reads shown represents the number of the reads recovered from total RNA deep sequencing of 293T cells [172]. For each miRNA, the percentile representation is shown.

293T Rank	miRNA	Total Reads	% of Total miRNAs
1	miR-92a-3p	657,322	19.59%
2	miR-10b-5p	510,752	15.22%
3	miR-10a-5p	163,875	4.88%
4	miR-25-3p	121,584	3.62%
5	miR-103a-3p	97,839	2.92%
6	miR-148a-3p	96,440	2.87%
7	miR-30d-5p	87,620	2.61%
8	miR-191-5p	80,058	2.39%
9	miR-16-5p	60,157	1.79%
10	miR-486-5p	54,993	1.64%
11	miR-221-3p	51,364	1.53%
12	miR-182-5p	48,223	1.44%
13	miR-93-5p	44,123	1.32%
14	miR-378a-3p	43,300	1.29%
15	miR-19b-3p	40,973	1.22%
16	miR-423-3p	39,790	1.19%
17	miR-222-3p	38,310	1.14%
18	miR-28-3p	33,619	1.00%
19	miR-99b-5p	32,809	0.98%
20	miR-550a-3p	32,445	0.97%
21	miR-320a-3p	30,877	0.92%
22	miR-186-5p	27,569	0.82%
23	miR-26a-5p	27,423	0.82%
24	miR-21-5p	25,266	0.75%
25	let-7a-5p	25,202	0.75%
26	miR-4454-5p	22,803	0.68%
27	miR-1307-5p	22,437	0.67%
28	miR-27b-3p	21,553	0.64%
29	miR-181a-5p	21,540	0.64%
30	miR-20a-5p	20,808	0.62%
31	miR-19a-3p	20,348	0.61%
32	miR-107-3p	20,099	0.60%
33	miR-17-3p	19,501	0.58%

34	miR-324-5p	18,842	0.56%
35	miR-744-5p	17,703	0.53%
36	miR-92b-3p	16,591	0.49%
37	miR-151a-3p	16,483	0.49%
38	miR-484-5p	15,853	0.47%
39	miR-17-5p	15,378	0.46%
40	miR-130b-3p	15,039	0.45%
41	miR-106b-3p	13,568	0.40%
42	let-7f-5p	13,550	0.40%
43	miR-423-5p	13,441	0.40%
44	miR-660-5p	13,389	0.40%
45	miR-589-3p	12,466	0.37%
46	miR-101-3p	11,833	0.35%
47	miR-148b-3p	11,256	0.34%
48	miR-324-3p	10,995	0.33%
49	miR-15a-5p	10,817	0.32%
50	miR-30e-5p	10,411	0.31%
51	miR-342-3p	9,994	0.30%
52	miR-30a-5p	9,595	0.29%
53	miR-22-3p	9,419	0.28%
54	miR-1307-3p	8,920	0.27%
55	miR-31-5p	8,524	0.25%
56	miR-339-5p	8,519	0.25%
57	miR-7706-3p	7,822	0.23%
58	miR-4286-5p	7,737	0.23%
59	miR-18a-5p	7,676	0.23%
60	miR-301a-3p	7,664	0.23%
61	miR-143-3p	7,616	0.23%
62	miR-652-3p	7,548	0.22%
63	miR-196b-5p	7,229	0.22%
64	miR-183-5p	7,149	0.21%
65	miR-151a-5p	6,835	0.20%
66	miR-18a-3p	6,680	0.20%
67	miR-140-3p	6,596	0.20%
68	miR-421-3p	6,005	0.18%
69	miR-532-5p	5,954	0.18%
70	miR-125a-5p	5,665	0.17%
71	miR-29a-3p	5,460	0.16%

72	miR-196a-5p	5,140	0.15%
73	miR-375-3p	5,009	0.15%
74	miR-192-5p	4,970	0.15%
75	miR-425-5p	4,887	0.15%
76	miR-181b-5p	4,761	0.14%
77	miR-15b-5p	4,755	0.14%
78	miR-185-5p	4,679	0.14%
79	miR-126-5p	4,640	0.14%
80	miR-218-5p	4,575	0.14%
81	let-7i-5p	4,513	0.13%
82	miR-9-5p	4,487	0.13%
83	miR-1180-3p	4,339	0.13%
84	miR-320c-3p	4,320	0.13%
85	miR-99a-5p	4,309	0.13%
86	miR-361-5p	4,219	0.13%
87	miR-26b-5p	4,187	0.12%
88	miR-320b-3p	3,910	0.12%
89	miR-320b-5p	3,769	0.11%
90	miR-181c-5p	3,711	0.11%
91	miR-941-3p	3,584	0.11%
92	let-7g-5p	3,507	0.10%
93	miR-296-3p	3,465	0.10%
94	miR-340-5p	3,448	0.10%

References

1. Bartel DP: **MicroRNAs: target recognition and regulatory functions**. *Cell* 2009, **136**(2):215-233.

2. Lee RC, Feinbaum RL, Ambros V: **The C. elegans heterochronic gene lin-4 encodes small RNAs with antisense complementarity to lin-14**. *Cell* 1993, **75**:843-854.

3. Mendell JT, Olson EN: **MicroRNAs in stress signaling and human disease**. *Cell* 2012, **148**(6):1172-1187.

4. Melar-New M, Laimins LA: **Human papillomaviruses modulate expression of microRNA 203 upon epithelial differentiation to control levels of p63 proteins**. *J Virol* 2010, **84**(10):5212-5221.

5. Cimmino A, Calin GA, Fabbri M, Iorio MV, Ferracin M, Shimizu M, Wojcik SE, Aqeilan RI, Zupo S, Dono M *et al*: **miR-15 and miR-16 induce apoptosis by targeting BCL2**. *Proc Natl Acad Sci U S A* 2005, **102**(39):13944-13949.

6. Friedman RC, Farh KK, Burge CB, Bartel DP: **Most mammalian mRNAs are conserved targets of microRNAs**. *Genome Res* 2009, **19**(1):92-105.

7. Lai EC: **Micro RNAs are complementary to 3' UTR sequence motifs that mediate negative post-transcriptional regulation**. *Nat Genet* 2002, **30**(4):363-364.

8. Lewis BP, Shih IH, Jones-Rhoades MW, Bartel DP, Burge CB: **Prediction of mammalian microRNA targets**. *Cell* 2003, **115**:787-798.

9. Loeb GB, Khan AA, Canner D, Hiatt JB, Shendure J, Darnell RB, Leslie CS, Rudensky AY: **Transcriptome-wide miR-155 binding map reveals widespread noncanonical microRNA targeting**. *Mol Cell* 2012, **48**(5):760-770.

10. Mullokandov G, Baccarini A, Ruzo A, Jayaprakash AD, Tung N, Israelow B, Evans MJ, Sachidanandam R, Brown BD: **High-throughput assessment of microRNA activity and function using microRNA sensor and decoy libraries**. *Nat Methods* 2012, **9**(8):840-846.

11. Cai X, Hagedorn CH, Cullen BR: **Human microRNAs are processed from capped, polyadenylated transcripts that can also function as mRNAs**. *RNA* 2004, **10**:1957-1966.

12. Cullen BR: **RNAi the natural way**. *Nat Genet* 2005, **37**(11):1163-1165.

13. Cullen BR: **Transcription and processing of human microRNA precursors**. *Mol Cell* 2004, **16**(6):861-865.

14. Zeng Y, Yi R, Cullen BR: **Recognition and cleavage of primary microRNA precursors by the nuclear processing enzyme Drosha**. *EMBO J* 2004, **24**:138-148.

15. Lee Y, Ahn C, Han J, Choi H, Kim J, Yim J, Lee J, Provost P, Radmark O, Kim S *et al*: **The nuclear RNase III Drosha initiates microRNA processing**. *Nature* 2003, **425**:415-419.

16. Zeng Y, Yi R, Cullen BR: **Recognition and cleavage of primary microRNA precursors by the nuclear processing enzyme Drosha**. *EMBO J* 2005, **24**(1):138-148.

17. Han J, Lee Y, Yeom KH, Nam JW, Heo I, Rhee JK, Sohn SY, Cho Y, Zhang BT, Kim VN: **Molecular basis for the recognition of primary microRNAs by the Drosha-DGCR8 complex**. *Cell* 2006, **125**:887-901.

18. Bogerd HP, Karnowski HW, Cai X, Shin J, Pohlers M, Cullen BR: **A mammalian herpesvirus uses noncanonical expression and processing mechanisms to generate viral microRNAs**. *Mol Cell* 2010, **37**:135-142.

19. Kincaid RP, Burke JM, Sullivan CS: **RNA virus microRNA that mimics a B-cell oncomiR**. *Proc Natl Acad Sci U S A* 2012, **109**(8):3077-3082.

20. Sibley CR, Seow Y, Saayman S, Dijkstra KK, El Andaloussi S, Weinberg MS, Wood MJ: **The biogenesis and characterization of mammalian microRNAs of mirtron origin**. *Nucleic Acids Res* 2012, **40**(1):438-448.

21. Yi R, Qin Y, Macara IG, Cullen BR: **Exportin-5 mediates the nuclear export of pre-microRNAs and short hairpin RNAs**. *Genes Dev* 2003, **17**:3011-3016.

22. Zhang H, Kolb FA, Brondani V, Billy E, Filipowicz W: **Human Dicer preferentially cleaves dsRNAs at their termini without a requirement for ATP**. *EMBO J* 2002, **21**:5875-5885.

23. Chendrimada TP, Gregory RI, Kumaraswamy E, Norman J, Cooch N, Nishikura K, Shiekhattar R: **TRBP recruits the Dicer complex to Ago2 for microRNA processing and gene silencing**. *Nature* 2005, **436**:740-744.

24. Eulalio A, Huntzinger E, Izaurralde E: **GW182 interaction with Argonaute is essential for miRNA-mediated translational repression and mRNA decay**. *Nat Struct Mol Biol* 2008, **15**(4):346-353.

25. Cheloufi S, Dos Santos CO, Chong MM, Hannon GJ: **A dicer-independent miRNA biogenesis pathway that requires Ago catalysis**. *Nature* 2010, **465**(7298):584-589.

26. Liu J, Carmell MA, Rivas FV, Marsden CG, Thomson JM, Song JJ, Hammond SM, Joshua-Tor L, Hannon GJ: **Argonaute2 is the catalytic engine of mammalian RNAi**. *Science* 2004, **305**:1437-1441.

27. Zekri L, Kuzuoğlu-Öztürk D, Izaurralde E: **GW182 proteins cause PABP dissociation from silenced miRNA targets in the absence of deadenylation**. *EMBO J* 2013, **32**(7):1052-1065.

28. Eulalio A, Behm-Ansmant I, Izaurralde E: **P bodies: at the crossroads of post-transcriptional pathways**. *Nat Rev Mol Cell Biol* 2007, **8**(1):9-22.

29. Liu J, Valencia-Sanchez MA, Hannon GJ, Parker R: **MicroRNA-dependent localization of targeted mRNAs to mammalian P-bodies**. *Nat Cell Biol* 2005, **7**:719-723.

30. Teixeira D, Sheth U, Valencia-Sanchez MA, Brengues M, Parker R: **Processing bodies require RNA for assembly and contain nontranslating mRNAs**. *RNA* 2005, **11**(4):371-382.

31. Cullen BR: **Viruses and microRNAs: RISCy interactions with serious consequences**. *Genes Dev* 2011, **25**(18):1881-1894.

32. Grundhoff A, Sullivan CS: **Virus-encoded microRNAs**. *Virology* 2011, **411**(2):325-343.

33. Kincaid RP, Sullivan CS: **Virus-encoded microRNAs: an overview and a look to the future**. *PLoS Pathog* 2012, **8**(12):e1003018.

34. Skalsky RL, Cullen BR: **Viruses, microRNAs, and host interactions**. *Annu Rev Microbiol* 2010, **64**:123-141.

35. Lu S, Cullen BR: **Adenovirus VA1 noncoding RNA can inhibit small interfering RNA and MicroRNA biogenesis**. *J Virol* 2004, **78**(23):12868-12876.

36. Andersson MG, Haasnoot PC, Xu N, Berenjian S, Berkhout B, Akusjarvi G: **Suppression of RNA interference by adenovirus virus-associated RNA**. *J Virol* 2005, **79**:9556-9565.

37. Pfeffer S, Sewer A, Lagos-Quintana M, Sheridan R, Sander C, Grasser FA, van Dyk LF, Ho CK, Shuman S, Chien M *et al*: **Identification of microRNAs of the herpesvirus family**. *Nat Methods* 2005, **2**(4):269-276.

38. Lin J, Cullen BR: **Analysis of the interaction of primate retroviruses with the human RNA interference machinery**. *J Virol* 2007, **81**(22):12218-12226.

39. Umbach JL, Yen HL, Poon LL, Cullen BR: **Influenza A virus expresses high levels of an unusual class of small viral leader RNAs in infected cells**. *MBio* 2010, **1**(4).

40. Parameswaran P, Sklan E, Wilkins C, Burgon T, Samuel MA, Lu R, Ansel KM, Heissmeyer V, Einav S, Jackson W *et al*: **Six RNA viruses and forty-one hosts: viral small RNAs and modulation of small RNA repertoires in vertebrate and invertebrate systems**. *PLoS Pathog* 2010, **6**(2):e1000764.

41. Ouellet DL, Plante I, Landry P, Barat C, Janelle ME, Flamand L, Tremblay MJ, Provost P: **Identification of functional microRNAs released through asymmetrical processing of HIV-1 TAR element**. *Nucleic Acids Res* 2008, **36**(7):2353-2365.

42. Klase Z, Kale P, Winograd R, Gupta MV, Heydarian M, Berro R, McCaffrey T, Kashanchi F: **HIV-1 TAR element is processed by Dicer to yield a viral micro-RNA involved in chromatin remodeling of the viral LTR**. *BMC Mol Biol* 2007, **8**:63.

43. Sanghvi VR, Steel LF: **The cellular TAR RNA binding protein, TRBP, promotes HIV-1 replication primarily by inhibiting the activation of double-stranded RNA-dependent kinase PKR**. *J Virol* 2011, **85**(23):12614-12621.

44. Bennasser Y, Le SY, Yeung ML, Jeang KT: **HIV-1 encoded candidate micro-RNAs and their cellular targets**. *Retrovirology* 2004, **1**:43.

45. Bennasser Y, Le SY, Benkirane M, Jeang KT: **Evidence that HIV-1 encodes an siRNA and a suppressor of RNA silencing**. *Immunity* 2005, **22**(5):607-619.

46. Zhang Y, Fan M, Geng G, Liu B, Huang Z, Luo H, Zhou J, Guo X, Cai W, Zhang H: **A novel HIV-1-encoded microRNA enhances its viral replication by targeting the TATA box region**. *Retrovirology* 2014, **11**:23.

47. Omoto S, Ito M, Tsutsumi Y, Ichikawa Y, Okuyama H, Brisibe EA, Saksena NK, Fujii YR: **HIV-1 nef suppression by virally encoded microRNA**. *Retrovirology* 2004, **1**:44.

48. Klase Z, Winograd R, Davis J, Carpio L, Hildreth R, Heydarian M, Fu S, McCaffrey T, Meiri E, Ayash-Rashkovsky M *et al*: **HIV-1 TAR miRNA protects against apoptosis by altering cellular gene expression**. *Retrovirology* 2009, **6**:18.

49. Omoto S, Fujii YR: **Regulation of human immunodeficiency virus 1 transcription by nef microRNA**. *J Gen Virol* 2005, **86**(Pt 3):751-755.

50. Kaul D, Amit K, Suman: **Evidence and nature of a novel miRNA encoded by HIV-1**. In: *Proceedings of the Indian National Science Academy, Part A: Physical Sciences.* vol. 72; 2006: 91-95.

51. Kaul D, Ahlawat A, Gupta SD: **HIV-1 genome-encoded hiv1-mir-H1 impairs cellular responses to infection**. *Mol Cell Biochem* 2009, **323**(1-2):143-148.

52. Yeung ML, Bennasser Y, Watashi K, Le SY, Houzet L, Jeang KT: **Pyrosequencing of small non-coding RNAs in HIV-1 infected cells: evidence for the processing of a viral-cellular double-stranded RNA hybrid**. *Nucleic Acids Res* 2009, **37**(19):6575-6586.

53. Schopman NC, Willemsen M, Liu YP, Bradley T, van Kampen A, Baas F, Berkhout B, Haasnoot J: **Deep sequencing of virus-infected cells reveals HIV-encoded small RNAs**. *Nucleic Acids Res* 2012, **40**(1):414-427.

54. Althaus CF, Vongrad V, Niederost B, Joos B, Di Giallonardo F, Rieder P, Pavlovic J, Trkola A, Gunthard HF, Metzner KJ *et al*: **Tailored enrichment strategy detects low abundant small noncoding RNAs in HIV-1 infected cells**. *Retrovirology* 2012, **9**:27.

55. Rouha H, Thurner C, Mandl CW: **Functional microRNA generated from a cytoplasmic RNA virus**. *Nucleic Acids Res* 2010, **38**(22):8328-8337.

56. Varble A, Chua MA, Perez JT, Manicassamy B, Garcia-Sastre A, tenOever BR: **Engineered RNA viral synthesis of microRNAs**. *Proc Natl Acad Sci U S A* 2010, **107**(25):11519-11524.

57. Shapiro JS, Varble A, Pham AM, Tenoever BR: **Noncanonical cytoplasmic processing of viral microRNAs**. *RNA* 2010, **16**(11):2068-2074.

58. Langlois RA, Shapiro JS, Pham AM, tenOever BR: **In vivo delivery of cytoplasmic RNA virus-derived miRNAs**. *Mol Ther* 2012, **20**(2):367-375.

59. Fields BN, Knipe DM, Howley PM: **Fields virology**, 5th edn. Philadelphia: Wolters Kluwer Health/Lippincott Williams & Wilkins; 2007.

60. Rosewick N, Momont M, Durkin K, Takeda H, Caiment F, Cleuter Y, Vernin C, Mortreux F, Wattel E, Burny A *et al*: **Deep sequencing reveals abundant noncanonical retroviral microRNAs in B-cell leukemia/lymphoma**. *Proc Natl Acad Sci U S A* 2013, **110**(6):2306-2311.

61. Schramke V, Allshire R: **Those interfering little RNAs! Silencing and eliminating chromatin**. *Curr Opin Genet Dev* 2004, **14**(2):174-180.

62. Lecellier CH, Dunoyer P, Arar K, Lehmann-Che J, Eyquem S, Himber C, Saib A, Voinnet O: **A cellular microRNA mediates antiviral defense in human cells**. *Science* 2005, **308**(5721):557-560.

63. Houzet L, Yeung ML, de Lame V, Desai D, Smith SM, Jeang KT: **MicroRNA profile changes in human immunodeficiency virus type 1 (HIV-1) seropositive individuals**. *Retrovirology* 2008, **5**:118.

64. Bignami F, Pilotti E, Bertoncelli L, Ronzi P, Gulli M, Marmiroli N, Magnani G, Pinti M, Lopalco L, Mussini C *et al*: **Stable changes in CD4+ T lymphocyte miRNA expression after exposure to HIV-1**. *Blood* 2012, **119**(26):6259-6267.

65. Witwer KW, Watson AK, Blankson JN, Clements JE: **Relationships of PBMC microRNA expression, plasma viral load, and CD4+ T-cell count in HIV-1-infected elite suppressors and viremic patients**. *Retrovirology* 2012, **9**:5.

66. Wang X, Ye L, Hou W, Zhou Y, Wang YJ, Metzger DS, Ho WZ: **Cellular microRNA expression correlates with susceptibility of monocytes/macrophages to HIV-1 infection**. *Blood* 2009, **113**(3):671-674.

67. Ma L, Shen CJ, Cohen É, Xiong SD, Wang JH: **miRNA-1236 inhibits HIV-1 infection of monocytes by repressing translation of cellular factor VprBP**. *PLoS One* 2014, **9**(6):e99535.

68. Chiang K, Sung TL, Rice AP: **Regulation of cyclin T1 and HIV-1 Replication by microRNAs in resting CD4+ T lymphocytes**. *J Virol* 2012, **86**(6):3244-3252.

69. Huang J, Wang F, Argyris E, Chen K, Liang Z, Tian H, Huang W, Squires K, Verlinghieri G, Zhang H: **Cellular microRNAs contribute to HIV-1 latency in resting primary CD4+ T lymphocytes**. *Nat Med* 2007, **13**:1241-1247.

70. Ahluwalia JK, Khan SZ, Soni K, Rawat P, Gupta A, Hariharan M, Scaria V, Lalwani M, Pillai B, Mitra D *et al*: **Human cellular microRNA hsa-miR-29a interferes with viral nef protein expression and HIV-1 replication**. *Retrovirology* 2008, **5**:117.

71. Nathans R, Chu CY, Serquina AK, Lu CC, Cao H, Rana TM: **Cellular microRNA and P bodies modulate host-HIV-1 interactions**. *Mol Cell* 2009, **34**(6):696-709.

72. Sun G, Li H, Wu X, Covarrubias M, Scherer L, Meinking K, Luk B, Chomchan P, Alluin J, Gombart AF *et al*: **Interplay between HIV-1 infection and host microRNAs**. *Nucleic Acids Res* 2012, **40**(5):2181-2196.

73. Cobos Jiménez V, Booiman T, de Taeye SW, van Dort KA, Rits MA, Hamann J, Kootstra NA: **Differential expression of HIV-1 interfering factors in monocyte-derived macrophages stimulated with polarizing cytokines or interferons**. *Sci Rep* 2012, **2**:763.

74. Mantri CK, Pandhare Dash J, Mantri JV, Dash CC: **Cocaine enhances HIV-1 replication in CD4+ T cells by down-regulating MiR-125b**. *PLoS One* 2012, **7**(12):e51387.

75. Didiano D, Hobert O: **Perfect seed pairing is not a generally reliable predictor for miRNA-target interactions**. *Nat Struct Mol Biol* 2006, **13**:849-851.

76. Yeung ML, Bennasser Y, Myers TG, Jiang G, Benkirane M, Jeang KT: **Changes in microRNA expression profiles in HIV-1-transfected human cells**. *Retrovirology* 2005, **2**:81.

77. Triboulet R, Mari B, Lin YL, Chable-Bessia C, Bennasser Y, Lebrigand K, Cardinaud B, Maurin T, Barbry P, Baillat V *et al*: **Suppression of microRNA-silencing pathway by HIV-1 during virus replication**. *Science* 2007, **315**(5818):1579-1582.

78. Chang ST, Thomas MJ, Sova P, Green RR, Palermo RE, Katze MG: **Next-generation sequencing of small RNAs from HIV-infected cells identifies phased microrna expression patterns and candidate novel microRNAs differentially expressed upon infection**. *MBio* 2013, **4**(1):e00549-00512.

79. Aqil M, Naqvi AR, Mallik S, Bandyopadhyay S, Maulik U, Jameel S: **The HIV Nef protein modulates cellular and exosomal miRNA profiles in human monocytic cells**. *J Extracell Vesicles* 2014, **3**.

80. Casey Klockow L, Sharifi HJ, Wen X, Flagg M, Furuya AK, Nekorchuk M, de Noronha CM: **The HIV-1 protein Vpr targets the endoribonuclease Dicer for proteasomal degradation to boost macrophage infection**. *Virology* 2013, **444**(1-2):191-202.

81. Sanghvi VR, Steel LF: **A re-examination of global suppression of RNA interference by HIV-1**. *PLoS ONE* 2011, **6**:e17246.

82. Aqil M, Naqvi AR, Bano AS, Jameel S: **The HIV-1 Nef protein binds argonaute-2 and functions as a viral suppressor of RNA interference**. *PLoS One* 2013, **8**(9):e74472.

83. Coburn GA, Cullen BR: **Potent and specific inhibition of human immunodeficiency virus type 1 replication by RNA interference**. *J Virol* 2002, **76**(18):9225-9231.

84. Jacque JM, Triques K, Stevenson M: **Modulation of HIV-1 replication by RNA interference**. *Nature* 2002, **418**(6896):435-438.

85. Lee NS, Dohjima T, Bauer G, Li H, Li MJ, Ehsani A, Salvaterra P, Rossi J: **Expression of small interfering RNAs targeted against HIV-1 rev transcripts in human cells**. *Nat Biotechnol* 2002, **20**(5):500-505.

86. Novina CD, Murray MF, Dykxhoorn DM, Beresford PJ, Riess J, Lee SK, Collman RG, Lieberman J, Shankar P, Sharp PA: **siRNA-directed inhibition of HIV-1 infection**. *Nat Med* 2002, **8**(7):681-686.

87. Park WS, Miyano-Kurosaki N, Hayafune M, Nakajima E, Matsuzaki T, Shimada F, Takaku H: **Prevention of HIV-1 infection in human peripheral blood mononuclear cells by specific RNA interference**. *Nucleic Acids Res* 2002, **30**(22):4830-4835.

88. Surabhi RM, Gaynor RB: **RNA interference directed against viral and cellular targets inhibits human immunodeficiency Virus Type 1 replication**. *J Virol* 2002, **76**(24):12963-12973.

89. Capodici J, Karikó K, Weissman D: **Inhibition of HIV-1 infection by small interfering RNA-mediated RNA interference**. *J Immunol* 2002, **169**(9):5196-5201.

90. Lee MT, Coburn GA, McClure MO, Cullen BR: **Inhibition of human immunodeficiency virus type 1 replication in primary macrophages by using Tat- or CCR5-specific small interfering RNAs expressed from a lentivirus vector**. *J Virol* 2003, **77**:11964-11972.

91. Song E, Lee SK, Dykxhoorn DM, Novina C, Zhang D, Crawford K, Cerny J, Sharp PA, Lieberman J, Manjunath N *et al*: **Sustained small interfering RNA-mediated human immunodeficiency virus type 1 inhibition in primary macrophages**. *J Virol* 2003, **77**:7174-7181.

92. Joshi PJ, North TW, Prasad VR: **Aptamers directed to HIV-1 reverse transcriptase display greater efficacy over small hairpin RNAs targeted to viral RNA in blocking HIV-1 replication**. *Mol Ther* 2005, **11**(5):677-686.

93. Westerhout EM, Vink M, Haasnoot PC, Das AT, Berkhout B: **A conditionally replicating HIV-based vector that stably expresses an antiviral shRNA against HIV-1 replication**. *Mol Ther* 2006, **14**(2):268-275.

94. ter Brake O, Konstantinova P, Ceylan M, Berkhout B: **Silencing of HIV-1 with RNA interference: a multiple shRNA approach**. *Mol Ther* 2006, **14**(6):883-892.

95. Konstantinova P, de Vries W, Haasnoot J, ter Brake O, de Haan P, Berkhout B: **Inhibition of human immunodeficiency virus type 1 by RNA interference using long-hairpin RNA**. *Gene Ther* 2006, **13**(19):1403-1413.

96. Wu K, Mu Y, Hu J, Lu L, Zhang X, Yang Y, Li Y, Liu F, Song D, Zhu Y *et al*: **Simultaneously inhibition of HIV and HBV replication through a dual small interfering RNA expression system**. *Antiviral Res* 2007, **74**(2):142-149.

97. Liu YP, Haasnoot J, ter Brake O, Berkhout B, Konstantinova P: **Inhibition of HIV-1 by multiple siRNAs expressed from a single microRNA polycistron**. *Nucleic Acids Res* 2008, **36**(9):2811-2824.

98. ter Brake O, 't Hooft K, Liu YP, Centlivre M, von Eije KJ, Berkhout B: **Lentiviral vector design for multiple shRNA expression and durable HIV-1 inhibition**. *Mol Ther* 2008, **16**(3):557-564.

99. Zhou J, Li H, Li S, Zaia J, Rossi JJ: **Novel dual inhibitory function aptamer-siRNA delivery system for HIV-1 therapy**. *Mol Ther* 2008, **16**(8):1481-1489.

100. Tan X, Lu ZJ, Gao G, Xu Q, Hu L, Fellmann C, Li MZ, Qu H, Lowe SW, Hannon GJ *et al*: **Tiling genomes of pathogenic viruses identifies potent antiviral shRNAs and reveals a role for secondary structure in shRNA efficacy**. *Proc Natl Acad Sci U S A* 2012, **109**(3):869-874.

101. Low JT, Knoepfel SA, Watts JM, ter Brake O, Berkhout B, Weeks KM: **SHAPE-directed discovery of potent shRNA inhibitors of HIV-1**. *Mol Ther* 2012, **20**(4):820-828.

102. Boden D, Pusch O, Lee F, Tucker L, Ramratnam B: **Human immunodeficiency virus type 1 escape from RNA interference**. *J Virol* 2003, **77**(21):11531-11535.

103. Das AT, Brummelkamp TR, Westerhout EM, Vink M, Madiredjo M, Bernards R, Berkhout B: **Human immunodeficiency virus type 1 escapes from RNA interference-mediated inhibition**. *J Virol* 2004, **78**:2601-2605.

104. Westerhout EM, Ooms M, Vink M, Das AT, Berkhout B: **HIV-1 can escape from RNA interference by evolving an alternative structure in its RNA genome**. *Nucleic Acids Res* 2005, **33**(2):796-804.

105. Westerhout EM, Berkhout B: **A systematic analysis of the effect of target RNA structure on RNA interference**. *Nucleic Acids Res* 2007, **35**(13):4322-4330.

106. Leonard JN, Shah PS, Burnett JC, Schaffer DV: **HIV evades RNA interference directed at TAR by an indirect compensatory mechanism**. *Cell Host Microbe* 2008, **4**(5):484-494.

107. Nevot M, Martrus G, Clotet B, Martínez MA: **RNA interference as a tool for exploring HIV-1 robustness**. *J Mol Biol* 2011, **413**(1):84-96.

108. Shah PS, Pham NP, Schaffer DV: **HIV develops indirect cross-resistance to combinatorial RNAi targeting two distinct and spatially distant sites**. *Mol Ther* 2012, **20**(4):840-848.

109. Yu SF, Lujan P, Jackson DL, Emerman M, Linial ML: **The DEAD-box RNA helicase DDX6 is required for efficient encapsidation of a retroviral genome**. *PLoS Pathog* 2011, **7**(10):e1002303.

110. Lanford RE, Hildebrandt-Eriksen ES, Petri A, Persson R, Lindow M, Munk ME, Kauppinen S, Orum H: **Therapeutic silencing of microRNA-122 in primates with chronic hepatitis C virus infection**. *Science* 2010, **327**:198-201.

111. Cullen BR: **MicroRNAs as mediators of viral evasion of the immune system**. *Nat Immunol* 2013, **14**:205-210.

112. Yao Y, Smith LP, Nair V, Watson M: **An avian retrovirus uses canonical expression and processing mechanisms to generate viral microRNA**. *J Virol* 2013, **88**:2-9.

113. Liu YP, Vink MA, Westerink JT, Ramirez de Arellano E, Konstantinova P, Ter Brake O, Berkhout B: **Titers of lentiviral vectors encoding shRNAs and miRNAs are reduced by different mechanisms that require distinct repair strategies**. *RNA* 2010, **16**:1328-1339.

114. Brandl A, Wittmann J, Jack HM: **A facile method to increase titers of miRNA-encoding retroviruses by inhibition of the RNaseIII enzyme Drosha**. *Eur J Immunol* 2011, **41**:549-551.

115. Skalsky RL, Kang D, Linnstaedt SD, Cullen BR: **Evolutionary conservation of primate lymphocryptovirus microRNA targets**. *J Virol* 2013, **88**:1617-1635.

116. Hechler T, Materniak M, Kehl T, Kuzmak J, Löchelt M: **Complete genome sequences of two novel European clade bovine foamy viruses from Germany and Poland**. *J Virol* 2012, **86**:10905-10906.

117. Yu SF, Linial ML: **Analysis of the role of the bel and bet open reading frames of human foamy virus by using a new quantitative assay**. *J Virol* 1993, **67**:6618-6624.

118. Materniak M, Bicka L, Kuzmak J: **Isolation and partial characterization of bovine foamy virus from Polish cattle**. *Polish journal of veterinary sciences* 2006, **9**(4):207-211.

119. Materniak M, Hechler T, Löchelt M, Kuzmak J: **Similar patterns of infection with bovine foamy virus in experimentally inoculated calves and sheep**. *J Virol* 2013, **87**:3516-3525.

120. Romen F, Backes P, Materniak M, Sting R, Vahlenkamp TW, Riebe R, Pawlita M, Kuzmak J, Löchelt M: **Serological detection systems for identification of cows shedding bovine foamy virus via milk**. *Virology* 2007, **364**:123-131.

121. Bolger AM, Lohse M, Usadel B: **Trimmomatic: a flexible trimmer for Illumina sequence data**. *Bioinformatics* 2014, **30**(15):2114-2120.

122. Langmead B, Trapnell C, Pop M, Salzberg SL: **Ultrafast and memory-efficient alignment of short DNA sequences to the human genome**. *Genome Biol* 2009, **10**:R25.

123. Kozomara A, Griffiths-Jones S: **miRBase: integrating microRNA annotation and deep-sequencing data**. *Nucleic Acids Res* 2011, **39**(Database issue):D152-157.

124. Flicek P, Ahmed I, Amode MR, Barrell D, Beal K, Brent S, Carvalho-Silva D, Clapham P, Coates G, Fairley S *et al*: **Ensembl 2013**. *Nucleic Acids Res* 2013, **41**(Database issue):D48-55.

125. Livak KJ, Schmittgen TD: **Analysis of relative gene expression data using real-time quantitative PCR and the 2(-Delta Delta C(T)) Method**. *Methods* 2002, **25**:402-408.

126. Newman MA, Mani V, Hammond SM: **Deep sequencing of microRNA precursors reveals extensive 3' end modification**. *RNA* 2011, **17**:1795-1803.

127. Arimbasseri AG, Rijal K, Maraia RJ: **Transcription termination by the eukaryotic RNA polymerase III**. *Biochim Biophys Acta* 2012, **1829**:318-330.

128. Dieci G, Conti A, Pagano A, Carnevali D: **Identification of RNA polymerase III-transcribed genes in eukaryotic genomes**. *Biochim Biophys Acta* 2012, **1829**:296-305.

129. Cai X, Schäfer A, Lu S, Bilello JP, Desrosiers RC, Edwards R, Raab-Traub N, Cullen BR: **Epstein-Barr virus microRNAs are evolutionarily conserved and differentially expressed**. *PLoS Pathog* 2006, **2**:e23.

130. Kehl T, Tan J, Materniak M: **Non-simian foamy viruses: molecular virology, tropism and prevalence and zoonotic/interspecies transmission**. *Viruses* 2013, **5**:2169-2209.

131. Meiering CD, Linial ML: **Historical perspective of foamy virus epidemiology and infection**. *Clin Microbiol Rev* 2001, **14**:165-176.

132. Wolfe ND, Switzer WM, Carr JK, Bhullar VB, Shanmugam V, Tamoufe U, Prosser AT, Torimiro JN, Wright A, Mpoudi-Ngole E *et al*: **Naturally acquired simian retrovirus infections in central African hunters**. *Lancet* 2004, **363**:932-937.

133. Schweizer M, Falcone V, Gange J, Turek R, Neumann-Haefelin D: **Simian foamy virus isolated from an accidentally infected human individual**. *J Virol* 1997, **71**:4821-4824.

134. Rethwilm A: **Foamy virus vectors: an awaited alternative to gammaretro- and lentiviral vectors**. *Curr Gene Ther* 2007, **7**:261-271.

135. Erlwein O, McClure M: **Gene delivery the key to gene therapy: the case for foamy viruses**. *Ther Deliv* 2012, **2**:681-684.

136. Schwantes A, Truyen U, Weikel J, Weiss C, Löchelt M: **Application of chimeric feline foamy virus-based retroviral vectors for the induction of antiviral immunity in cats**. *J Virol* 2003, **77**:7830-7842.

137. Glazov EA, Horwood PF, Assavalapsakul W, Kongsuwan K, Mitchell RW, Mitter N, Mahony TJ: **Characterization of microRNAs encoded by the bovine herpesvirus 1 genome**. *J Gen Virol* 2009, **91**:32-41.

138. Cullen BR, Lomedico PT, Ju G: **Transcriptional interference in avian retroviruses--implications for the promoter insertion model of leukaemogenesis**. *Nature* 1984, **307**:241-245.

139. Erlwein O, McClure M: **Gene delivery the key to gene therapy: the case for foamy viruses**. *Therapeutic delivery* 2011, **2**(6):681-684.

140. Trobridge GD, Russell DW: **Helper-free foamy virus vectors**. *Hum Gene Ther* 1998, **9**:2517-2525.

141. Neilson JR, Zheng GX, Burge CB, Sharp PA: **Dynamic regulation of miRNA expression in ordered stages of cellular development**. *Genes Dev* 2007, **21**:578-589.

142. Gartner S, Markovits P, Markovitz DM, Kaplan MH, Gallo RC, Popovic M: **The role of mononuclear phagocytes in HTLV-III/LAV infection**. *Science* 1986, **233**:215-219.

143. Hwang SS, Boyle TJ, Lyerly HK, Cullen BR: **Identification of the envelope V3 loop as the primary determinant of cell tropism in HIV-1**. *Science* 1991, **253**:71-74.

144. Adachi A, Gendelman HE, Koenig S, Folks T, Willey R, Rabson A, Martin MA: **Production of acquired immunodeficiency syndrome-associated retrovirus in human and nonhuman cells transfected with an infectious molecular clone**. *J Virol* 1986, **59**:284-291.

145. Westervelt P, Gendelman HE, Ratner L: **Identification of a determinant within the human immunodeficiency virus 1 surface envelope glycoprotein critical for productive infection of primary monocytes**. *Proc Natl Acad Sci U S A* 1991, **88**:3097-3101.

146. Umbach JL, Cullen BR: **In-depth analysis of Kaposi's sarcoma-associated herpesvirus microRNA expression provides insights into the mammalian microRNA-processing machinery**. *J Virol* 2009, **84**:695-703.

147. Gottwein E, Cullen BR: **A human herpesvirus microRNA inhibits p21 expression and attenuates p21-mediated cell cycle arrest**. *J Virol* 2010, **84**:5229-5237.

148. Wei X, Decker JM, Liu H, Zhang Z, Arani RB, Kilby JM, Saag MS, Wu X, Shaw GM, Kappes JC: **Emergence of resistant human immunodeficiency virus type 1 in patients receiving fusion inhibitor (T-20) monotherapy**. *Antimicrob Agents Chemother* 2002, **46**:1896-1905.

149. Salahuddin SZ, Markham PD, Wong-Staal F, Franchini G, Kalyanaraman VS, Gallo RC: **Restricted expression of human T-cell leukemia--lymphoma virus (HTLV) in transformed human umbilical cord blood lymphocytes**. *Virology* 1983, **129**:51-64.

150. Hafner M, Landthaler M, Burger L, Khorshid M, Hausser J, Berninger P, Rothballer A, Ascano M, Jr., Jungkamp AC, Munschauer M *et al*: **Transcriptome-wide identification of RNA-binding protein and microRNA target sites by PAR-CLIP**. *Cell* 2010, **141**(1):129-141.

151. Gottwein E, Corcoran DL, Mukherjee N, Skalsky RL, Hafner M, Nusbaum JD, Shamulailatpam P, Love CL, Dave SS, Tuschl T *et al*: **Viral microRNA targetome of KSHV-infected primary effusion lymphoma cell lines**. *Cell Host Microbe* 2011, **10**(5):515-526.

152. Kozomara A, Griffiths-Jones S: **miRBase: integrating microRNA annotation and deep-sequencing data**. *Nucleic Acids Res* 2010, **39**:D152-157.

153. Flicek P, Amode MR, Barrell D, Beal K, Brent S, Carvalho-Silva D, Clapham P, Coates G, Fairley S, Fitzgerald S *et al*: **Ensembl 2012**. *Nucleic Acids Res* 2011, **40**:D84-90.

154. Mituyama T, Yamada K, Hattori E, Okida H, Ono Y, Terai G, Yoshizawa A, Komori T, Asai K: **The Functional RNA Database 3.0: databases to support mining and annotation of functional RNAs**. *Nucleic Acids Res* 2008, **37**:D89-92.

155. Corcoran DL, Georgiev S, Mukherjee N, Gottwein E, Skalsky RL, Keene JD, Ohler U: **PARalyzer: definition of RNA binding sites from PAR-CLIP short-read sequence data**. *Genome Biol* 2011, **12**(8):R79.

156. Dutko JA, Schäfer A, Kenny AE, Cullen BR, Curcio MJ: **Inhibition of a yeast LTR retrotransposon by human APOBEC3 cytidine deaminases**. *Curr Biol* 2005, **15**:661-666.

157. Bogerd HP, Skalsky RL, Kennedy EM, Furuse Y, Whisnant AW, Flores O, Schultz KL, Putnam N, Barrows NJ, Sherry B *et al*: **Replication of many human viruses**

is refractory to inhibition by endogenous cellular microRNAs. *J Virol* 2014, **88**:8065-8076.

158. Wiegand HL, Doehle BP, Bogerd HP, Cullen BR: **A second human antiretroviral factor, APOBEC3F, is suppressed by the HIV-1 and HIV-2 Vif proteins**. *EMBO J* 2004, **23**:2451-2458.

159. Diamond TL, Roshal M, Jamburuthugoda VK, Reynolds HM, Merriam AR, Lee KY, Balakrishnan M, Bambara RA, Planelles V, Dewhurst S *et al*: **Macrophage tropism of HIV-1 depends on efficient cellular dNTP utilization by reverse transcriptase**. *J Biol Chem* 2004, **279**:51545-51553.

160. Sharova N, Wu Y, Zhu X, Stranska R, Kaushik R, Sharkey M, Stevenson M: **Primate lentiviral Vpx commandeers DDB1 to counteract a macrophage restriction**. *PLoS Pathog* 2008, **4**(5):e1000057.

161. Giedroc DP, Cornish PV: **Frameshifting RNA pseudoknots: structure and mechanism**. *Virus Res* 2008, **139**:193-208.

162. Zeng Y, Cullen BR: **Efficient processing of primary microRNA hairpins by Drosha requires flanking nonstructured RNA sequences**. *J Biol Chem* 2005, **280**:27595-27603.

163. Linnstaedt SD, Gottwein E, Skalsky RL, Luftig MA, Cullen BR: **Virally induced cellular microRNA miR-155 plays a key role in B-cell immortalization by Epstein-Barr virus**. *J Virol* 2010, **84**(22):11670-11678.

164. Libri V, Helwak A, Miesen P, Santhakumar D, Borger JG, Kudla G, Grey F, Tollervey D, Buck AH: **Murine cytomegalovirus encodes a miR-27 inhibitor disguised as a target**. *Proc Natl Acad Sci U S A* 2012, **109**(1):279-284.

165. Cazalla D, Yario T, Steitz JA: **Down-regulation of a host microRNA by a Herpesvirus saimiri noncoding RNA**. *Science* 2010, **328**:1563-1566.

166. Jopling CL, Yi M, Lancaster AM, Lemon SM, Sarnow P: **Modulation of hepatitis C virus RNA abundance by a liver-specific microRNA**. *Science* 2005, **309**:1577-1581.

167. Ho BC, Yu SL, Chen JJ, Chang SY, Yan BS, Hong QS, Singh S, Kao CL, Chen HY, Su KY *et al*: **Enterovirus-induced miR-141 contributes to shutoff of host protein translation by targeting the translation initiation factor eIF4E**. *Cell Host Microbe* 2011, **9**:58-69.

168. Marcinowski L, Tanguy M, Krmpotic A, Radle B, Lisnic VJ, Tuddenham L, Chane-Woon-Ming B, Ruzsics Z, Erhard F, Benkartek C *et al*: **Degradation of cellular mir-27 by a novel, highly abundant viral transcript is important for efficient virus replication in vivo**. *PLoS Pathog* 2012, **8**(2):e1002510.

169. Simon V, Ho DD: **HIV-1 dynamics in vivo: implications for therapy**. *Nat Rev Microbiol* 2003, **1**(3):181-190.

170. Backes S, Shapiro JS, Sabin LR, Pham AM, Reyes I, Moss B, Cherry S, tenOever BR: **Degradation of host microRNAs by poxvirus poly(A) polymerase reveals terminal RNA methylation as a protective antiviral mechanism**. *Cell Host Microbe* 2012, **12**(2):200-210.

171. Islam S, Kjallquist U, Moliner A, Zajac P, Fan JB, Lonnerberg P, Linnarsson S: **Characterization of the single-cell transcriptional landscape by highly multiplex RNA-seq**. *Genome Res* 2011, **21**(7):1160-1167.

172. Bogerd HP, Whisnant AW, Kennedy EM, Flores O, Cullen BR: **Derivation and characterization of Dicer- and microRNA-deficient human cells**. *RNA* 2014, **20**:923-937.

173. Watts JM, Dang KK, Gorelick RJ, Leonard CW, Bess JW, Jr., Swanstrom R, Burch CL, Weeks KM: **Architecture and secondary structure of an entire HIV-1 RNA genome**. *Nature* 2009, **460**:711-716.

174. Pfeffer S, Zavolan M, Grasser FA, Chien M, Russo JJ, Ju J, John B, Enright AJ, Marks D, Sander C *et al*: **Identification of virus-encoded microRNAs**. *Science* 2004, **304**:734-736.

175. Flores O, Nakayama S, Whisnant AW, Javanbakht H, Cullen BR, Bloom DC: **Mutational inactivation of herpes simplex virus 1 microRNAs identifies viral mRNA targets and reveals phenotypic effects in culture**. *J Virol* 2013, **87**(12):6589-6603.

176. Skalsky RL, Kang D, Linnstaedt SD, Cullen BR: **Evolutionary conservation of primate lymphocryptovirus microRNA targets**. *J Virol* 2014, **88**:1617-1635.

177. Tsichlis PN, Donehower L, Hager G, Zeller N, Malavarca R, Astrin S, Skalka AM: **Sequence comparison in the crossover region of an oncogenic avian retrovirus recombinant and its nononcogenic parent: genetic regions that control growth rate and oncogenic potential**. *Mol Cell Biol* 1982, **2**(11):1331-1338.

178. Kincaid RP, Chen Y, Cox JE, Rethwilm A, Sullivan CS: **Noncanonical microRNA (miRNA) biogenesis gives rise to retroviral mimics of lymphoproliferative and immunosuppressive host miRNAs**. *MBio* 2014, **5**(2):e00074.

179. Lagos D, Pollara G, Henderson S, Gratrix F, Fabani M, Milne RS, Gotch F, Boshoff C: **miR-132 regulates antiviral innate immunity through suppression of the p300 transcriptional co-activator**. *Nat Cell Biol* 2010, **12**(5):513-519.

180. Choi SY, Faller DV: **A transcript from the long terminal repeats of a murine retrovirus associated with trans activation of cellular genes**. *J Virol* 1995, **69**(11):7054-7060.

181. Xia T, O'Hara A, Araujo I, Barreto J, Carvalho E, Sapucaia JB, Ramos JC, Luz E, Pedroso C, Manrique M *et al*: **EBV microRNAs in primary lymphomas and targeting of CXCL-11 by ebv-mir-BHRF1-3**. *Cancer Res* 2008, **68**:1436-1442.

182. Bouttier M, Saumet A, Peter M, Courgnaud V, Schmidt U, Cazevieille C, Bertrand E, Lecellier CH: **Retroviral GAG proteins recruit AGO2 on viral RNAs without affecting RNA accumulation and translation**. *Nucleic Acids Res* 2011, **40**:775-786.

183. Phalora PK, Sherer NM, Wolinsky SM, Swanson CM, Malim MH: **HIV-1 replication and APOBEC3 antiviral activity are not regulated by P bodies**. *J Virol* 2012, **86**(21):11712-11724.

184. Llano M, Saenz DT, Meehan A, Wongthida P, Peretz M, Walker WH, Teo W, Poeschla EM: **An essential role for LEDGF/p75 in HIV integration**. *Science* 2006, **314**(5798):461-464.

Biography

Adam Wesley Whisnant

Born August 28, 1988 in Morgantown, West Virginia, USA

Education

2010-2014	Ph.D., Molecular Genetics and Microbiology
	Certificate in College Teaching
	Duke University, Durham, NC, USA
2006-2010	B.S., Zoology
	B.S., Biochemistry
	B.A., Chemistry
	North Carolina State University, Raleigh, NC, USA

Publications

Kennedy EM, Kornepati AVR, Goldstein M, Bogerd HP, Poling BC, **Whisnant AW**, Kastan MB, Cullen BR. 2014. *Inactivation of the human papillomavirus E6 or E7 gene in cervical carcinoma cells using a bacterial CRISPR/Cas RNA-guided endonuclease*. J Virol 88(20):11965-72.

Bogerd HP, Skalsky RL, Kennedy EM, Furuse Y, **Whisnant AW**, Flores O, Schultz KL, Putnam N, Barrows NJ, Sherry B, Scholle F, Garcia-Blanco MA, Griffin DE, Cullen BR. 2014. *Replication of Many Human Viruses Is Refractory to Inhibition by Endogenous Cellular MicroRNAs*. J Virol 88(14):8065-76.

Bogerd HP, **Whisnant AW**, Kennedy EM, Flores O, Cullen BR. 2014. *Derivation and characterization of Dicer- and microRNA-deficient human cells*. RNA 20(6):923-37.

Whisnant AW, Kehl T, Bao Q, Materniak M, Kuzmak J, Löchelt M, Cullen BR. 2014. *Identification of novel, highly expressed retroviral microRNAs in cells infected by bovine foamy virus*. J Virol 88(9):4679-86.

Whisnant AW, Bogerd HP, Flores O, Ho P, Powers JG, Sharova N, Stevenson M, Chen CH, Cullen BR. 2013. *In-Depth Analysis of the Interaction of HIV-1 with Cellular microRNA Biogenesis and Effector Mechanisms*. MBio 4(2). E00193-13.

Flores O, Nakayama S, **Whisnant AW**, Javanbakht H, Cullen BR, Bloom DC. 2013. *Mutational Inactivation of Herpes Simplex Virus 1 MicroRNAs Identifies Viral mRNA Targets and Reveals Phenotypic Effects in Culture*. J Virol 87(12):6589-603.

Awards and Honors

Anne T. and Robert M. Bass Instructional Fellowship